MOMENTUM AND MASS TRANSFER BETWEEN FOREST STANDS AND THE ATMOSPHERE: A NUMERICAL STUDY OF CANOPY BULK EXCHANGE COEFFICIENTS AND CANOPY RESISTANCES

Anno van Dijken

Momentum and Mass Transfer between Forest Stands and the Atmosphere: A Numerical Study of Canopy Bulk Exchange Coefficients and Canopy Resistances

Anno van Dijken

June 1988

U.S.D.A./U.S. Forest Service
Rocky Mountain Forest and Range Experiment Station
Fort Collins, Colorado 80526

PREFACE

As part of my graduate study in Air Pollution and Meteorology at the Agricultural University in Wageningen (The Netherlands), I have spent the past five months at the Rocky Mountain Forest and Range Experiment Station of the U.S. Forest Service in Fort Collins, Colorado.

This report on the exchange of momentum and mass between forest stands and the atmosphere is the formal result of my work at the Rocky Mountain Station, which undoubtedly has led to an improvement of my understanding of the exchange processes between vegetation and atmosphere. For me however, the value of my stay here goes far beyond that which is reflected by this report. Especially, meeting a lot of new people, during office-hours as well as after office-hours, has been a great experience.

Therefore, I would like to thank everyone who has made this stay possible, and everyone who has contributed to making it what it was: a marvellous time! My special thanks go to Bill Massman; it has been a great pleasure working with him during the past five months.

Fort Collins
June 20, 1988

Anno van Dijken

CONTENTS

NOTATION

A	parameter in stomatal resistance model	[kPa^{-1}]
$Ai(x)$	Airy function Ai of argument x	
B	parameter in stomatal resistance model	[$\mu E\ m^{-2}s^{-1}$]
B^{-1}	inverse surface Stanton number	
$Bi(x)$	Airy function Bi of argument x	
C_a	CO_2 concentration in the ambient air	[kg/m^3]
C_d	leaf drag coefficient	
C_{ds}	drag coefficient for the surface underlying the canopy	
C_f	stand drag coefficient	
C_t	leaf bulk transfer coefficient for water vapor	
C_t'	leaf bulk transfer coefficient for water vapor vapor evaluated at the top of the canopy	
C_t''	leaf bulk transfer coeffcient for heat evaluated at the top of the canopy	
D	characteristic dimension of a foliage element	[m]
DAH	absolute humidity difference from leaf to air	[kg/m^3]
$E(\zeta)$	vapor pressure deficit e_f-$e(\zeta)$	[kPa]
E_1	vapor pressure deficit at the top of the canopy	[kPa]
F	vertical specific flux of an admixture of the flow	[$kg\ m^{-2}s^{-1}$]
G	soil heat flux	[W/m^2]
$G(\delta)$	relative projected area of the foliage elements in the direction $\cos^{-1}\delta$	
$I_\lambda(x)$	modified Bessel function I of order λ of argument x	

K_c	turbulent diffusivity for an admixture of the flow	[m^2/s]
K_e	turbulent diffusivity for water vapor	[m^2/s]
K_h	turbulent diffusivity for heat	[m^2/s]
K_m	turbulent diffusivity for momentum	[m^2/s]
$K_\lambda(x)$	modified Bessel function K of order λ of argument x	
L	accumulated leaf area from the top of the canopy down to ζ	
LAI	leaf area index	
LE	latent heat flux from the surface	[W/m^2]
LE_s	latent heat flux from the soil	[W/m^2]
P_m	CO_2-saturated rate of photosynthesis at a particular PPFD	[mol $m^{-2}s^{-1}$]
P_{ml}	PPFD and CO_2-satureated rate of photosynthesis	[mol $m^{-2}s^{-1}$]
PPFD	photosynthetic photon flux density	[μE $m^{-2}s^{-1}$]
$PPFD_0$	PPFD at the top of the canopy	[μE $m^{-2}s^{-1}$]
Q_n	net radiation	[W/m^2]
Q_p	photon flux density	[μE $m^{-2}s^{-1}$]
R	solar global radiation	[W/m^2]
Re	local Reynolds number	
Re_h	local Reynolds number evaluated at the top of the canopy	
Sc	Schmidt number	
S_f	flux of admixture to or from the surface of foliage elements	[kg $m^{-2}s^{-1}$]
T	mean atmospheric temperature of the ambient air	[K]
T_f	foliage temperature	[K]
T_h	mean atmospheric temperature at the top of the canopy	[K]

$a(z)$, $a(\xi)$	one sided leaf area per unit volume of the canopy	[m^{-1}]
a_m,a_1	maximum value of the foliage area density a(z)	[m^{-1}]
a_0	value of the foliage area density at the surface	[m^{-1}]
$c(z)$	mean concentration of an admixture in the ambient air	[kg/m^3]
c_f	concentration of an admixture in the foliage elements	[kg/m^3]
c_p	specific heat of air at constant pressure	[J/kgK]
d	displacement height for momentum transfer	[m]
d_s	displacement height for water vapor transfer	[m]
$e(\xi)$	mean water vapor pressure in the ambient air	[kPa]
e_f	water vapor pressure in substomatal cavity	[kPa]
$f(\xi)$	$a(\xi)/a_m$	
g_s	stomatal conductance	[m/s]
$g_{s,min}$	minimal stomatal conductance	[m/s]
$g_{s,max}$	maximal stomatal conductance	[m/s]
g_1	light extinction coefficient	
g_2	parameter for soil moisture flux	
h	height of the top of the canopy	[m]
k	von Karman constant = 0.41	
p	atmospheric pressure	[kPa]
r_a	aerodynamic resistance for momentum exchange	[s/m]
r_{ah}	aerodunamic resistance for heat exchange	[s/m]
r_b	boundary-layer resistance	[s/m]

r_c	canopy resistance	[s/m]
r_{cut}	cuticular resistance	[s/m]
r_m	mesophyll resistance	[s/m]
r_s	stomatal resistance	[s/m]
$r_{s,bulk}$	bulk stomatal resistance	[s/m]
$r_{s,min}$	minimal stomatal resistance	[s/m]
s	change of saturation vapor pressure with temperature	[kPa/K]
u	mean horizontal wind speed	[m/s]
u_h	mean horizontal wind speed at the top of the canopy	[m/s]
u*	friction velocity	[m/s]
v_d	deposition velocity	[m/s]
z	height	[m]
z_m	height of the top of the roughness sublayer	[m]
z_0	roughness length for momentum	[m]
z_{0s}	scalar roughness length associated with water vapor	[m]
α_k	K_e/K_m	
β	extinction coefficient for the profile of mean horizontal wind speed for constant foliage distributions	
β_I	idem , but for triangular foliage distributions (region I)	
β_{II}	idem , but for triangular foliage distributions (region II)	
γ	psychrometric constant	[kPa/K]
δ	cosine of the zenith angle of an incident beam of radiation	
ε	molecular diffusivity of water vapor in the air	[m^2/s]

ς	molecular diffusivity of gaseous air pollutant in air	[m^2/s]
θ	$(T_f - T)/(T_f - T_h)$	
λ_1	parameter arising from the roughness sublayer	
μ	integral of $f(\xi)$ from the bottom of the canopy to the top	
ν	molecular viscosity of air	[m^2/s]
ξ	normalized height z/h	
ξ_m	normalized height at which the maximum foliage density occurs	
ρ	density of air	[kg/m^3]
σ	$K_m/(u\ h) = K_m(h)/(u_h\ h)$	
τ	horizontal shear stress	[N/m^2]
φ	solar elevation angle	[degrees]
ψ_l	leaf water potential	[MPa]
ψ_s	soil water potential	[MPa]
ω	scattering coefficient	
χ	normalized mean horizontal wind speed for constant foliage distributions u/u_h	
χ_I	idem , but for triangular foliage distributions (region I)	
χ_{II}	idem , but for triangular foliage distributions (region II)	
τ_*	normalized horizontal shear stress $\tau/(\rho\ u_h^2)$	

SUMMARY

Simple first-order closure methods are used to describe the exchange of momentum and mass between forest stands and the atmosphere. Analytical expressions are derived for the within-canopy profiles of mean wind speed and horizontal shear stress for constant and triangular foliage distributions, and displacement heights and roughness lengths are presented as a function of C_dLAI and canopy structure. The effects of mutual aerodynamic interference of canopy elements are included in the model by assuming that for full canopies $0.25 \leq C_dLAI \leq 0.50$.

The model is extended to mass transfer by taking into account the leaf boundary-layer resistance and the stomatal resistance to transport of a scalar admixture of the flow. The Pohlhausen model for laminar boundary layers is used to describe the leaf boundary-layer resistance. The stomatal resistance is assumed to be a function of two environmental factors only: (1) the within-canopy profile of photosynthetic photon flux density, and (2) the water vapor pressure deficit at the top of the canopy. The obtained transfer equation is solved numerically, using a very efficient relaxation method. The model is then used to investigate the influence of canopy density, canopy structure, and shelter on the bulk transfer coefficient (in terms of kB^{-1}), and canopy resistance, both for the transfer of water vapor, and on the deposition velocity for ozone.

The results for water vapor transfer showed that canopy density and canopy structure have a considerable influence on kB^{-1} and canopy resistance, but including shelter effects in the model tends to diminish the dependency on canopy structure. Also, including the effects of sheltering caused kB^{-1} values to decrease by as much as 70% for full deciduous canopies, and 45% for coniferous canopies. Furthermore, it was found that the commonly used assumption that the canopy resistance is equal to the bulk stomatal resistance is probably accurate only to within about 20% for full canopies.

Computed deposition velocities for ozone were also strongly influenced by shelter effects, and ranged from 1.0 to 4.7 cm/s (depending on LAI) for full deciduous canopies, and from 0.15 to 0.6 cm/s for coniferous canopies.

1. INTRODUCTION

Much effort is (and already has been) directed towards modeling the exchange of momentum, heat and mass between the atmosphere and vegetated surfaces, because it is of interest to several scientific problems. For the development of large-scale models (e.g. Global Circulation Models) descriptions of the interaction between vegetation and atmosphere are required to model the large-scale radiation balance and the partitioning of net radiation into sensible and latent heat fluxes, simply because large parts of the earth's surface are vegetated. Estimating (future) effects of air pollutants (like e.g. O_3 and SO_2) on forest stands also requires studying this interaction, in order to determine the amount of pollutant transported to the leaves or needles.

Generally, the turbulent air flow within plant canopies is described using so called conservation equations (e.g. Raupach and Thom, 1981). Solving these equations introduces a closure problem, i.e. the number of unknowns is larger than the number of equations available, which can only be solved by making additional assumptions.

In the past decades, most studies used a simple first-order closure approach, assuming an analogy between molecular diffusion and turbulent transport, and describing the fluxes of momentum, heat and mass in terms of a local gradient-diffusion equation only (e.g. Inoue, 1963; Cowan, 1968). This approach implies, that the length scale over which the mean gradients (of wind speed, temperature, and concentration) change is much larger than the length scale of the turbulence (Corrsin, 1974).

Measurements showed that this concept is not able to describe all observed features of the exchange processes which occur within plant stands. E.g. Shaw (1977) notes the presence of secondary maxima in wind speed in the lower region of forest canopies, and regions of zero-shear in wind speed within crop canopies, which imply counter-gradient and zero-gradient momentum fluxes respectively, when using a local gradient-diffusion equation. Therefore, other solutions are sought, e.g. in more realistic first-order closure approaches (Li et al., 1985), and in

higher-order closure schemes (e.g. Wilson and Shaw, 1977; Yamada, 1982; Meyers and Paw, 1986).

However, these more sophisticated models generally have the disadvantage of being computationally very complicated, and therefore rather time consuming and expensive. Moreover, the general applicability of these models has not yet been proved. Consequently, simple gradient-diffusion models remain useful to provide insight in the exchange of momentum, heat and mass within plant canopies, especially when their limitations are recognized, and are therefore still employed (e.g. Sellers et al., 1986; Taconet et al., 1986).

In this work simple first-order closure assumptions are used to model the exchange of momentum and mass between a forest stand and the atmosphere. Chapter 2 deals with the transfer of momentum from the atmosphere to a vegetated surface. In chapter 3 the turbulent transport of mass in general is described, and a transfer equation is derived for the special case of water vapor. Stomates at the surface of the leaves or needles play an important role in the process of mass exchange between canopy and atmosphere, and their behaviour is modeled in chapter 4. The method used to solve the water vapor transfer equation, and the boundary conditions applied to this equation, are described in chapter 5. Chapter 6 deals with the canopy bulk exchange coefficients for water vapor, and model results are presented in this chapter. In chapter 7 values for the canopy resistance, computed with the model, are presented and compared with values for the bulk stomatal resistance. The transfer of air pollutants (in particular ozone) from atmosphere to forest stand is described in chapter 8. Finally, chapter 9 provides a discussion of the results, and the conclusions.

2. EXCHANGE OF MOMENTUM BETWEEN VEGETATED SURFACES AND THE ATMOSPHERE

2.1. Introduction

Modeling the exchange of momentum between vegetated surfaces and the atmosphere, requires assumptions about the mechanics of this process. Here, simple first-order closure approaches will be used to supply the within-canopy profiles of mean horizontal wind speed and horizontal shear stress, although the deficiencies of these methods are recognized (e.g. Shaw, 1977; Finnigan, 1985). For the purpose of this study however, the use of a computationally much simpler (and cheaper) first-order closure scheme is probably sufficient.

The within-canopy air flow will be joined to the flow above the canopy, by assuming the presence of roughness sublayer between the canopy sublayer and the inertial sublayer, accompagnied by assumptions concerning the eddy diffusivity. Furthermore, expressions will be provided for the roughness length, displacement height and friction velocity (in terms of a stand drag coeffcient) for the air flow above the canopy.

To investigate the influence of the canopy structure, constant foliage distributions will be considered as well as triangular distributions, and attention is paid to mutual aerodynamic interference of foliage elements.

2.2. The first-order closure equations for momentum exchange

Most first-order closure methods use a turbulent diffusivity K_m and a drag coefficient C_d to describe the momentum transfer within a canopy. Following Seginer (1974) K_m and C_d are defined by equations (2.1) and (2.2):

$$\tau = \rho K_m \frac{du}{dz} \qquad (2.1)$$

$$\frac{d\tau}{dz} = \rho C_d a(z) u^2 \qquad (2.2)$$

where τ is the horizontal shear stress within the canopy; ρ is the density of the air; u is the mean horizontal wind speed; z is the height above the surface; and a(z) is the foliage distribution or foliage area density (i.e. the one sided leaf area per unit volume of the canopy) as a function of height. C_d is assumed to be a constant throughout the depth of the canopy (den Hartog and Shaw, 1975; Raupach and Thom, 1981). Furthermore, it is assumed that the profiles of mean horizontal wind speed and turbulent diffusivity are similar within the canopy (Cowan, 1968).

Equations (2.1) and (2.2) can be normalized to yield (2.3) and (2.4) (Massman, 1987a):

$$\chi_* = \frac{\sigma}{2}\frac{d\chi}{d\zeta} \qquad (2.3)$$

$$\frac{d\chi_*}{d\zeta} = \frac{C_d\, LAI\, f(\zeta)\, \chi}{\mu} \qquad (2.4)$$

where $\chi_* = \tau/(\rho u_h^2)$; u_h is the mean horizontal wind speed at the top of the canopy; $\chi = u^2/u_h^2$; $\zeta = z/h$; h is the height of the canopy; $\sigma = K_m/(u\,h) = K_m(h)/(u_h\,h)$ (because of the assumed similarity between the mean wind speed profile and the turbulent diffusivity profile); LAI is the leaf area index ($= {}_0\int^h a(z)\,dz$); $f(\zeta) = a(\zeta)/a_m$, with a_m representing the maximum value of the foliage area density; and $\mu = {}_0\int^1 f(\zeta)\,d\zeta$. (2.3) and (2.4) can be decoupled by differentiating (2.3) with respect to ζ, resulting in (2.5), followed by a substitution of (2.5) in (2.4), yielding (2.6):

$$\frac{d\chi_*}{d\zeta} = \frac{\sigma}{2}\frac{d^2\chi}{d\zeta^2} \qquad (2.5)$$

$$\frac{d^2\chi}{d\zeta^2} = \beta^2 f(\zeta)\chi \qquad (2.6)$$

where β is the profile extinction coefficient:

$$\beta = \left[\frac{2\ C_d\ LAI}{\mu\ \sigma}\right]^{1/2} \qquad (2.7)$$

2.3. Solving the equations for momentum exchange

2.3.1. Boundary conditions

Considering the definition of χ, the boundary condition at z = h (i.e. $\zeta = 1$) for solving (2.6), in order to obtain the wind profile within the canopy, is simply:

$$\chi(1) = 1 \qquad (2.8)$$

The lower boundary condition (i.e. at $\zeta = 0$) for this equation can take several forms. Cowan (1968) assumed the mean horizontal wind speed to be zero (2.9), and Inoue (1963) assumed that the flow above the canopy interacts mainly with the upper part of the canopy, and that the influence of the surface is not important (2.10). Neither of these two boundary conditions reproduce the frequently observed zero wind shear within the lower part of the canopy (e.g. Shaw, 1977). So a third boundary condition can be applied by assuming a zero wind gradient within the lower region of the canopy (2.11).

$$\chi(0) = 0 \qquad (2.9)$$

$$\lim_{\zeta \to -\infty} \chi(\zeta) = 0 \qquad (2.10)$$

$$\frac{d\chi(0)}{d\zeta} = 0 \qquad (2.11)$$

Once the within-canopy wind profile is found, it can be used to calculate the profile of horizontal shear stress within the canopy from (2.5). The lower boundary condition on χ_* is chosen following Wilson and Shaw (1977) and Shaw and Pereira (1982):

$$\chi_*(0) = C_{ds}\,\chi(0.05) \qquad (2.12)$$

where C_{ds} equals 0.032, based on a surface roughness length z_{0s} of 0.005h. The upper boundary condition on χ_* is that $\chi_*(1)$ is a constant, which will be determined as part of the solution, but by connecting the canopy sublayer to the inertial sublayer through the roughness sublayer, $\chi_*(1)$ can be related to other parameters, which will be outlined in the next section.

2.3.2. Joining the flow within the canopy to the flow above the canopy

Figure 2.1 shows the assumed presence of a roughness sublayer between the canopy sublayer and the inertial sublayer. Inserting this roughness sublayer implicates that the value of turbulent diffusivity at the top of the canopy (i.e. $K_m(h)$) will be larger than its logarithmic extrapolation from the inertial sublayer (Raupach and Thom, 1981):

$$K_m(h) = \alpha\, u_*\, k\, (h - d) \qquad (2.13)$$

where α is a constant between 1.0 and 2.0 (Raupach and Thom, 1981) and assumed to be 1.5, as was estimated from observed wind profiles within several different canopies; $u_* = (\tau/\rho)^{1/2}$ is the friction velocity, which is assumed to be constant throughout the depth of the roughness sublayer; k = 0.41 is the von Karman constant; and d is the displacement height. Normalizing (2.13) yields (2.14):

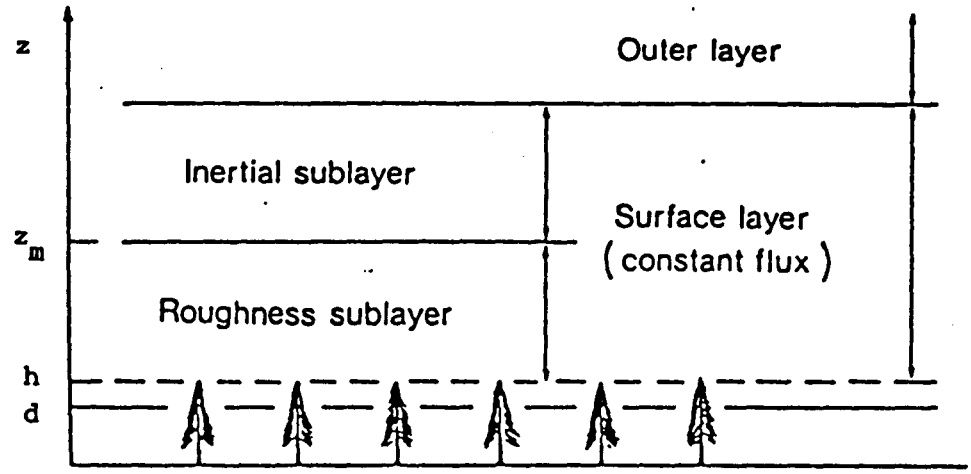

Figure 2.1: The roughness sublayer as intermediate layer between the canopy sublayer and the inertial sublayer. The height of the roughness sublayer is denoted by z_m.

$$\sigma' = \alpha \; k \, \chi_*(1)^{1/2} \, (1 - d/h) \qquad (2.14)$$

According to Thom (1971) the displacement height corresponds to the level of mean drag upon the individual canopy elements, and can be written as (Shaw and Pereira, 1982):

$$\frac{d}{h} = \frac{C_d \, LAI}{\mu} \; \frac{\int_0^1 \zeta' \, f(\zeta') \, \chi(\zeta') \, d\zeta'}{\chi_*(1)} \qquad (2.15)$$

2.3.3. Solutions for constant foliage distributions

In the case of a constant foliage distribution (figure 2.2), it can easily be seen that $f(\zeta) = 1$ and $\mu = 1$. Then (2.6) is a simple differential equation, with a general solution as given in (2.16):

$$\chi = c_1 \, e^{\beta \zeta} + c_2 \, e^{-\beta \zeta} \qquad (2.16)$$

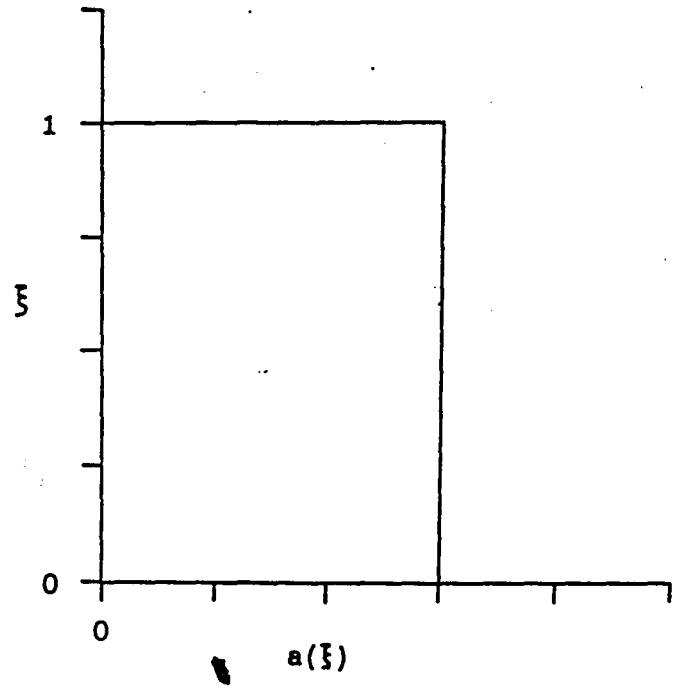

Figure 2.2: A constant foliage distribution.

where c_1 and c_2 are constants to be determined by applying boundary conditions (see 2.3.1.).

Cowans (1968) lower boundary condition (2.9) results in (2.17) for χ:

$$\chi = \sinh(\beta\xi)/\sinh(\beta) \qquad (2.17)$$

whereas Inoues (1963) condition (2.10) results in an exponential wind profile (2.18):

$$\chi = e^{-\beta(1-\xi)} \qquad (2.18)$$

Finally, the assumption of zero wind shear at the surface (2.11) yields (2.19):

$$\chi = \cosh(\beta\xi)/\cosh(\beta) \qquad (2.19)$$

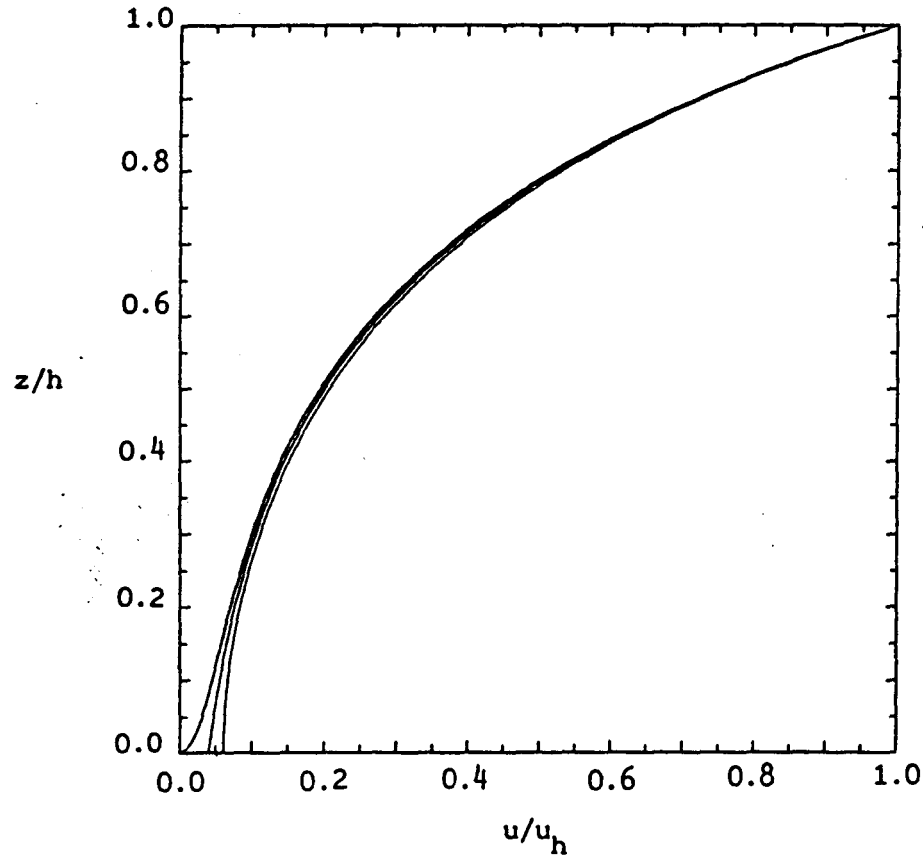

Figure 2.3: Wind speed profiles for constant foliage distributions. The upper curve represents the sinh profile, the middle one the exponential profile, and the lower one the cosh profile. $C_d LAI = 0.6$.

Integrating the equation for the horizontal shear stress (2.5) results in (2.20):

$$\chi_*(\zeta) = \chi_*(0) + \frac{C_d\ LAI}{\mu} \int_0^{\zeta} f(\zeta')\ \chi(\zeta')\ d\zeta' \qquad (2.20)$$

where $\chi_*(0)$ is defined by the lower boundary condition; and $f(\zeta') = 1$ in the case of a constant foliage distribution. Knowing the mean horizontal

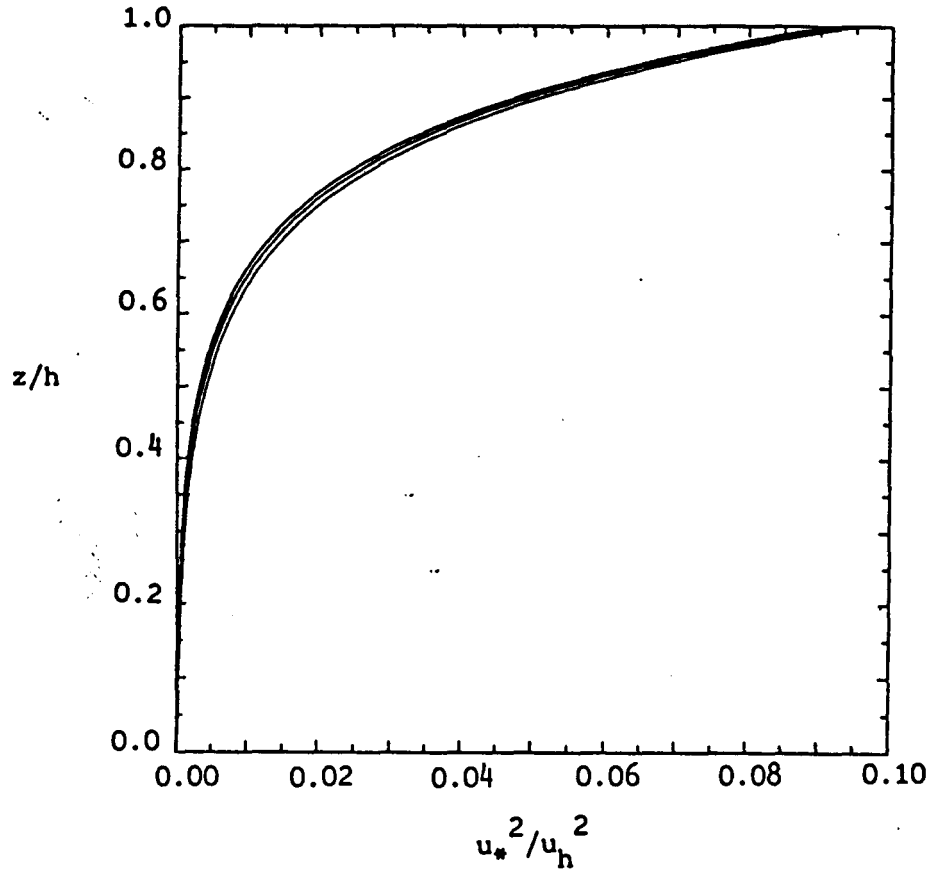

Figure 2.4: Shear stress profiles for constant foliage distributions. The upper curve is associated with the sinh wind profile, the middle one with the exponential profile, and the lower one with the cosh profile. $C_dLAI = 0.6$.

wind speed profile from (2.17)-(2.19), it is easy to calculate the shear stress profile from (2.20).

Therefore, given the boundary conditions on (2.5) and (2.6), equations (2.6), (2.7), (2.14), (2.15) and (2.20) can be solved iteratively for σ, β, d/h, $\lambda_*(0)$ and $\lambda_*(1)$, each as a function of C_dLAI. Given a value for C_dLAI and a starting value for σ, β can be computed. Once β is known the wind profile $\lambda(\zeta)$ can be calculated, providing the necessary information for computation of the shear stress profile. Then the displacement height

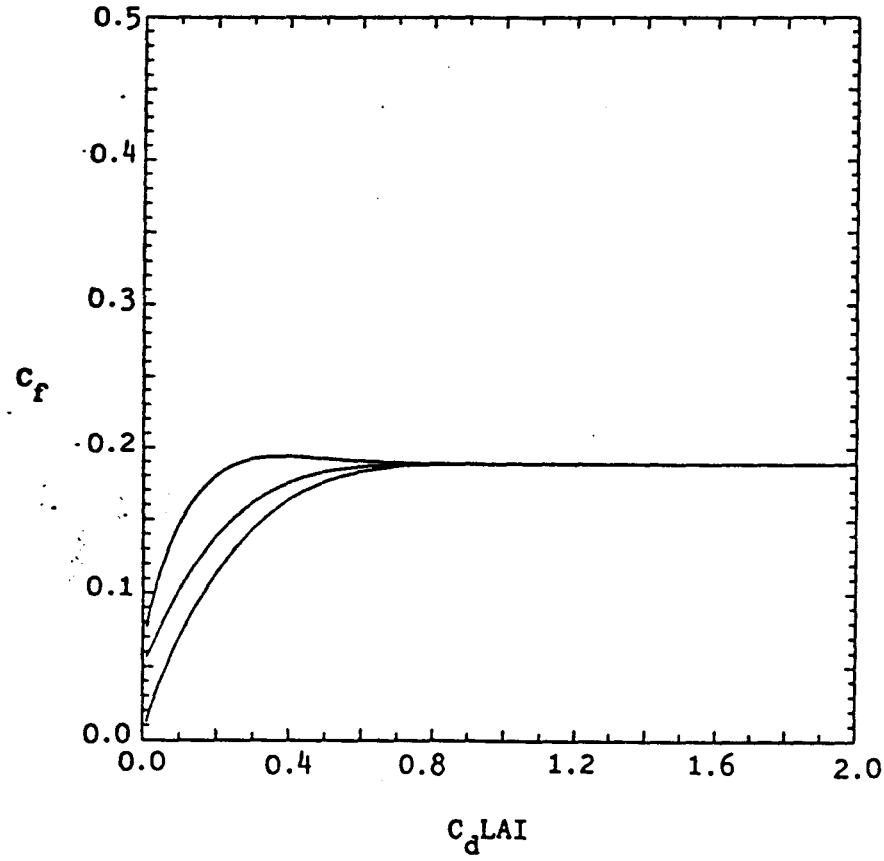

Figure 2.5: The stand drag coefficient as a function of C_dLAI for constant foliage distributions. The upper curve is associated with the cosh wind profile, the middle one with the exponential profile, and the lower one with the sinh profile.

d/h is calculated from (2.15), using Simpson's rule. Finally, $\chi_*(1)$ and d/h are substituted in (2.14), resulting in an improved value for σ.

Figure 2.3 shows the calculated wind speed profiles for the different boundary conditions, and figure 2.4 the corresponding profiles for the shear stress within the canopy. In figure 2.5 the stand drag coefficient $C_f = 2(u_*^2/u_h^2)_{z=h}$ is shown as a function of C_dLAI. Finally, figure 2.6 shows the normalized displacement height d/h as a function of C_dLAI.

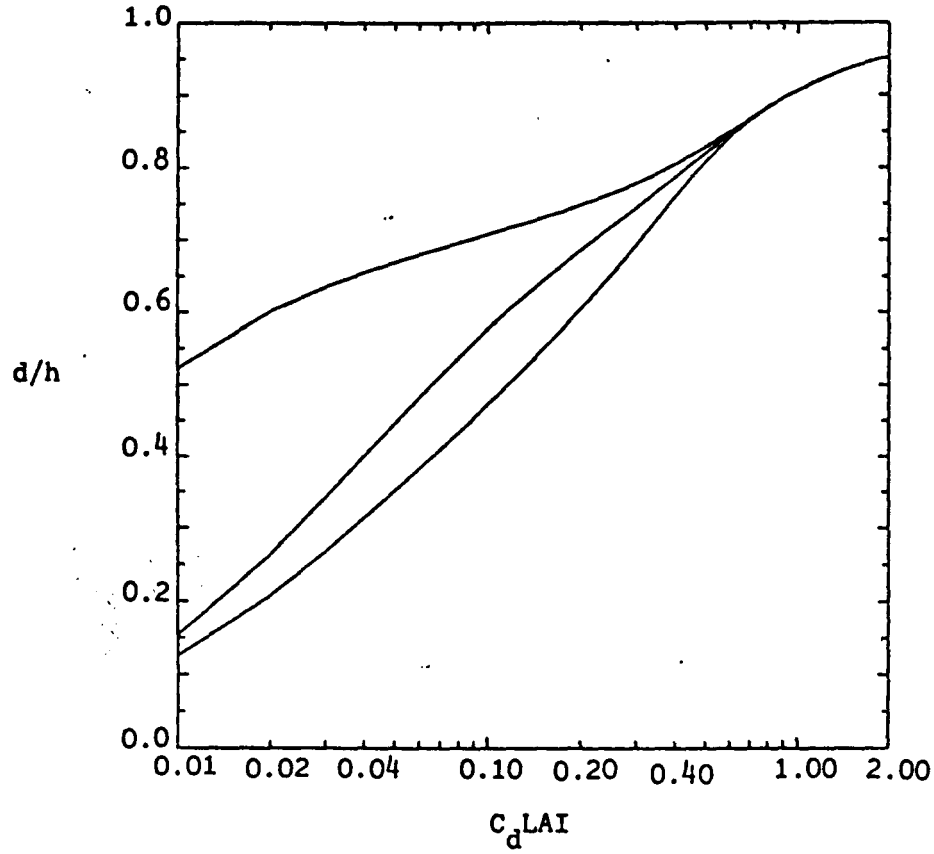

Figure 2.6: Normalized displacement height as a function of C_dLAI for constant foliage distributions. The upper curve is associated with the sinh wind profile, the middle one with the exponential profile, and the lower one with the cosh profile.

2.3.4. Solutions for triangular foliage distributions

Assuming a triangular foliage distribution, instead of a constant foliage distribution, provides a different solution to (2.5) and (2.6).

Let $a(\zeta)$ be defined as (see also figure 2.7):

$$a(\zeta) = a_1 (1 - \zeta)/(1 - \zeta_m) \qquad \text{if } \zeta_m \leq \zeta \leq 1 \qquad (2.21a)$$

$$a(\zeta) = a_0 (a_1 - a_0) \zeta / \zeta_m \qquad \text{if } 0 \leq \zeta \leq \zeta_m \qquad (2.21b)$$

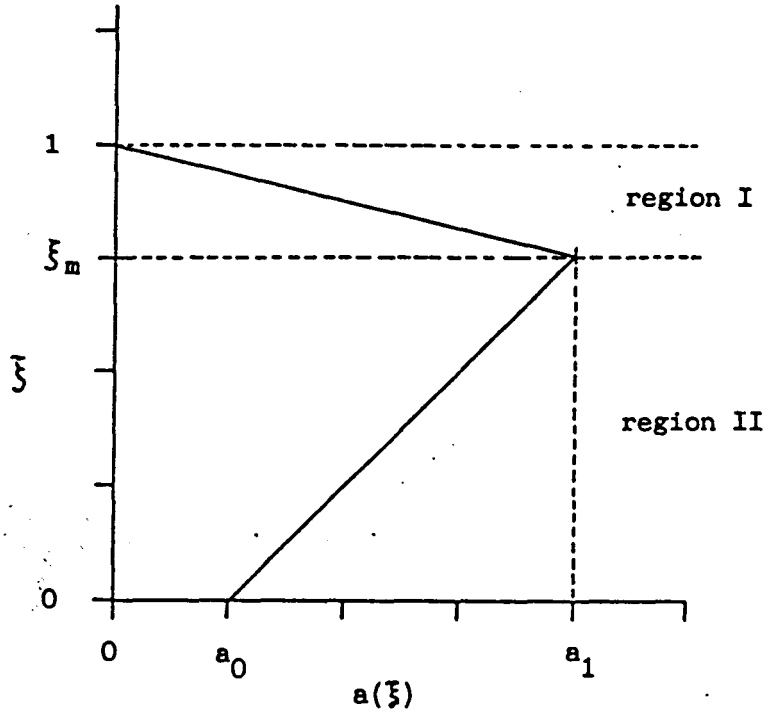

Figure 2.7: A triangular foliage distribution.

where ξ_m is the (normalized) height at which the maximum foliage density occurs; $a_1 = a_m$ is the maximum foliage density; and a_0 is the foliage density at the surface. Now, $f(\xi)$ is a function of height and it can be derived that

$$\mu = \frac{LAI}{h\, a_1} = 0.5\,(1 + \frac{a_0}{a_1}\,\xi_m) \qquad (2.22)$$

Substituting for $f(\xi)$ in (2.4) results in (2.23):

$$\frac{d\chi_*}{d\xi} = \frac{C_d\, LAI}{\mu(1 - \xi_m)}\,(1 - \xi)\,\chi \qquad \text{if } \xi_m \leq \xi \leq 1 \qquad (2.23a)$$

$$\frac{d\chi_*}{d\xi} = \frac{C_d\, LAI}{\mu}\,\{\,(1 - \frac{a_0}{a_1})\,\frac{\xi}{\xi_m} + \frac{a_0}{a_1}\,\}\chi \quad \text{if } 0 \leq \xi \leq \xi_m \qquad (2.23b)$$

Now, decoupling of (2.3) and (2.23) results in (2.5) and (2.24):

$$\frac{d^2\chi}{d\zeta'^2} = \beta_I^3 \zeta' \chi \qquad \text{if } \zeta_m \leq \zeta \leq 1 \qquad (2.24a)$$

$$\frac{d^2\chi}{d\zeta''^2} = \beta_{II}^3 \zeta'' \chi \qquad \text{if } 0 \leq \zeta \leq \zeta_m \qquad (2.24b)$$

where $\zeta' = 1 - \zeta$; $\zeta'' = (1 - a_0/a_1)\zeta + (a_0/a_1)\zeta_m$; and:

$$\beta_I = \left[\frac{2\, C_d\, LAI}{\kappa^2 \sigma\, (1 - \zeta_m)}\right]^{1/3} \qquad (2.25a)$$

$$\beta_{II} = \left[\frac{2\, C_d\, LAI}{\kappa^2 \sigma\, \zeta_m\, (1-a_0/a_1)^2}\right]^{1/3} \qquad (2.25b)$$

The solutions for χ to (2.24) can be related to Airy functions (e.g. Abramowitz and Stegun, 1964):

$$\chi_I = a_I\, Ai(\beta_I\, \zeta') + b_I\, Bi(\beta_I\, \zeta') \qquad (2.26a)$$

$$\chi_{II} = a_{II}\, Ai(\beta_{II}\, \zeta'') + b_{II}\, Bi(\beta_{II}\, \zeta'') \qquad (2.26b)$$

where χ_I represents the wind speed profile for $\zeta_m \leq \zeta \leq 1$, and χ_{II} for $0 \leq \zeta \leq \zeta_m$; Ai and Bi are the Airy functions; a_I, b_I, a_{II} and b_{II} are constants to be determined by application of boundary conditions.

Apart from the boundary conditions mentioned in 2.3.1., additional conditions are required to obtain a complete profile throughout the depth of the canopy, because of the different solutions for region I and II. Therefore, the solutions have to match at ζ_m (2.27), and the same applies for their first derivatives (2.28).

$$a_I \, Ai(\beta_I (1-\zeta_m)) + b_I \, Bi(\beta_I (1-\zeta_m)) =$$

$$a_{II} \, Ai(\beta_{II} \zeta_m) + b_{II} \, Bi(\beta_{II} \zeta_m) \qquad (2.27)$$

$$a_I \{-\beta_I \, Ai'(\beta_I (1-\zeta_m))\} + b_I \{-\beta_I \, Bi'(\beta_I (1-\zeta_m))\} =$$

$$a_{II} \{\beta_{II} (1-a_0/a_1) \, Ai'(\beta_{II} \zeta_m)\} +$$

$$b_{II} \{\beta_{II} (1-a_0/a_1) \, Bi'(\beta_{II} \zeta_m)\} \qquad (2.28)$$

Since assuming a lower boundary condition of zero shear at the surface (2.11) is most consistent with observations, only this case will be considered. Therefore, the upper boundary condition being

$$\chi(1) = a_I \, Ai(0) + b_I \, Bi(0) = 1 \qquad (2.29)$$

and the lower boundary condition being

$$\chi'(0) = a_{II} \, Ai'(\beta_{II} \, a_0/a_1 \, \zeta_m) \, \beta_{II} (1-a_0/a_1) +$$

$$b_{II} \, Bi'(\beta_{II} \, a_0/a_1 \, \zeta_m) \, \beta_{II} (1-a_0/a_1) = 0 \qquad (2.30)$$

the set of equations (2.27), (2.28), (2.29) and (2.30) can be written as:

$$\begin{pmatrix} C_{11} & C_{12} & 0 & 0 \\ C_{21} & C_{22} & C_{23} & C_{24} \\ C_{31} & C_{32} & C_{33} & C_{34} \\ 0 & 0 & C_{43} & C_{44} \end{pmatrix} \begin{pmatrix} a_I \\ b_I \\ a_{II} \\ b_{II} \end{pmatrix} = \begin{pmatrix} 1 \\ 0 \\ 0 \\ 0 \end{pmatrix} \qquad (2.31)$$

where: $C_{11} = Ai(0)$

$C_{12} = Bi(0)$

$C_{21} = Ai(\beta_I (1-\zeta_m))$

$C_{22} = Bi(\beta_I (1-\zeta_m))$

$C_{23} = -Ai(\beta_{II} \zeta_m)$

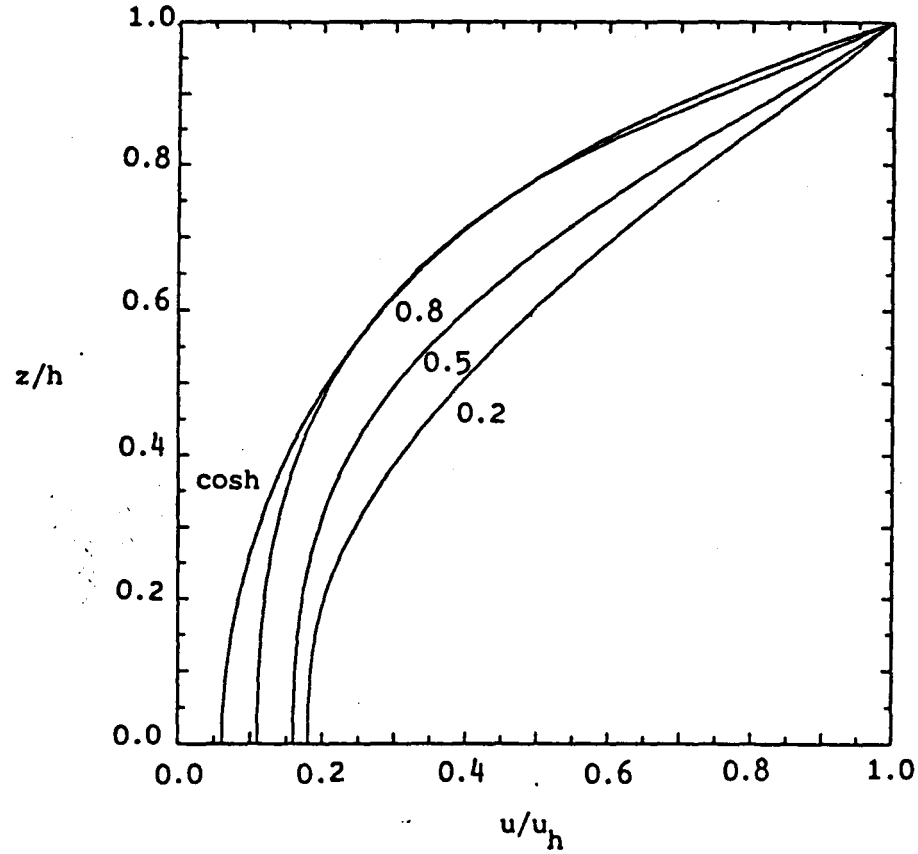

Figure 2.8: Wind speed profiles for three triangular foliage distributions with the maximum foliage density at ζ = 0.2, 0.5, and 0.8, and the cosh profile for constant distributions. $C_d LAI$ = 0.6.

$$C_{24} = -Bi(\beta_{II}\,\zeta_m)$$
$$C_{31} = -\beta_I\,Ai'(\beta_I\,(1-\zeta_m))$$
$$C_{32} = -\beta_I\,Bi'(\beta_I\,(1-\zeta_m))$$
$$C_{33} = -\beta_{II}\,(1-a_0/a_1)\,Ai'(\beta_{II}\,\zeta_m)$$
$$C_{34} = -\beta_{II}\,(1-a_0/a_1)\,Bi'(\beta_{II}\,\zeta_m)$$
$$C_{43} = \beta_{II}\,(1-a_0/a_1)\,Ai'(\beta_{II}\,a_0/a_1\,\zeta_m)$$
$$C_{44} = \beta_{II}\,(1-a_0/a_1)\,Bi'(\beta_{II}\,a_0/a_1\,\zeta_m)$$

To solve (2.31) for a_I, b_I, a_{II} and b_{II} a matrix LU-decomposition method is used (Press et al., 1986). Once these coefficients are

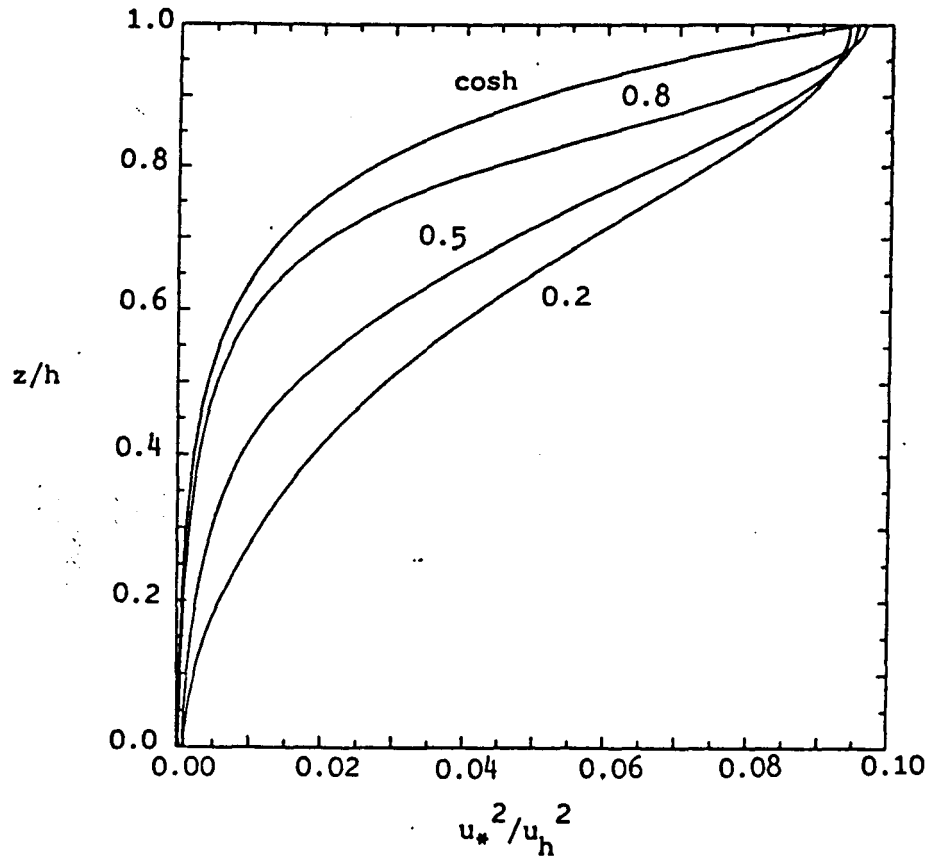

Figure 2.9: Canopy shear stress profiles for the same foliage distributions as in figure 2.8. $C_dLAI = 0.6$.

determined, the mean horizontal wind speed profile can be computed from (2.26). Then it is easy to calculate the horizontal shear stress profile from (2.20), using Simpson's rule for the integration.

Therefore, given the boundary conditions on (2.5) and (2.24), equations (2.14), (2.15), (2.20), (2.24) and (2.25) can be solved iteratively for β_I, β_{II}, σ, d/h, $\chi_*(0)$ and $\chi_*(1)$, each as a function of C_dLAI (see 2.3.3.).

Figure 2.8 shows the calculated wind speed profiles for $\int_m = 0.2$, $\int_m = 0.5$ and $\int_m = 0.8$, and also the cosh wind speed profile for a constant foliage distribution is included. Figure 2.9 shows the corresponding within-canopy shear stress profiles. For all profiles it is

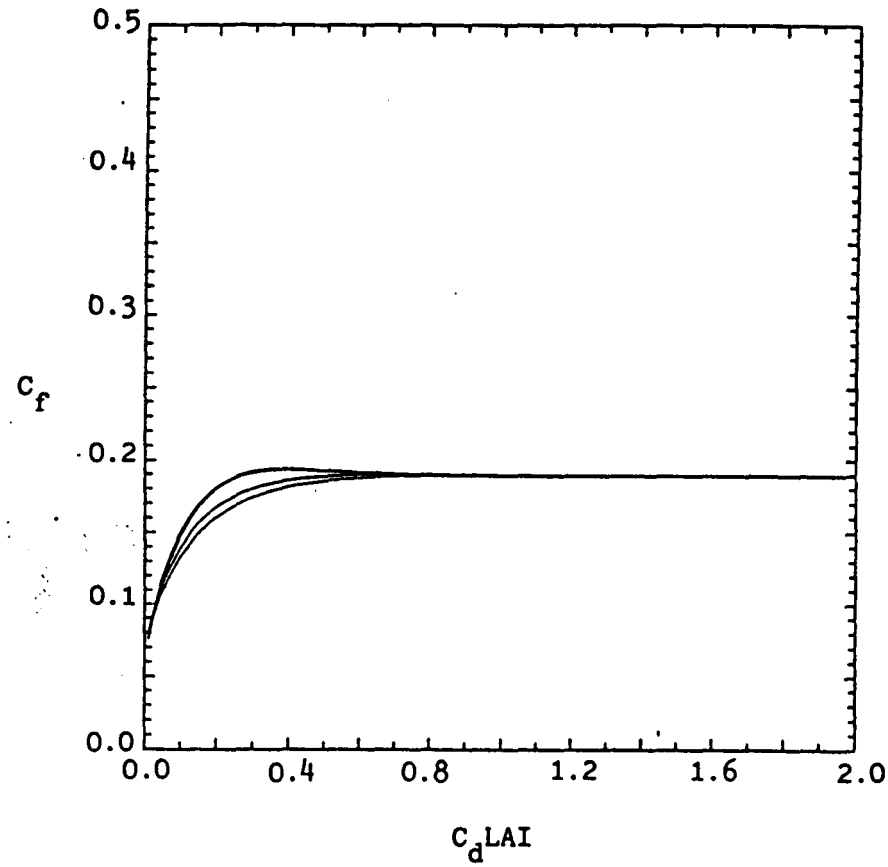

Figure 2.10: Stand drag coefficient as a function of C_dLAI. The upper curve is associated with the cosh wind profile for constant foliage distributions, while the lower three are associated with the triangular distributions with maximum foliage density at ζ = 0.8 (upper), 0.5 (middle), and 0.2 (lower).

assumed that C_dLAI = 0.6. Finally, figure 2.10 shows the stand drag coefficient C_f, and figure 2.11 the normalized displacement height d/h, both as a function of C_dLAI. In all cases a_0/a_1 = 0.1.

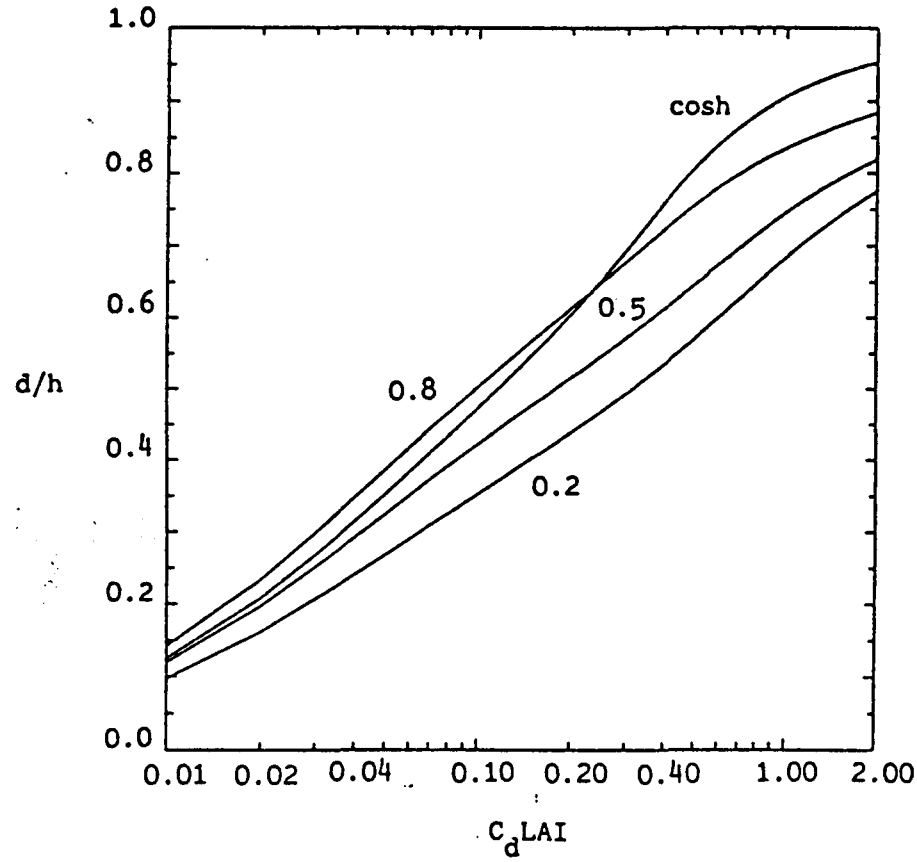

Figure 2.11: Normalized displacement height as a function of C_dLAI for the same foliage distributions as in figure 2.8.

2.3.5. Computation of the roughness length for momentum

In 2.3.2. the existance of a roughness sublayer between the canopy sublayer and the inertial sublayer was assumed. According to Raupach et al. (1980) the diffusivity within the roughness sublayer is assumed to be constant with the height. Then the mean wind speed at the top of the roughness sublayer (where it joins the inertial sublayer) is:

$$u(z_m) = u_h - u* \, g(x_h)/k \qquad (2.32)$$

where $x_h = (h-d)/(z_m-d)$; $g(x_h) = (1-x_h)$; and z_m is the top of the roughness sublayer. At the bottom of the inertial sublayer the mean wind speed is:

$$u(z_m) = u*/k \ln\{ (z_m-d)/z_0 \} \qquad (2.33)$$

Substituting for $u(z_m)$ in (2.32) and solving for z_0/h yields (2.34):

$$\frac{z_0}{h} = \lambda_1 (1 - \frac{d}{h}) \exp\{ -k/\{ (C_f/2)^{1/2} \} \qquad (2.34)$$

where $\lambda_1 = \exp\{-g(x_h)\}/x_h$; and $x_h = 1/\alpha$ as can be derived from equation (2.13).

Garratt (1980) assumed the diffusivity within the roughness sublayer to be linearly related to height, and used an influence function to account for the presence of the roughness sublayer under neutral stability conditions. Massman (1987a) showed that both models result in approximately the same values for the parameter λ_1. In 2.3.2. α was chosen to be 1.5, and consequently $\lambda_1 = 1.075$.

Figure 2.12 shows the normalized roughness length z_0/h as a function of C_dLAI for the three triangular foliage distributions and the constant foliage distribution, associated with the cosh wind speed profile.

2.4. Mutual aerodynamic interference of canopy elements

The exchange of momentum between the atmosphere and plant canopies, consisting of many smaller foliage elements, can be seen as a summation of exchange processes occurring at the surface of these smaller elements. However, Landsberg and Thom (1971) pointed out, that the (total) canopy drag is not necessarily equal to the summed drag upon the canopy elements, due to mutual aerodynamic interference of the individual elements, becoming more and more important as the number of elements in any given volume increases.

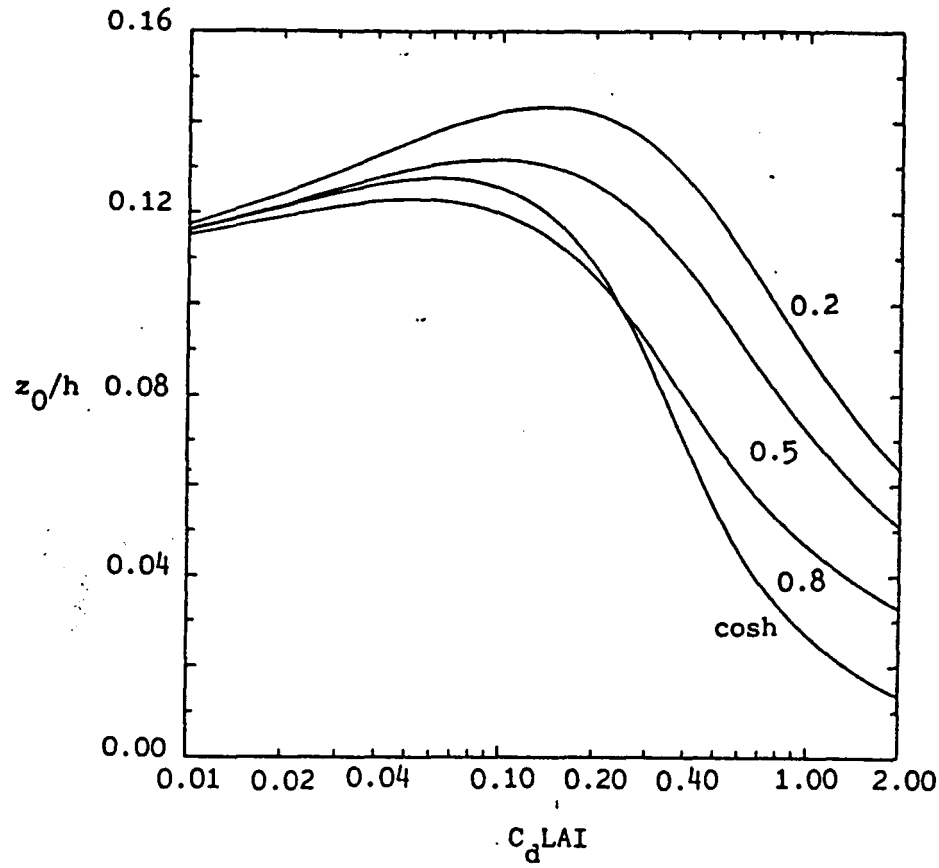

Figure 2.12: Normalized roughness length as a function of C_dLAI for the same foliage distributions as in figure 2.8.

Massman (1987a) hypothesized that for full canopies this shelter effect could be characterized by a narrow range of effective values of C_dLAI: $0.25 \leqslant C_dLAI(\text{effective}) \leqslant 0.50$. Accordingly, the effect of mutual aerodynamic interference is included in the presented model by limiting the maximum effective C_dLAI to a value of 0.5.

The effect of limiting the effective C_dLAI results in constant profile extinction coefficients β, β_I and β_{II} after the product of C_d and LAI exceeds the maximum effective value of C_dLAI. Consequently, also z_0/h and d/h remain fixed.

2.5. Discussion and conclusions

First-order closure methods are used to derive simple analytical expressions for the profiles of mean horizontal wind speed and horizontal shear stress within plant canopies. Although these methods are not able to reproduce observed profiles in detail (especially in the lower part of the vegetation, where e.g. secondary maxima in wind speed might occur), they have the advantage of being computationally much simpler than e.g. second-order closure techniques. For the purposes of this work however, first-order closure most probably provides a good enough representation of the profiles mentioned, at least in the dense foliated layers of the canopy.

The basic assumptions in deriving the model for momentum transfer are: (1) neutral atmospheric stability; (2) a constant value of the drag coefficient C_d throughout the depth of the canopy; (3) similarity between the profiles of mean horizontal wind speed and turbulent diffusivity within the canopy; (4) the presence of a roughness sublayer between the canopy sublayer and the inertial sublayer; (5) the displacement height corresponding to the effective level of mean drag upon the canopy elements. The assumption concerning C_d is probably crucial for the possibility of deriving analytical expressions for the profiles.

Massman (1987a) showed that a lower boundary condition on the mean horizontal wind speed profile of zero shear results in the best fit to observed profiles. As one might expect, the foliage distribution seemed to be important, the triangular distribution giving a better fit than the constant foliage distribution. The triangular distribution associated with the zero shear lower boundary condition on the wind speed also provided the best fit for the shear stress profile. Although model results are presented for a wide range of LAI values, including small values, more research is required in these cases of sparse canopies, because the employed lower boundary conditions might not be appropriate.

The calculated displacement heights are monotonically increasing as the density of the vegetation increases, a result to be expected, because increasing canopy density moves the effective level of mean drag to the

upper part of the canopy. For the same reason, the displacement height increases as the level of maximum foliage density is moved upwards in the canopy, as can be seen in the presented cases for a triangular foliage distribution. From figure 2.6 it seems that a lower boundary condition assuming zero wind speed is inappropriate, since the calculated values for the displacement height are significantly different from the other results presented. The displacement heights for the triangular distributions are in good agreement with those obtained by Shaw and Pereira (1982), based on second-order closure, at least for C_dLAI values larger than 0.2. For smaller values, the values calculated by Shaw and Pereira are up to 0.1 higher at C_dLAI = 0.05, but as already mentioned, more research is required concerning sparse canopies.

The curves for the computed roughness lengths reach a maximum value for values of C_dLAI between 0.05 and 0.18. This is slightly different from values obtained by Shaw and Pereira (1982), their maximum values occurring at a C_dLAI between 0.10 and 0.24. Increasing the foliage density leads to a decrease in roughness length, the exposed surface becoming increasingly smoother to the air flow above. Similarly, having the heighest foliage density in the upper levels of the canopy, results in asmoother surface, and hence a lower roughness length than obtained for a canopy with the heighest foliage density near the bottom, being relatively open at the top. The values for z_0/h computed for these higher foliage densities are in agreement with those of Shaw and Pereira (1982). For foliage densities smaller than those at which the peak values occur, the calculated roughness lengths differ from those obtained by Shaw and Pereira (1982), showing a much smaller decrease with decreasing C_dLAI. However, Dolman (1986) found that the roughness length might be relative insenstive to C_dLAI, at least for a certain region of C_dLAI values, and that is in better agreement with the results shown in figure 2.12.

Following Massman (1987a) mutual aerodynamic interference of foliage elements is included in the model by limiting the range of effective values for full canopies to $0.25 \leq C_dLAI(\text{effective}) \leq 0.50$. However, this being a rather crude assumption, modeling the shelter factor as a function of

foliage distribution seems a more realistic approach, resulting in an aerodynamically more uniform distribution than the observed a(z).

3. TURBULENT TRANSPORT OF SCALAR ADMIXTURES OF THE FLOW WITHIN A CANOPY

3.1. Introduction

In addition to the exchange of momentum, the exchange of scalar quantities, like heat, moisture, CO_2 and air pollutants (e.g. SO_2, O_3 and NO_2), between vegetated surfaces and the atmosphere is of considerable importance. Again, simple one-dimensional turbulent diffusion approaches can be employed, to provide descriptions for these exchange processes, and resistance terms play an important role.

E.g. Thom (1975) pointed out, that momentum transfer to foliage elements is accomplished by a combination of normal pressure forces and molecular skin friction drag, where the former is usually more important than the latter, whereas the simultaneous transfer of heat and mass to or from the elements is restricted to the mechanism of molecular diffusion alone. Therefore, additional to the aerodynamic resistance for momentum exchange, other resistances have to be taken into account to describe the transfer of scalar quantities. Massman (1987b) extended his (1987a) momentum exchange model to include the exchange of heat, by also considering a quasi-laminar leaf boundary-layer resistance. This resistance accounts for the transport of heat by molecular diffusion from the surfaces of the individual foliage elements through the boundary layer associated with each of these individual elements.

Modeling the transfer of other admixtures to or from a plant canopy, again requires accounting for additional transport resistances, as will be outlined in the next section. The attention is mainly directed towards moisture exchange between vegetation and atmosphere, and a transfer equation for water vapor will be derived.

3.2. General considerations

According to Brutsaert (1979), the governing equation for the turbulent transport of any scalar inert admixture (or pollutant) of the flow is

$$\frac{dF}{dz} - S_f = 0 \qquad (3.1)$$

where F is the vertical specific flux of the admixture in the canopy air; and S_f the source (or negative sink) term, resulting from the flux of the admixture to or from the surfaces of the foliage elements.

The transfer of the scalar quantity under consideration can, like in the case of momentum transfer, be described using an eddy diffusivity:

$$F = -\rho K_c \frac{dc}{dz} \qquad (3.2)$$

where K_c is the eddy diffusivity; and $c = c(z)$ is the mean concentration of the admixture in the air surrounding the foliage elements.

The source (or sink) term S_f can be expressed as

$$S_f = a(z)\rho \frac{(c_f(z) - c)}{r_b + r_r} \qquad (3.3)$$

where $r_b = r_b(z)$ is the boundary-layer resistance, accounting for the molecular diffusion of the admixture from the surfaces of the foliage elements through the boundary layer associated with these elements; $c_f(z)$ is the concentration of the admixture in the leaves (or needles). The resistance term $r_r = r_r(z)$ is, when e.g. the transfer of gaseous air pollutants is considered, composed of the stomatal resistance r_s, the mesophyll resistance r_m, and the cuticular resistance r_{cut} (Baldocchi et al., 1987). The stomatal resistance and the mesophyll resistance are in series with each other, while the cuticular resistance acts parallel to

these two resistances (figure 3.1). Stomatal resistance accounts for the molecular diffusion of the admixture from the substomatal cavity to the boundary layer associated with the leaf or needle, while the mesophyll resistance accounts for the transport from substomatal cavity into the mesophyll cells. The cuticular resistance is associated with the uptake at the surface of the leaf.

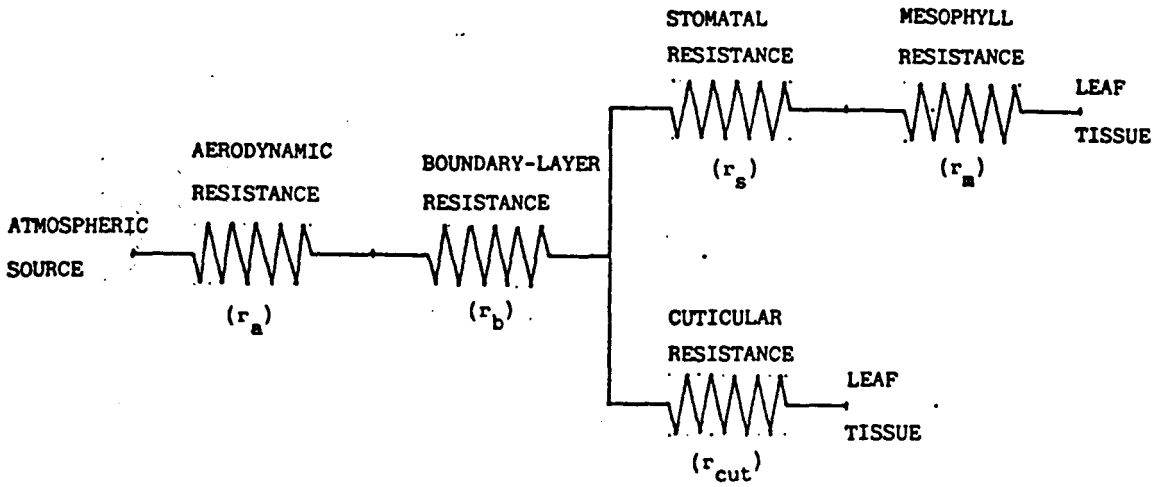

Figure 3.1: Resistances to the transfer of gaseous air pollutants.

For the transfer of water vapor however, the following two assumptions are made: (1) water vapor transport occurs from an always saturated substomatal cavity, and (2) the cuticular resistance to evaporation from leaf tissue is very high compared to the stomatal resistance. Consequently, the resistance term r_r is assumed to be equal to the stomatal resistance r_s. Therefore, modeling the exchange of water vapor between vegetation and atmosphere, the source term S_f can be written as:

$$S_f = a(z) \rho \frac{(c_f - c)}{r_b + r_s} \qquad (3.4)$$

with c_f the concentration of water vapor in the substomatal cavity.

3.3. The transfer equation for water vapor

Substitution of (3.2) and (3.4) in (3.1) yields a second-order differential equation (3.5), describing the transport of water vapor from canopy to atmosphere:

$$\frac{d}{dz}\left[-K_e \frac{de}{dz}\right] - a(z)\,\frac{(e_f - e)}{r_b + r_s} = 0 \qquad (3.5)$$

where $e = e(z)$ is the mean water vapor pressure within the canopy, used instead of the concentration $c(z)$; e_f is the water vapor pressure in the substomatal cavity of the leaves or needles; and K_e is the eddy diffusivity for water vapor.

The boundary-layer resistance can be expressed in terms of a leaf bulk transfer coefficient C_t as follows:

$$r_b = 1/(C_t\, u(z)) \qquad (3.6)$$

According to Brutsaert (1979), but using the mean horizontal wind speed $u(z)$ as a velocity scale, instead of the friction velocity u_*, the leaf bulk transfer coefficient probably has the form

$$C_t = C_1\, Re^{-m}\, Sc^{-n} \qquad (3.7)$$

where C_1, m and n are parameters, which may depend on shape, density and orientation of the foliage elements and on the intensity of the turbulence; $Re = (u(z)\, D/\nu)$ is the local Reynolds number, with D the characteristic dimension of a foliage element (assumed to be constant throughout the depth of the canopy) and ν the molecular viscosity of air; and $Sc = (\nu/\mathcal{E})$, with $\mathcal{E}$ the molecular diffusivity of water vapor in the air.

The determination of values for the parameters C_1, m and n is difficult, because of the complicated structures of most canopies. Brutsaert (1979) presents some conceptual models, based on different assumptions concerning the extent of interaction between the foliage

elements, and the nature of the flow within the boundary layer. Following Massman (1987b), the Pohlhausen model for laminar boundary layers is applied, assuming values of m = 1/2 and n = 2/3. C_1 is assumed to be a constant, and field observations suggest a value for C_1 between 1.0 and 1.2, depending on the structure of the foliage (e.g. Pearman et al., 1972; Gates, 1980).

Therefore, (3.5) can be written as:

$$\frac{d}{dz}\left[K_e \frac{de}{dz}\right] = \frac{-a(z)\ (e_f - e)}{(C_1\ Re^{-1/2}\ Sc^{-2/3}\ u(z))^{-1} + r_s} \qquad (3.8)$$

Finally, some rearranging yields equation (3.9):

$$\frac{d}{dz}\left[K_e \frac{de}{dz}\right] = \frac{-a(z)\ C_t\ u(z)\ (e_f - e)}{1 + r_s\ C_t\ u(z)} \qquad (3.9)$$

with $C_t = C_1\ Re^{-1/2}\ Sc^{-2/3}$.

Applying the same conventions as in 2.2., equation (3.9) can be recast into the following form:

$$\frac{d}{d\zeta}\left[\frac{K_e}{K_m}\ \chi^{1/2}\sigma' \frac{dE}{d\zeta}\right] = \frac{f(\zeta)\ C_t'\ LAI\ \chi^{1/4}\ E}{\mu\ (1 + r_s\ C_t'\ \chi^{1/4}\ u_h)} \qquad (3.10)$$

where $E = e_f - e$ is the water vapor pressure deficit between the (saturated) substomatal cavity and the air surrounding the leaf or needle; and $C_t' = C_1\ Sc^{-2/3}\ Re_h^{-1/2}$ with $Re_h = (u_h\ D/\nu)$. It is assumed that the ratio K_e/K_m is constant, and equal to its value at the top of the canopy, denoted by α_k, requiring the same functional dependence for K_m and K_e on height. Therefore, (3.10) can be written as:

$$\frac{d^2E}{d\zeta^2} + \frac{1}{2}\frac{\chi'}{\chi}\frac{dE}{d\zeta} = \frac{f(\zeta)\ C_t'\ LAI\ \chi^{-1/4}\ E}{\alpha_k\ \sigma'\ \mu\ (1 + r_s\ C_t'\ \chi^{1/4}\ u_h)} \qquad (3.11)$$

The mean horizontal wind speed χ appearing in the denominator of the second term on the left-hand side of (3.11), requires a non-zero wind speed everywhere within the canopy.

4. STOMATAL RESISTANCE

4.1. Introduction

Stomates are pores in the epidermal surface of leaves and needles, typically approximately 10 μm in length and 2 to 7 μm in width. Although stomates cover only approximately 1% of the leaf surface, they are generally able to meet the demand of plants, concerning the exchange of CO_2, O_2 and water vapor with the atmosphere, by adjusting the stomatal aperture.

Opening and closing of stomates (and therefore a change in stomatal resistance) is caused by several environmental and plant physiological parameters: the amount of incident photosynthetically active radiation on the leaf, the vapor pressure deficit between the air in the substomatal cavity and the leaf surrounding air, intercellular CO_2 concentrations, the temperature of the air, and the leaf water potential, the one being of more importance than the other. The stomates respond to these factors by active transport of ions into and out of the so called guard cells, thereby modifying turgidity by changing osmotic concentrations within the cell.

In this chapter a simple model will be presented for the computation of stomatal resistance as a function of height within a canopy, in order to solve the transfer eqation for water vapor (3.11).

4.2. Modeling the stomatal resistance

Several models for stomatal resistance have been suggested in the past, mostly considering the role of some, and sometimes all, of the above mentioned resistance determining parameters.

Jarvis (1976) hypothesized a model for the stomatal conductance g_s ($= 1/r_s$), taking into account its dependence on photon flux density Q_p, leaf temperature T, vapor pressure deficit E, leaf water potential ψ_l,

and ambient air CO_2 concentration C_a, of the form

$$g_s(Q_p,T,E,\psi_1,C_a) = g_{s1}(Q_p)\, g_{s2}(T)\, g_{s3}(E)\, g_{s4}(\psi_1)\, g_{s5}(C_a) \qquad (4.1)$$

assuming no synergistic interactions, and providing submodels for the dependence of the stomatal conductance on each single variable.

The model proposed by Avissar and Mahrer (1982) is given in (4.2), where $g_{s,min}$ is the minimal conductance, occurring only through leaf cuticle when the stomates are closed, and $g_{s,max}$ is the maximal stomatal conductance, occurring when the stomates are completely opened.

$$g_s = g_{s,min} + (g_{s,max}-g_{s,min})\, g_{s1}(R)g_{s2}(T)g_{s3}(E)g_{s4}(\psi_s)g_{s5}(C_a) \qquad (4.2)$$

The functions g_{si} provide the dependence on solar global radiation (R), leaf temperature (T), vapor pressure deficit (E), ambient air CO_2 concentration (C_a) and soil water potential (ψ_s), and are all given by the mathematical expression

$$g_{si} = 1/\{1 + \exp[-S(X_i-b)]\} \qquad (4.3)$$

with different values for S and b, depending on the parameter under consideration, X_i being the intensity of this parameter.

Kaufmann (1982) proposed that the photosynthetic photon flux density (PPFD) and the absolute humidity difference from leaf to air (DAH) are the most important factors determining the stomatal conductance for plants growing in their natural environment. The other factors mentioned, play a secondary role, except when plants are considered growing outside their natural range. His "Two-Factor Model of Leaf Conductance" is given in (4.4), b_1, b_2 and b_3 being species dependent parameters, based on experimental data.

$$g_s = b_1(\sqrt{PPFD}/\sqrt{DAH}) + b_2(\sqrt{PPFD}/DAH) + b_3(\sqrt{PPFD}/DAH^2) \qquad (4.4)$$

Therefore, making the restriction of dealing with plants in their natural range, the stomatal resistance is assumed to be a function of photosynthetic photon flux density and vapor pressure deficit only, i.e. $r_s = f(PPFD,E)$. The form of the proposed model however, is chosen to be similar to the model of Jarvis (1976):

$$r_s(PPFD,E) = r_s(PPFD)\ r_s(E) \qquad (4.5)$$

The dependence of the stomatal resistance on photosynthetic photon flux density is often described, using a relationship based on simple Michaelis-Menten kinetics for the process of photosynthesis (e.g. Jarvis, 1976; Sellers, 1985). Smith (1937, 1938) however, noted that the region of CO_2 and PPFD-saturated conditions is reached more rapidly than would be expected using Michaelis-Menten kinetics. Gates et al. (1985) present a net photosynthesis model, using the empirical relation suggested by Smith, and their equation (2) describes the CO_2-saturated response of the rate of photosynthesis to various levels of PPFD. Now, assuming that

$$\frac{P_m}{P_{ml}} = \frac{r_{s,min}}{r_s} \qquad (4.6)$$

where P_{ml} is the PPFD and CO_2-saturated rate of photosynthesis; P_m is the CO_2-saturated rate of photosynthesis at a particular PPFD; r_s is the stomatal resistance at this particular PPFD; and $r_{s,min}$ is the minimal stomatal resistance, occurring under PPFD-saturated conditions, the following relation is proposed:

$$r_s(PPFD) = r_{s,min}\ \{(B^2/PPFD^2) + 1\}^{1/2} \qquad (4.7)$$

where B is a constant depending on plant species.

Stomatal response to vapor pressure deficit E is modeled following Jarvis (1976), assuming a linear increase of resistance with increasing vapor pressure deficit. Although, the leaves or needles within a canopy are exposed to varying values of E with height, it is assumed that all the

leaves or needles respond to a "canopy value" of the vapor pressure deficit (Choudbury and Monteith, 1986). This "canopy value" is chosen to be equal to the deficit at the top of the canopy, E_1 (= $E(\zeta=1)$). Consequently, equation (4.8) describes the proposed stomatal response to vapor pressure deficit:

$$r_s(E) = 1/\{1 - (A\ E_1)\} \qquad (4.8)$$

where is A is constant depending on species.

Therefore, substitution of (4.7) and (4.8) in (4.5) results in the model for stomatal resistance, used throughout this work:

$$r_s = r_{s,min}\ \frac{\{(B^2/PPFD^2) + 1\}^{1/2}}{\{1 - (A\ E_1)\}} \qquad (4.9)$$

Following Choudbury and Monteith (1986), A is chosen to be equal to 0.15 kPA^{-1} for annual deciduous forest and 0.30 kPa^{-1} for coniferous forest, and the corresponding values for $r_{s,min}$ are 100 s/m and 1000 s/m, respectively. According to Massman (personal communication) the values for B are 10 $\mu E\ m^{-2}s^{-1}$ for deciduous forest and 100 $\mu E\ m^{-2}s^{-1}$ for coniferous forest.

4.3. The attenuation of radiation within a canopy

For the computation of the stomatal resistance at different levels within the canopy, using (4.9), a description of the photosynthetic photon flux density as a function of height is required. Sophisticated models for the attenuation of radiation within canopies are available (e.g. Suits, 1972; Goudriaan, 1977; Kimes, 1984), but their complexity makes the calculations rather time consuming, and therefore expensive. For the purposes of this work a simple model is probably sufficient.

Monsi and Saeki (1953) described the attenuation of direct beam radiation, incident on a canopy of randomly distributed foliage elements, using a zero-scattering approach, given in (4.10):

$$PPFD(\zeta) = PPFD_0 \exp(-g_1 L) \qquad (4.10)$$

where $PPFD_0$ is the PPFD at the top of the canopy; g_1 is an empirical constant depending on plant species; and L is the accumulated leaf area from the top of the canopy (= 1) down to , i.e.:

$$L = \int_{\zeta}^{1} a(\zeta)\, d\zeta \qquad (4.11)$$

Goudriaan (1977) included scattering in the above model by defining the light extinction coefficient g_1 being

$$g_1 = G(\delta)\ (1 - \omega)^{1/2} \qquad (4.12)$$

for small values of the scattering coeffcient ω ($\omega \leq 0.2$, for photosynthetically active radiation). In (4.12) δ is the cosine of the zenith angle of the incident beam of radiation; $G(\delta)$ is the relative projected area of the foliage elements in the direction $\cos^{-1}\delta$. $\delta = \sin\varphi$, with φ the solar elevation angle.

Several works (Ross and Nilson, 1965; Warren Wilson, 1967; Anderson, 1970; Kuroiwa, 1970) give an analysis of the term $G(\delta)/\sin\varphi$. Assuming a constant inclination of leaves, an uniform distribution of azimuth orientation, and a spherical leaf distribution, e.g. Ross (1975) provides:

$$\frac{G(\delta)}{\sin\varphi} = \frac{1}{2 \sin\varphi} \qquad (4.13)$$

Following Sellers (1985), no distinction is made between leaves or needles exposed to full sunlight and those in shade regions. Consequently,

equation (4.14) describes the photosynthetic photon flux density as a function of height within the canopy:

$$PPFD(\zeta) = PPFD_0 \exp[\, -(1-\omega)^{1/2} L/(2 \sin\varphi)] \qquad (4.14)$$

Figures 4.1 and 4.2 show the PPFD as a function of ζ for a constant foliage distribution and three triangular distributions. The flux density at the top of the canopy is assumed to be 1000 μE $m^{-2}s^{-1}$, the solar elevation angle is set to be 30^o in figure 4.1, and 90^o in figure 4.2, and the scattering coefficient $\omega = 0.175$ (Dickinson, 1983).

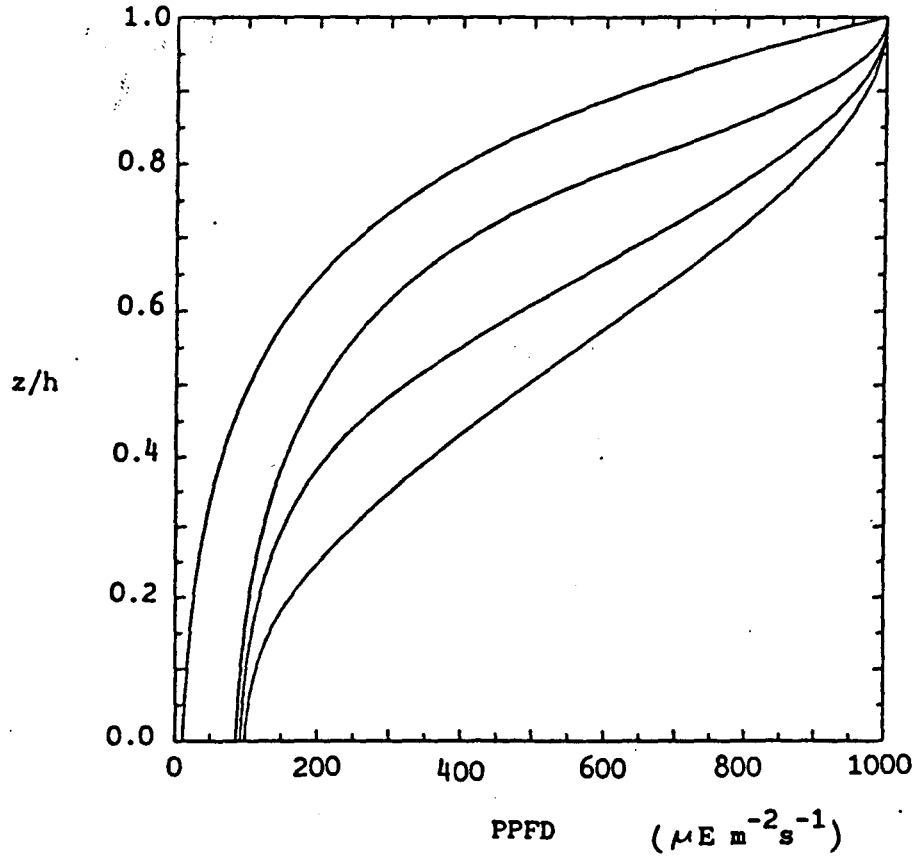

Figure 4.1: Photosynthetic photon flux density as a function of height within the canopy. The upper curve is associated with the constant foliage distribution, while the lower three are associated with triangular distributions with the level of maximum foliage density at ζ = 0.8 (upper), 0.5 (middle) and 0.2 (lower). a_0/a_1 = 0.1, LAI = 5, and $\varphi = 30^o$.

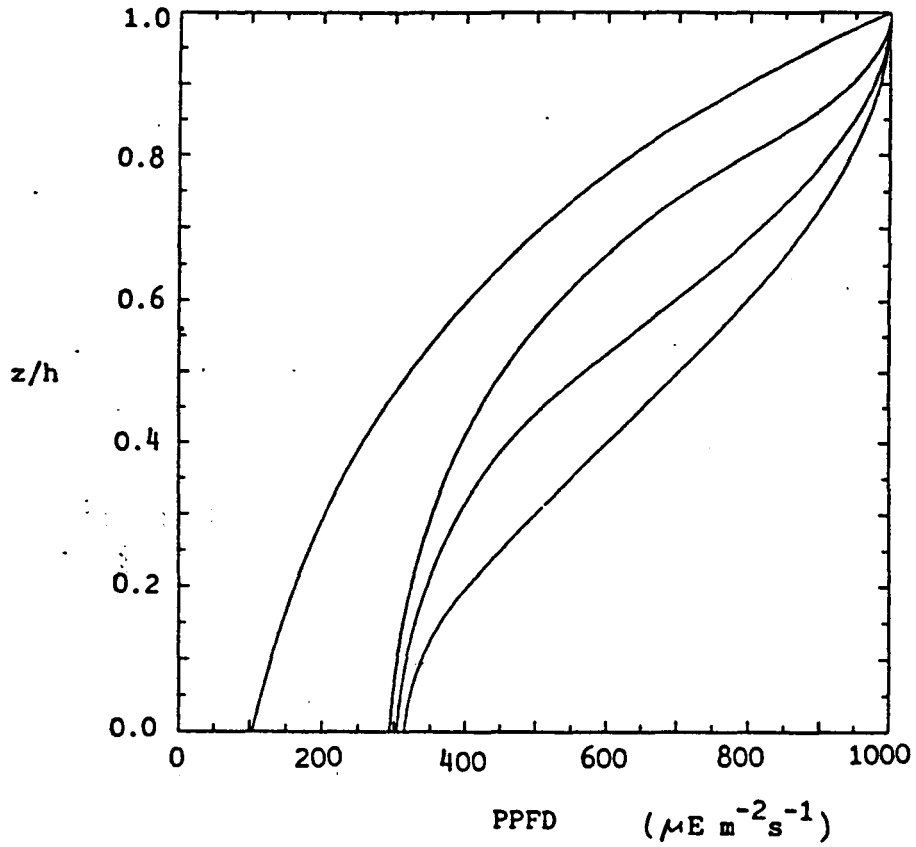

Figure 4.2: Photosynthetic photon flux density as a function of height within the canopy for the same foliage distributions as shown in figure 4.1. a_0/a_1 = 0.1, LAI = 5, and φ= 90°.

5. SOLVING THE TRANSFER EQUATION FOR WATER VAPOR

5.1. Introduction

To solve the second-order differential equation (3.11), first of all boundary conditions have to be defined at the bottom and top of the canopy. A numerical method, a so called "relaxation method", will be applied to obtain a solution. For this purpose, the second-order differential equation is replaced by two coupled first-order differential equations, which, on their turn, are replaced by finite difference equations. Initial guesses of the solution to (3.11) for the constant and triangular foliage distribution, obtained by making simplifying assumptions, are then iteratively improved to satisfy the exact transfer equation for water vapor.

5.2. Boundary conditions

At the top of the canopy a constant vapor pressure deficit E (= e_f-e) is assumed, which is not affected by the exchange of heat and moisture between the canopy and the atmosphere:

$$E(\zeta = 1) = E_1 = \text{constant} \qquad (5.1)$$

Massman (1987b), describing the transfer of heat to and from a canopy, assumed that the flow is interacting mainly with the upper part of the canopy, using a lower boundary condition of the form $\lim_{\zeta \to -\infty} \Theta(\zeta) = 0$, where $\Theta = (T_f-T)/(T_f-T_h)$. $T = T(\zeta)$ is the mean atmospheric temperature within the canopy; T_f is the foliage temperature; and T_h is the temperature at the top of the canopy. However, since the transfer equation for water vapor will be solved numerically, it is impossible to apply a similar lower boundary condition to (3.11). Therefore, a different

lower boundary condition must be used. In (5.2) this alternative condition, equivalent with assuming the presence of a soil moisture flux, which vanishes for large values of LAI, is given.

$$\left.\frac{dE}{d\zeta}\right|_{\zeta=0} = E'_0 = g_2 \exp(-g_1 \, LAI) \qquad (5.2)$$

where g_1 is the light extinction coefficient (see equation (4.12); and g_2 is a parameter.

5.3. Applying the relaxation method

The second-order differential equation (3.11) can be replaced by two coupled first-order differential equations as follows:

$$\frac{dE}{d\zeta} = W \qquad (5.3a)$$

$$\frac{dW}{d\zeta} + \frac{1}{2}\frac{\chi'}{\chi} W = \frac{f(\zeta)\, C_t' \, LAI \, \chi^{-1/4} \, E}{\alpha_k \sigma \mu (1 + r_s(\zeta)\, C_t' \, \chi^{1/4} \, u_h)} \qquad (5.3b)$$

A mesh is defined within the canopy consisting of M points, ζ_1 to ζ_M, where ζ_1 corresponds to the bottom of the canopy, and therefore is 0, while ζ_M represents the top of the canopy, being equal to 1.

The first-order differential equations can be replaced by (approximate) finite difference equations of the form

$$D_{1,k} = E_k - E_{k-1} - 0.5\,(\zeta_k - \zeta_{k-1})\,(W_k + W_{k-1}) \qquad (5.4a)$$

$$D_{2,k} = W_k - W_{k-1} - 0.5\,(J_k - J_{k-1})\,(a_k(W_k + W_{k-1}) + b_k(E_k + E_{k-1}) \qquad (5.4b)$$

where $D_{1,k} = D_{2,k} = 0$; $k = 2, 3, \ldots\ldots, M-1, M$; and

$$a_k = -0.5\,\frac{\chi'(0.5\,(J_k+J_{k-1}))}{\chi\,(0.5\,(J_k+J_{k-1}))}$$

$$b_k = \frac{f(0.5(J_k+J_{k-1}))\;C_t'\;LAI\;\chi(0.5(J_k+J_{k-1}))^{-1/4}}{\alpha_k\sigma\mu(1 + r_s(0.5(J_k+J_{k-1}))\;C_t'\chi(0.5(J_k+J_{k-1}))^{1/4}\;u_h)}$$

The finite difference equations for $D_{1,k}$ and $D_{2,k}$ couple 4 variables, i.e. E_k, E_{k-1}, W_k and W_{k-1} at two mesh points J_k and J_{k-1}. (5.4) provides 2(M-1) equations for 2M unknowns, the remaining 2 equations being provided by the boundary conditions:

$$D_{1,M+1} = E_{k=M} - E_{J=1} \qquad (5.5a)$$

$$D_{2,1} = W_{k=1} - E'_{J=0} \qquad (5.5b)$$

Press et al. (1986) provide an algorithm for determining the values of the variables E_k and W_k for $k = 1, 2, \ldots, M$. This algorithm requires initial guesses for E_k and W_k, which will be discussed in section 5.4. Assuming the initial guesses have been provided, the next step is to determine increments ΔE_k and ΔW_k such that $E_k+\Delta E_k$ and $W_k+\Delta W_k$ are improved approximations to the desired solution.

Expanding the finite difference equations (5.4) and (5.5) in first-order Taylor series results in equations for the increments at the interior points:

$$D_{1,k}(E_k+\Delta E_k, E_{k-1}+\Delta E_{k-1}, W_k+\Delta W_k, W_{k-1}+\Delta W_{k-1}) \approx$$

$$D_{1,k}(E_k, E_{k-1}, W_k, W_{k-1}) + \frac{\partial D_{1,k}}{\partial E_k}\Delta E_k + \frac{\partial D_{1,k}}{\partial E_{k-1}}\Delta E_{k-1}$$
$$+ \frac{\partial D_{1,k}}{\partial W_k}\Delta W_k + \frac{\partial D_{1,k}}{\partial W_{k-1}}\Delta W_{k-1} \qquad (5.6a)$$

$$D_{2,k}(E_k+\Delta E_k, E_{k-1}+\Delta E_{k-1}, W_k+\Delta W_k, W_{k-1}+\Delta W_{k-1}) \approx$$

$$D_{2,k}(E_k, E_{k-1}, W_k, W_{k-1}) + \frac{\partial D_{2,k}}{\partial E_k}\Delta E_k + \frac{\partial D_{2,k}}{\partial E_{k-1}}\Delta E_{k-1}$$
$$+ \frac{\partial D_{2,k}}{\partial W_k}\Delta W_k + \frac{\partial D_{2,k}}{\partial W_{k-1}}\Delta W_{k-1} \qquad (5.6b)$$

and at the boundaries:

$$D_{1,M+1}(E_M+\Delta E_M, W_M+\Delta W_M) \approx D_{1,M+1}(E_M, W_M)$$
$$+ \frac{\partial D_{1,M+1}}{\partial E_M}\Delta E_M + \frac{\partial D_{1,M+1}}{\partial W_M}\Delta W_M \qquad (5.7a)$$

$$D_{2,1}(E_1+\Delta E_1, W_1+\Delta W_1) \approx D_{2,1}(E_1, W_1)$$
$$+ \frac{\partial D_{2,1}}{\partial E_1}\Delta E_1 + \frac{\partial D_{2,1}}{\partial W_1}\Delta W_1 \qquad (5.7b)$$

Now, the requirement for a solution is that the terms on the left-hand side of equations (5.7a) and (5.7b) are equal to zero. Consequently, the set of equations can be written as

$$-D_{1,k}(E_k, E_{k-1}, W_k, W_{k-1}) = R_{1,k}\Delta E_k + R_{1,k-1}\Delta E_{k-1}$$
$$+ S_{1,k}\Delta W_k + S_{1,k-1}\Delta W_{k-1} \qquad (5.8a)$$

$$-D_{2,k}(E_k,E_{k-1},W_k,W_{k-1}) = R_{2,k}\Delta E_k + R_{2,k-1}\Delta E_{k-1} + S_{2,k}\Delta W_k + S_{2,k-1}\Delta W_{k-1} \qquad (5.8b)$$

at the interior points of the mesh, and

$$-D_{1,M+1}(E_M,W_M) = U_{1,M}\Delta E_M + V_{1,M}\Delta W_M \qquad (5.9a)$$

$$-D_{2,1}(E_1,W_1) = U_{2,1}\Delta E_1 + V_{2,1}\Delta W_M \qquad (5.9b)$$

at the boundaries, where

$$R_{1,x} = \frac{\partial D_{1,k}}{\partial E_x} \quad S_{1,x} = \frac{\partial D_{1,k}}{\partial W_x} \quad R_{2,x} = \frac{\partial D_{2,k}}{\partial E_x} \quad S_{2,x} = \frac{\partial D_{2,k}}{\partial W_x}$$

$$U_{1,M} = \frac{\partial D_{1,M+1}}{\partial E_M} \quad V_{1,M} = \frac{\partial D_{1,M+1}}{\partial W_M} \quad U_{2,1} = \frac{\partial D_{2,1}}{\partial E_1} \quad V_{2,1} = \frac{\partial D_{2,1}}{\partial W_M}$$

The values of these coefficients are obtained by differentiating equations (5.4) and (5.5), yielding:

$R_{1,k} = 1$ $\qquad$ $R_{1,k-1} = -1$

$S_{1,k} = -0.5(\int_k - \int_{k-1})$ $\qquad$ $S_{1,k-1} = S_{1,k}$

$R_{2,k} = -0.5\,(\int_k - \int_{k-1})\,b_k$ $\qquad$ $R_{2,k-1} = R_{2,k}$

$S_{2,k} = -0.5(\int_k - \int_{k-1})\,a_k + 1$ $\qquad$ $S_{2,k-1} = -0.5(\int_k - \int_{k-1})\,a_k - 1$

$U_{1,M} = 1$ $\qquad$ $U_{2,1} = 0$

$V_{1,M} = 0$ $\qquad$ $V_{2,1} = 1$

Now, the set of 2M linear equations can be written in matrix form as follows:

$$\begin{pmatrix} X & X & 0 & 0 & 0 & 0 & \cdots & 0 & 0 & 0 & 0 & 0 & 0 \\ X & X & X & X & 0 & 0 & \cdots & 0 & 0 & 0 & 0 & 0 & 0 \\ X & X & X & X & 0 & 0 & \cdots & 0 & 0 & 0 & 0 & 0 & 0 \\ 0 & 0 & X & X & X & X & \cdots & 0 & 0 & 0 & 0 & 0 & 0 \\ 0 & 0 & X & X & X & X & \cdots & 0 & 0 & 0 & 0 & 0 & 0 \\ \cdot & \cdot & \cdot & \cdot & \cdot & \cdot & \cdots & \cdot & \cdot & \cdot & \cdot & \cdot & \cdot \\ \cdot & \cdot & \cdot & \cdot & \cdot & \cdot & \cdots & \cdot & \cdot & \cdot & \cdot & \cdot & \cdot \\ 0 & 0 & 0 & 0 & 0 & 0 & \cdots & X & X & X & X & 0 & 0 \\ 0 & 0 & 0 & 0 & 0 & 0 & \cdots & X & X & X & X & 0 & 0 \\ 0 & 0 & 0 & 0 & 0 & 0 & \cdots & 0 & 0 & X & X & X & X \\ 0 & 0 & 0 & 0 & 0 & 0 & \cdots & 0 & 0 & X & X & X & X \\ 0 & 0 & 0 & 0 & 0 & 0 & \cdots & 0 & 0 & 0 & 0 & X & X \end{pmatrix} \begin{pmatrix} Y \\ Y \\ Y \\ Y \\ Y \\ \cdot \\ \cdot \\ Y \\ Y \\ Y \\ Y \\ Y \end{pmatrix} = \begin{pmatrix} Z \\ Z \\ Z \\ Z \\ Z \\ \cdot \\ \cdot \\ Z \\ Z \\ Z \\ Z \\ Z \end{pmatrix} \quad (5.10)$$

where the elements X of the (2M x 2M) matrix correspond with the coefficients of the finite difference equations, the elements Y of the 2M vector on the left-hand side represent the increments ΔE and ΔW, and the elements Z of the 2M vector on the right-hand side are equal to the differences $-D_{1,x}$ and $-D_{2,x}$. The 1 x 2 block in the top left-hand corner of the matrix comes from the upper boundary condition, while the one in the bottom right-hand corner results from the lower-boundary condition. The 2 x 4 blocks each correspond to an interior point of the mesh.

Therefore, knowing the values of the coefficients X in the matrix, and the values of each Z from (5.8) and (5.9), values of all increments Y can be determined.

A special Gaussian elimination procedure is used, which takes advantage of the special structure of the matrix, to minimize (1) the total number of operations, and (2) the storage of matrix coefficients by packing the elements in a special blocked structure. This elimination procedure yields (5.11).

$$\begin{pmatrix} 1 & X' & 0 & 0 & 0 & 0 & \cdots & 0 & 0 & 0 & 0 & 0 & 0 \\ 0 & 1 & 0 & X' & 0 & 0 & \cdots & 0 & 0 & 0 & 0 & 0 & 0 \\ 0 & 0 & 1 & X' & 0 & 0 & \cdots & 0 & 0 & 0 & 0 & 0 & 0 \\ 0 & 0 & 0 & 1 & 0 & X' & \cdots & 0 & 0 & 0 & 0 & 0 & 0 \\ 0 & 0 & 0 & 0 & 1 & X' & \cdots & 0 & 0 & 0 & 0 & 0 & 0 \\ \cdots & & & & & & & & & & & & \cdots \\ \cdots & & & & & & & & & & & & \cdots \\ 0 & 0 & 0 & 0 & 0 & 0 & \cdots & 0 & 1 & 0 & X' & 0 & 0 \\ 0 & 0 & 0 & 0 & 0 & 0 & \cdots & 0 & 0 & 1 & X' & 0 & 0 \\ 0 & 0 & 0 & 0 & 0 & 0 & \cdots & 0 & 0 & 0 & 1 & 0 & X' \\ 0 & 0 & 0 & 0 & 0 & 0 & \cdots & 0 & 0 & 0 & 0 & 1 & X' \\ 0 & 0 & 0 & 0 & 0 & 0 & \cdots & 0 & 0 & 0 & 0 & 0 & 1 \end{pmatrix} \begin{pmatrix} Y \\ Y \\ Y \\ Y \\ Y \\ \cdots \\ \cdots \\ Y \\ Y \\ Y \\ Y \\ Y \end{pmatrix} = \begin{pmatrix} Z' \\ Z' \\ Z' \\ Z' \\ Z' \\ \cdots \\ \cdots \\ Z' \\ Z' \\ Z' \\ Z' \\ Z' \end{pmatrix} \quad (5.11)$$

where X' and Z' represent the adjusted values of X and Z.

Consequently, backsubstitution provides the values for the increments Y. Starting with the bottom row and working up towards the top, each step defines one unknown in terms of known quantities.

The calculated corrections ΔE and ΔW at all mesh points k = 1, 2, ..., M are then applied to the corresponding E_k and W_k, resulting in an improvement of the solution to (3.11). New values of $-D_{1,x}$ and $-D_{2,x}$ can be calculated, and again increments can be determined. This iterative procedure is continued until the increments are considered sufficiently small.

5.4. Initial guesses for the profiles of E and W

5.4.1. Constant foliage distributions

In order to obtain an initial guess for the profiles of E and W, when considering constant foliage distributions, it is assumed that (1) $r_s = r_{s,min}$ at all levels within the canopy, (2) the within-canopy profile for the mean horizontal wind speed is exponential (see equation

(2.18)), and (3) the term $r_s\, C_t'\, \lambda^{1/4}\, u_h >> 1$. Consequently, equation (3.11) can be written as

$$\frac{d^2E}{d\zeta^2} + \frac{1}{2}\beta\frac{dE}{d\zeta} = \frac{C_t'\ LAI\ \exp[0.5\,\beta(1-\zeta)]\ E}{\alpha_k\,\sigma\ r_{s,min}\ C_t'\ u_h} \qquad (5.12)$$

because $f(\zeta) = 1$ and $\mu = 1$. Introducing the constants $C_1 = -\beta/2$, $C_2 = C_t'\ LAI/(\alpha_k\,\sigma\ r_{s,min}\ C_t'\ u_h)$, and $N = \beta/2$ yields

$$\frac{d^2E}{d\zeta'^2} + C_1\frac{dE}{d\zeta'} - C_2\, e^{N\zeta'}\, E = 0 \qquad (5.13)$$

where $\zeta' = (1 - \zeta)$.

Brutsaert (1979) showed that the solutions to (5.13) are related to the modified Bessel functions I_λ and K_λ, where λ denotes the order of these Bessel functions. Then

$$E = e^{-C1\zeta'/2}\ \{\ C_3\ I_1(e^{N\ \zeta'/2}\ [4\ C_2]^{1/2}/N) + C_4\ K_1(e^{N\ \zeta'/2}\ [4\ C_2]^{1/2}/N)\ \} \qquad (5.14)$$

where I_1 and K_1 are the modified Bessel functions of the order 1. C_3 and C_4 have to be determined by applying the boundary conditions. Using (5.1) and (5.2) for the upper and lower boundary respectively, gives

$$C_4 = \{\ E'_0\ C_2^{-1/2}\ e^{C1/2}\ e^{-N/2}\ I_1([2\ C_2^{1/2}/N) + I_0(e^{N/2}\ 2\ C_2^{1/2}/N)\ \}\ /\ \{\ K_1(2\ C_2^{1/2}/N)\ I_0(e^{N/2}\ 2\ C_2^{1/2}/N) + I_1(2\ C_2^{1/2}/N)\ K_0(e^{N/2}\ 2\ C_2^{1/2}/N)\ \} \qquad (5.15a)$$

$$C_3 = \{ E_1 - C_4 K_1(2 C_2^{1/2}/N) \} / I_1(2 C_2^{1/2}/N) \qquad (5.15b)$$

with I_0 and K_0 representing the modified Bessel functions of the order 0.

The initial guess for W is obtained by simply differentiating (5.14):

$$W = e^{-C1 \xi'/2} C_2^{1/2} e^{N \xi'/2} \{ -C_3 I_0(e^{N \xi'/2} [4 C_2]^{1/2}/N) + C_4 K_0(e^{N \xi'/2} [4 C_2]^{1/2}/N) \} \qquad (5.16)$$

5.4.2. Triangular foliage distributions

Massman's (1987b) analytical solution to the transfer equation for heat is used to provide initial guesses for the profiles of $\dot{E}$ and W, for the triangular foliage distributions.

The transfer equation for heat is given by (5.17):

$$\frac{d^2\Theta}{d\xi^2} + \frac{1}{2}\frac{\chi'}{\chi}\frac{d\Theta}{d\xi} = \frac{C_t'' \, LAI}{\alpha_k' \, \sigma \mu} \chi^{-1/4} f(\xi) \Theta \qquad (5.17)$$

where $\Theta = (T_f - T)/(T_f - T_h)$; $T = T(\xi)$ is the mean atmospheric temperature within the canopy; T_f is the foliage temperature; T_h is the temperature at the top of the canopy; C_t'' is the leaf bulk transfer coefficient for heat; and α_k' is equal to K_m/K_h, with K_h the eddy diffusivity for heat.

Using the transformation $\Theta(\xi) = y(\xi) \, h(\xi)$, with $h(\xi)$ chosen to be equal to $\chi^{-1/4}$, yields

$$\frac{d^2y}{d\xi^2} = \left\{ -\frac{3}{16}\left[\frac{\chi'}{\chi}\right]^2 + \frac{1}{4}\left[\frac{\chi''}{\chi}\right] + \delta \chi^{-1/4} f(\xi) \right\} y \qquad (5.18)$$

with $\delta = C_t'' \, LAI/(\alpha_k' \sigma \mu)$.

Using the approximations $\chi^{-1/4} = 1$, $3/16 \, (\chi'/\chi)^2 = \beta_I^3 \, \zeta'/8$ in the layer above the level of maximum foliage density, and $3/16 \, (\chi'/\chi)^2 = \beta_{II}^3 \, \zeta''/8$ below this level, and substituting from (2.24) for χ''/χ gives

$$\frac{d^2y}{d\zeta'^2} = [0.125 \, \beta_I^3 + \delta/(1-\zeta_m)] \, \zeta' \, y \quad \text{if } \zeta_m \leq \zeta \leq 1 \tag{5.19a}$$

$$\frac{d^2y}{d\zeta''^2} = \left[0.125 \, \beta_{II}^3 + \frac{\delta/\zeta_m}{(1-a_0/a_1)^2}\right] \zeta'' \, y \quad \text{if } 0 \leq \zeta \leq \zeta_m \tag{5.19b}$$

where ζ', ζ'', β_I, and β_{II} are defined in 2.3.4.

The solutions to (5.19) are again related to Airy functions (e.g. Abramowitz and Stegun, 1964). Massman (1987b) applied $y(1) = 1$ at the upper boundary, and $\lim_{\zeta \to -\infty} \Theta(\zeta) = 0$ at the lower boundary, implying that the flow interacts mainly with the upper portion of the canopy, to obtain a solution for $y(\zeta)$. $\Theta(\zeta)$ is then simply $y(\zeta) \, \chi^{-1/4}$.

The initial guess for $E(\zeta)$ is now obtained by substituting C_t' for C_t'' and α_k for α_k' in the above equations, and correcting the profile for the different upper boundary condition:

$$E = E_1 \, y(\zeta) \, \chi^{-1/4} = E_1 \, \Theta(\zeta) \tag{5.20}$$

Finally, it can be derived that the initial guess for $W(\zeta)$ is given by (5.21).

$$W = E_1 \, [\, y' - 0.25 \, (\chi'/\chi) \, y \,] \, \chi^{-1/4} \tag{5.21}$$

6. CANOPY BULK EXCHANGE COEFFICIENTS FOR WATER VAPOR

6.1. Introduction

In chapter 3 it has already been mentioned, that the transfer of heat and mass to the surfaces of leaves and needles depends on molecular diffusion alone, while momentum transfer is accomplished mainly by normal pressure forces (or bluff-body effects) acting on the individual foliage elements.

Owen and Thomson (1963) introduced the dimensionless surface Stanton number B as a measure for the discrepancy between the aerodynamic resistance for momentum exchange, and the aerodynamic resistance for heat or mass exchange. Chamberlain (1966) derived, that B could be expressed as a function of z_0, the surface roughness length for momentum, and z_{0s}, the surface roughness length for heat or mass, as follows:

$$k\,B^{-1} = \ln [z_0/z_{0s}] \qquad (6.1)$$

with k the von Karman constant.

Following e.g. Garratt and Hicks (1973), Brutsaert (1979) and Kondo and Kawanaka (1986), the term kB^{-1} will be used to represent the canopy bulk transfer coefficient for the exchange of scalar quantities. Therefore, in the following sections an expression will be derived for the scalar roughness length z_{0s}, associated with water vapor, and for kB^{-1}, and calculated values of kB^{-1} for a number of cases will be presented.

6.2. Derivation of an expression for kB^{-1}

In defining the scalar roughness length z_{0s} the basic assumption made is, that the exchange of momentum and water vapor are symmetric except for their associated roughness lengths, which implies a difference in effectiveness of the surface in the removal of momentum from and the

release of water vapor into the air stream. Therefore, similar to the case of momentum exchange, the presence of a roughness sublayer is assumed between the canopy sublayer and the inertial sublayer. The assumed similarity implies, that (1) the displacement heights for momentum, d, and for water vapor, d_s, are the same; (2) the depth of the roughness sublayer for momentum and water vapor are equal, because K_e shows the same dependence on height as K_m throughout the depth of the roughness sublayer; and (3) the turbulent diffusivity for water vapor at the top of the canopy (i.e. $K_e(h)$) is larger than its logarithmic extrapolation from the inertial sublayer. Consequently, α_k is set equal to 1.

The mean vapor pressure at the top of the roughness sublayer (where it joins the inertial sublayer) is:

$$e(z_m) = e_h - \frac{F_{e,h}\ g(x_h)}{\rho\, u_* \,k} \qquad (6.2)$$

where z_m is the top of the roughness sublayer; and h the top of the canopy (see also 2.3.5.). $F_{e,h}$ is equivalent with the moisture flux at the top of the canopy, and is given by

$$F_{e,h} = \sigma \rho\, u_h\, (e_f - e_h)\, (dE/df)_{f=1}/E_1 \qquad (6.3)$$

At the bottom of the inertial sublayer the mean vapor pressure is:

$$e(z_m) = e_f - \frac{F_{e,h}}{\rho\, u_* \,k} \ln\left[(z_m - d)/z_{0s}\right] \qquad (6.4)$$

Substituting for e_h in (6.2) from (6.3), and combining the result with (6.4) gives

$$\ln\left[(z_m - d)/z_{0s}\right] = \frac{u_* \,k\, E_1}{u_h\, \sigma\, (dE/df)_{f=1}} + g(x_h) \qquad (6.5)$$

which can be recast to the following form:

$$z_{0s}/h = \lambda_1(1-d/h)\ \exp\{-k\ E_1(C_f/2)^{1/2}/(\ (dE/d\zeta)_{\zeta=1})\} \quad (6.6)$$

where λ_1 has the same value as in the case of momentum transfer (= 1.075), because of the assumed similarity between the exchange processes.

The canopy bulk transfer coefficient for water vapor, kB^{-1}, being defined as $\ln [z_0/z_{0s}]$, can then be written as

$$kB^{-1} = \frac{k\ (C_f/2)^{1/2}\ E_1}{\sigma'\ (dE/d\zeta)_{\zeta=1}} - \frac{k}{(C_f/2)^{1/2}} \quad (6.7)$$

Therefore, given C_f and σ' as functions of C_dLAI and foliage distribution, $(dE/d\zeta)_{\zeta=1}$ from the solutions to (3.11), and E_1, kB^{-1} can be calculated as a function of C_t, C_dLAI and foliage distribution.

6.3. Boundary conditions

The general form of the lower boundary condition was presented in section 5.2. by equation (5.1). For all results presented in this chapter, the parameter $g_2 = 0.06$. Figure 6.1 shows the corresponding latent heat flux from the soil, LE_s, for a constant foliage distribution as a function of LAI and u_h, using the cosh wind profile and $\varphi = 60^o$. LE_s is computed using (6.8)

$$LE_s = \rho\ L\ \sigma'\ \chi^{1/2}\ u_h\ \frac{0.622}{p}\ \left.\frac{dE}{d\zeta}\right|_{\zeta=0} \quad (6.8)$$

where $L = 2.5\ 10^6$ J/kg is the latent heat of vaporization, and p is the atmospheric pressure, assumed to be 100 kPa. Changing φ to 30^o results in slightly lower fluxes, due to a change in the light extinction coefficient. For triangular foliage distributions the curves are very similar, and therefore not shown. As can be seen from the figure, LE_s approximately vanishes for values of LAI larger than 2.0.

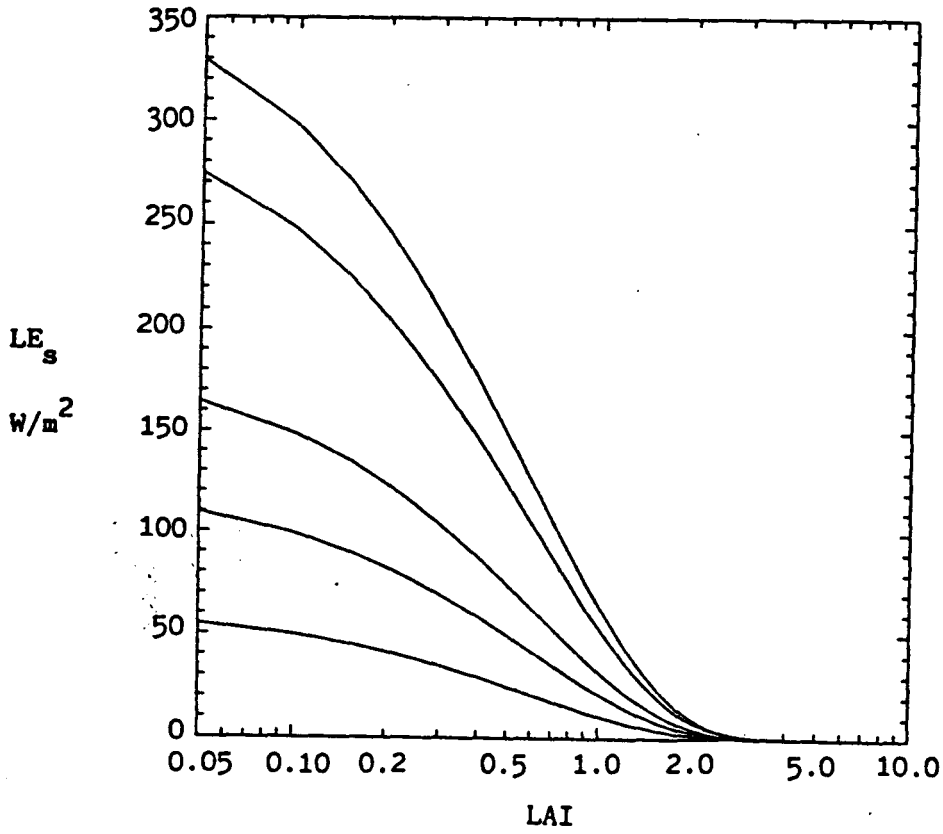

Figure 6.1: The latent heat flux from the soil in W/m^2, LE_s, as a function of LAI and u_h. The uppermost curve corresponds to u_h = 3.0 m/s, and each curve below it corresponds, respectively, to u_h = 2.5, 1.5, 1.0, and 0.5 m/s.

The upper boundary condition was also presented in a general form in section 5.2. (equation (5.1)). In this chapter two different cases will be studied concerning the value of E_1. First, E_1 is chosen to be equal to 0.2 kPa. This value is accompagnied by a solar elevation angle of 60 degrees. Furthermore, it is assumed that the photosynthetic photon flux density at the top of the canopy $PPFD_0 = 2000 \sin \varphi \ \mu E \ m^{-2}s^{-1}$. Consequently, this combination of E_1 = 0.2 kPa and $\varphi = 60^o$ allows all the stomates throughout the depth of the canopy to be nearly completely open, and therefore provides good conditions for moisture transport from canopy to atmosphere. Second, the combination of E_1 = 2.0 kPa and

$\varphi = 30^{o}$ will be used, which causes considerable stomatal closure, and therefore an increase of resistance to moisture transport is to be expected in this case.

6.4. Results

6.4.1. The leaf bulk transfer coefficient C_t'

Assuming that (1) the characteristic dimension of the foliage elements D lies between 0.01 and 0.1 m, (2) the mean horizontal wind speed at the top of the canopy u_h ranges from 0.5 to 3.0 m/s, (3) the parameter $C_1 = 1.2$, (4) $\mathcal{E} = 2.2\ 10^{-5}\ m^2/s$, and (5) $\upsilon = 1.5\ 10^{-5}\ m^2/s$, it can be shown that values for C_t' range from about 0.01 to 0.10. Therefore, in the following sections the computed values for kB^{-1} will be presented for $C_t' = 0.01$ ($u_h = 3.0$ m/s), 0.025 (2.5 m/s), 0.05 (1.5 m/s), 0.075 (1.0 m/s), and 0.10 (0.5 m/s).

6.4.2. Constant foliage distributions

In the figures 6.2 - 6.5 the computed kB^{-1} values for constant foliage distributions are shown as a function of LAI and C_t', using the cosh wind profile.

Figure 6.2 applies to an unstressed deciduous forest (i.e. $E_1 = 0.2$ kPa and $\varphi = 60^{o}$), while figure 6.3 shows a deciduous forest under stressed conditions ($E_1 = 2.0$ kPa and $\varphi = 30^{o}$). kB^{-1} is largely determined by the soil moisture flux for small values of LAI, but with increasing LAI the transport of water vapor from the canopy becomes more important, while the contribute of the soil moisture flux decreases (see figure 6.1). At first, the canopy is not able to compensate for the reduction in soil moisture flux, reflected in an increase in kB^{-1}, but a maximum value for kB^{-1} is reached when the canopy becomes more dense. After reaching the maximum, kB^{-1} decreases and finally becomes

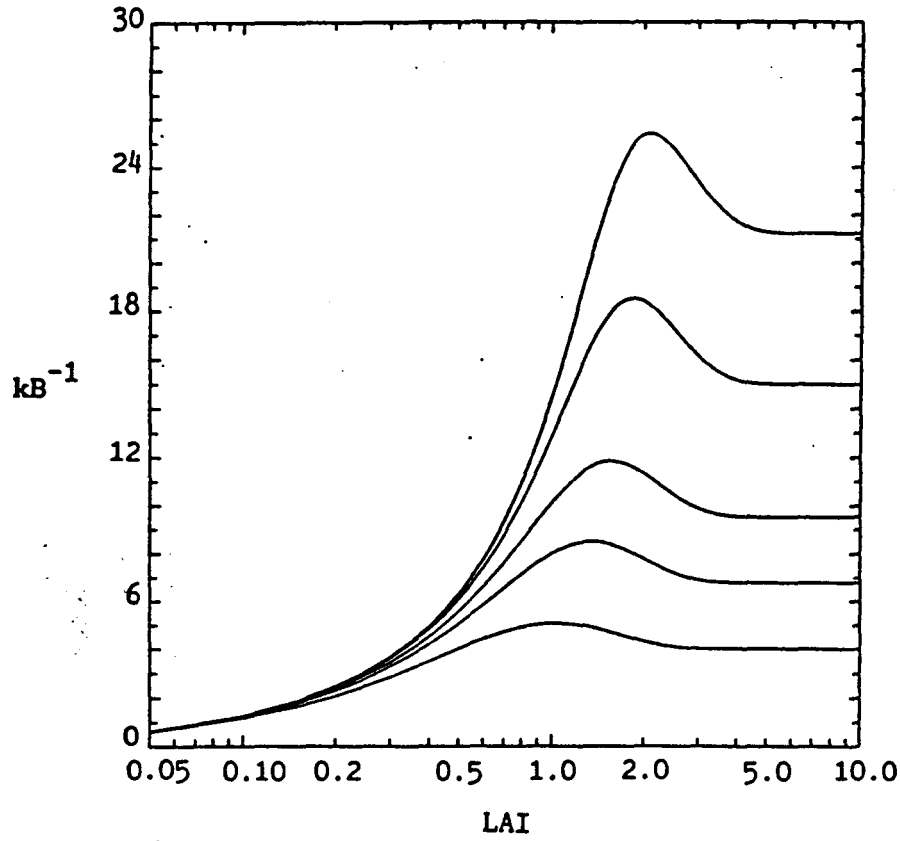

Figure 6.2: kB^{-1} for an unstressed deciduous forest as a function of LAI and C_t', assuming a constant foliage distribution and a cosh wind profile. The uppermost curve corresponds to $C_t' = 0.01$, and each curve below it corresponds, respectively, to $C_t' = 0.025, 0.05, 0.075, 0.10$.

independent of the LAI, the moisture flux at the top of the canopy being dominated or (for LAI > 2.0) completely determined by transpiration from the canopy. Comparing the kB^{-1} values for the unstressed and stressed case, shows that the latter are considerably larger, implying an increased resistance to water vapor transport.

One should be cautious with the kB^{-1} values computed for sparse canopies (vanishing LAI), because the formulation of the lower boundary condition becomes increasingly more important with decreasing LAI.

The figures 6.4 and 6.5 respectively, apply to an unstressed and stressed coniferous forest. Comparing the computed kB^{-1} values for full

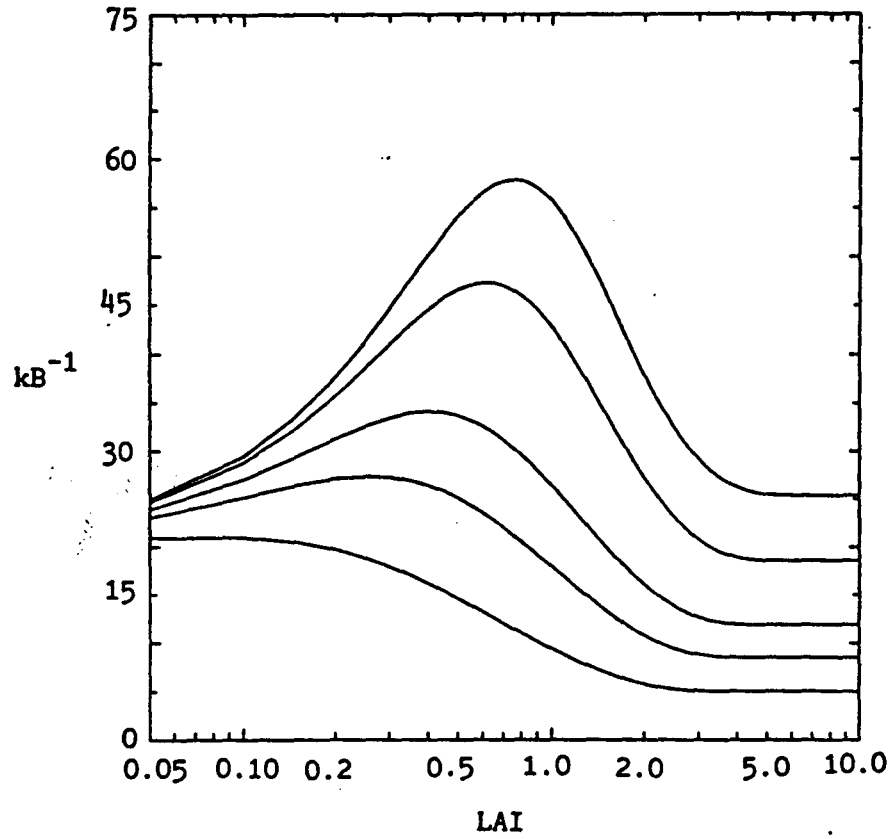

Figure 6.3: Same as figure 6.2, but for the case of a stressed deciduous forest.

coniferous canopies with those for annual deciduous forests, shows that the former are about 5 times higher in the unstressed case, and up to 12 times higher in the stressed case, implying a much higher resistance to water vapor transfer, and therefore less transpiration.

For full canopies, the differences in kB^{-1} in each single figure are largely due to the different values chosen for the wind speed at the top of the canopy, u_h.

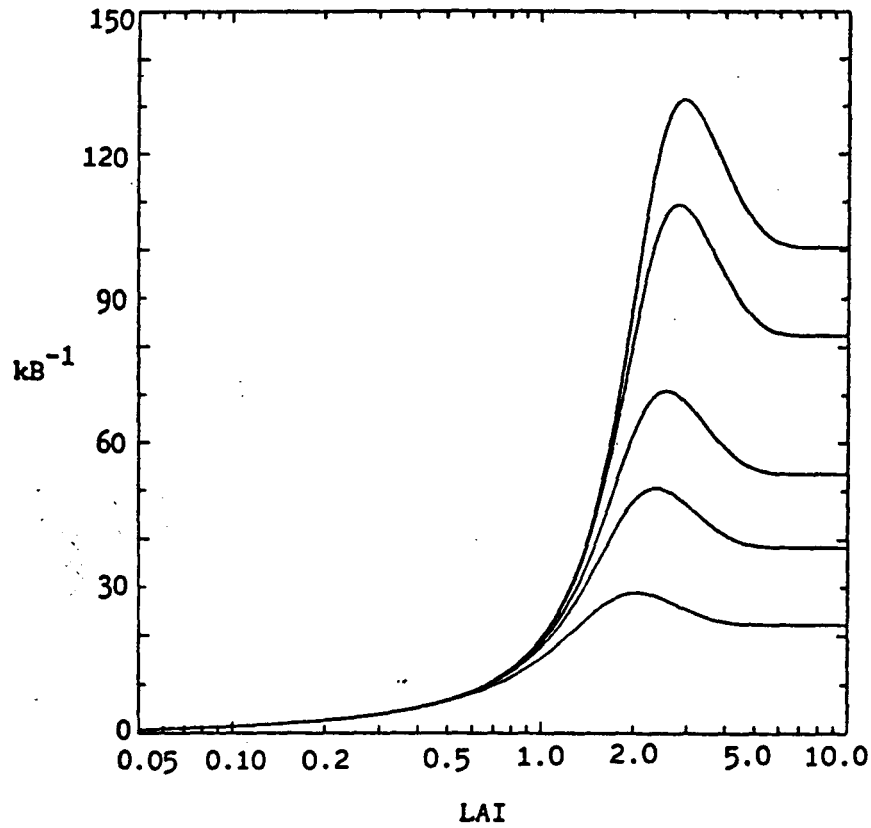

Figure 6.4: Same as figure 6.2, but for the case of an unstressed coniferous forest.

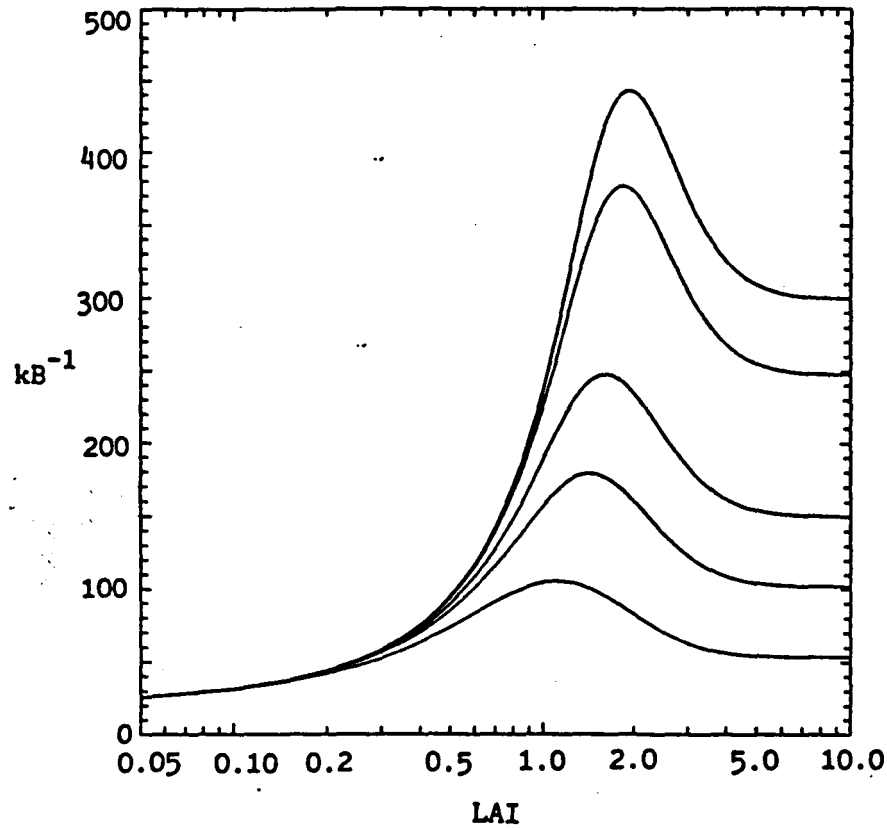

Figure 6.5: Same as figure 6.2, but for the case of a stressed coniferous forest.

6.4.3. Triangular foliage distributions

Computed values for kB^{-1} as a function of LAI and C_t' for three triangular foliage distributions (ζ_m = 0.2, 0.5 and 0.8) are shown in the figures 6.6 - 6.17. Again, the cases for unstressed and stressed annual deciduous and coniferous forests are presented. Everywhere, a_0/a_1 is assumed to be 0.1.

Disregarding small LAI values, where kB^{-1} is again largely determined by the soil moisture flux, all calculated kB^{-1} values for the triangular foliage distributions are smaller than those computed for the corresponding case with a constant distribution, the differences sometimes being almost 100%. Changing the position of the level of maximum foliage density causes differences in kB^{-1} of up to 40%, and the figures show a decrease in kB^{-1} with decreasing height of maximum density.

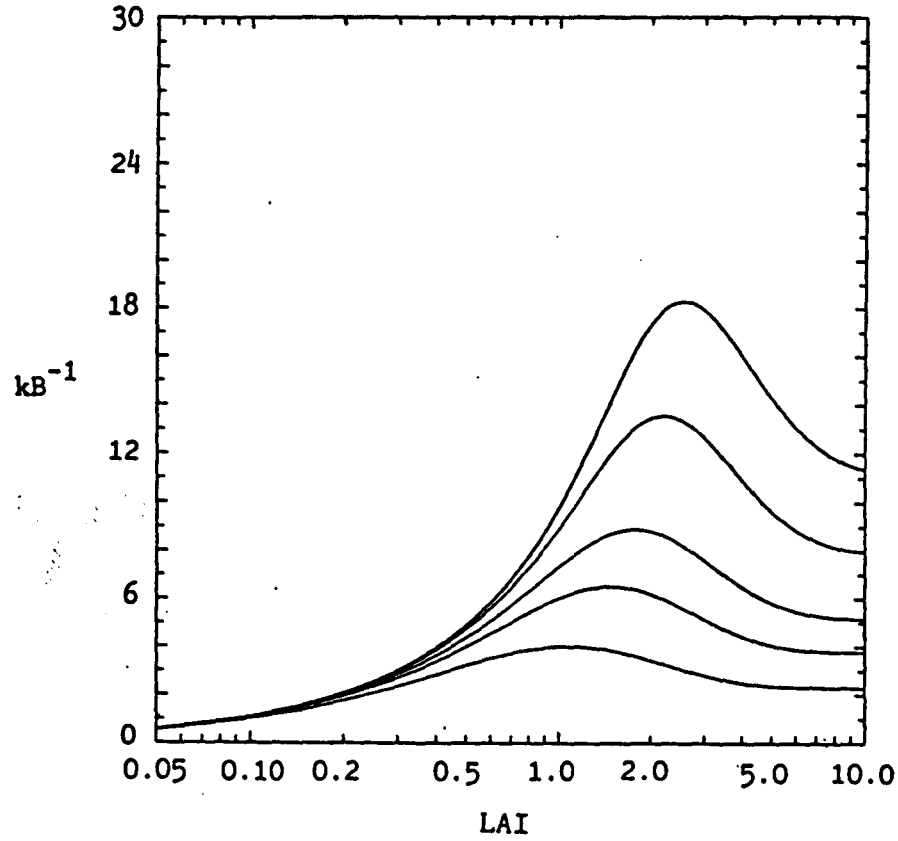

Figure 6.6: kB^{-1} for a deciduous forest as a function of LAI and C_t', assuming a triangular foliage distribution with $J_m = 0.2$. The uppermost curve corresponds to $C_t' = 0.01$, and each one below it corresponds, respectively, to $C_t' = 0.025$, 0.05, 0.075, and 0.10.

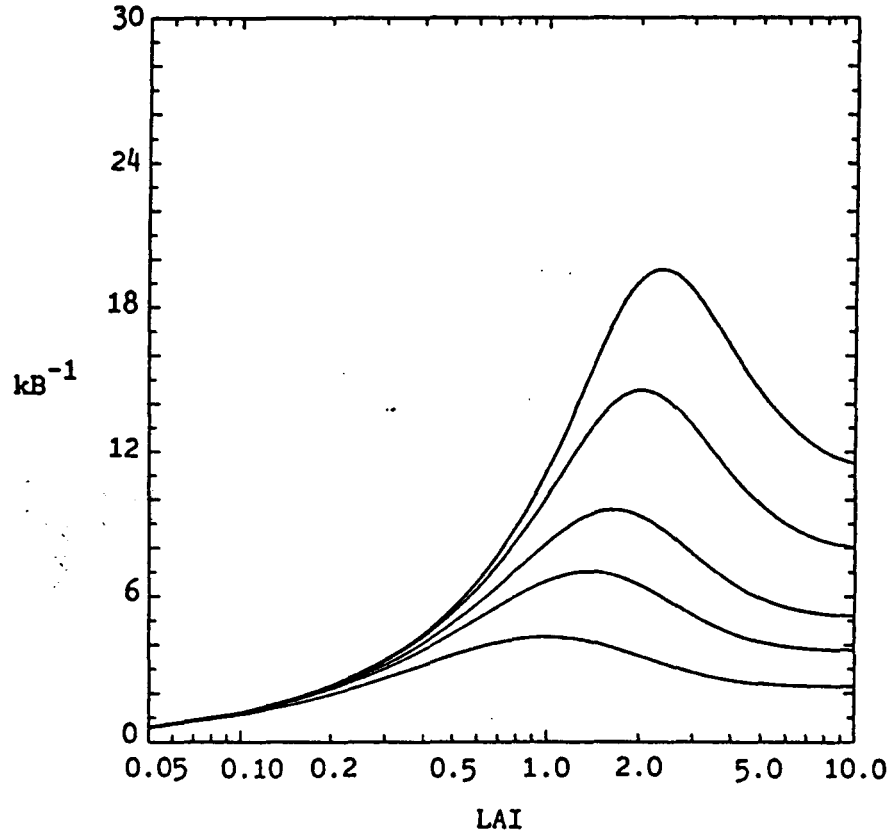

Figure 6.7: Same as figure 6.6, except f_m = 0.5.

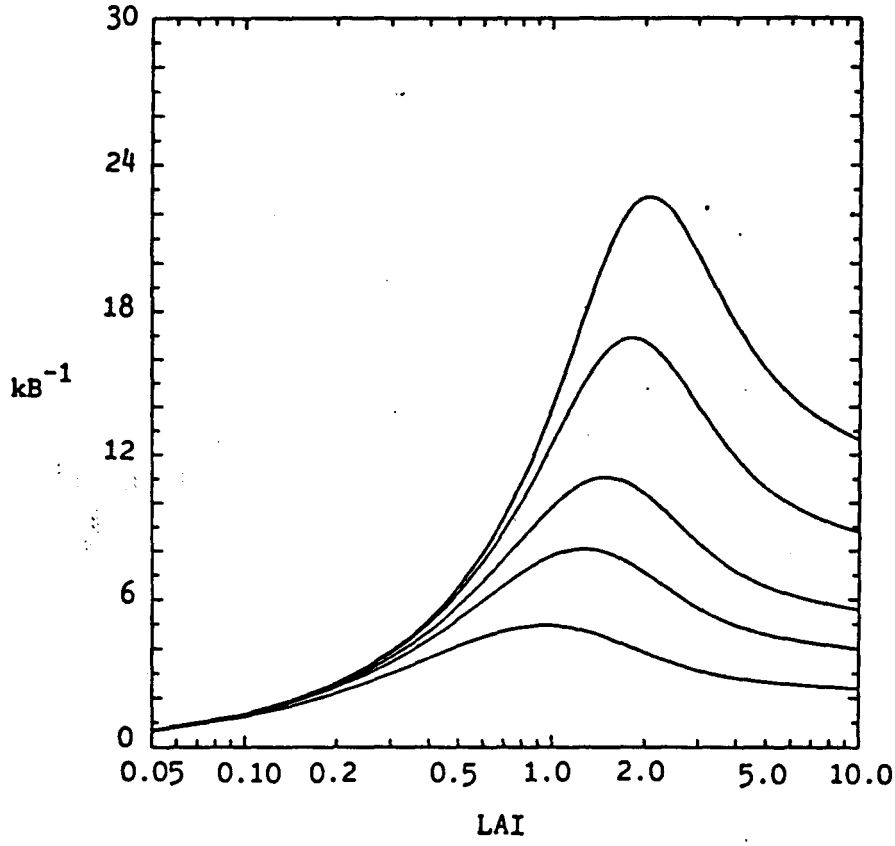

Figure 6.8: Same as figure 6.6, except ζ_m = 0.8.

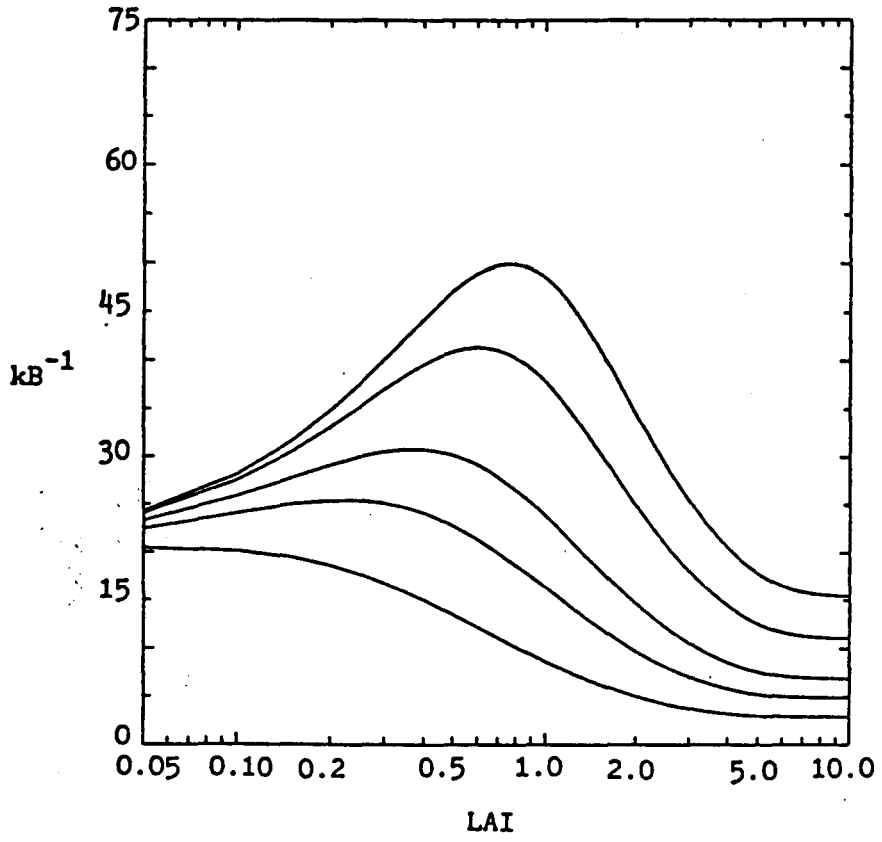

Figure 6.9: Same as figure 6.6, but now for a stressed deciduous forest ($\int_m$ = 0.2).

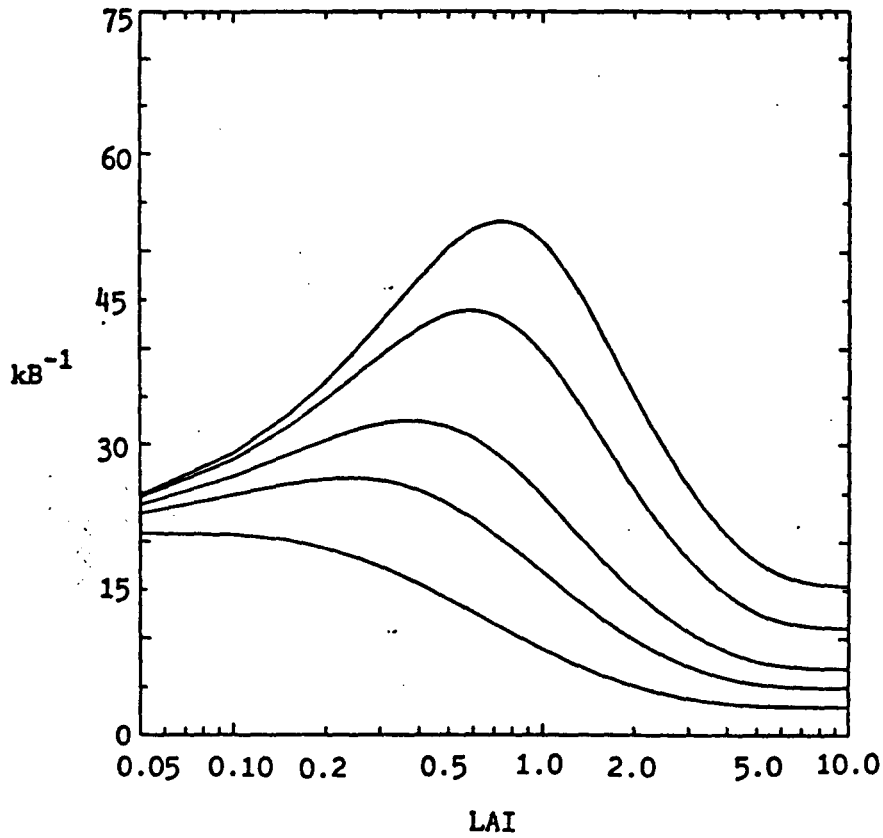

Figure 6.10: Same as figure 6.9, except ζ_m = 0.5.

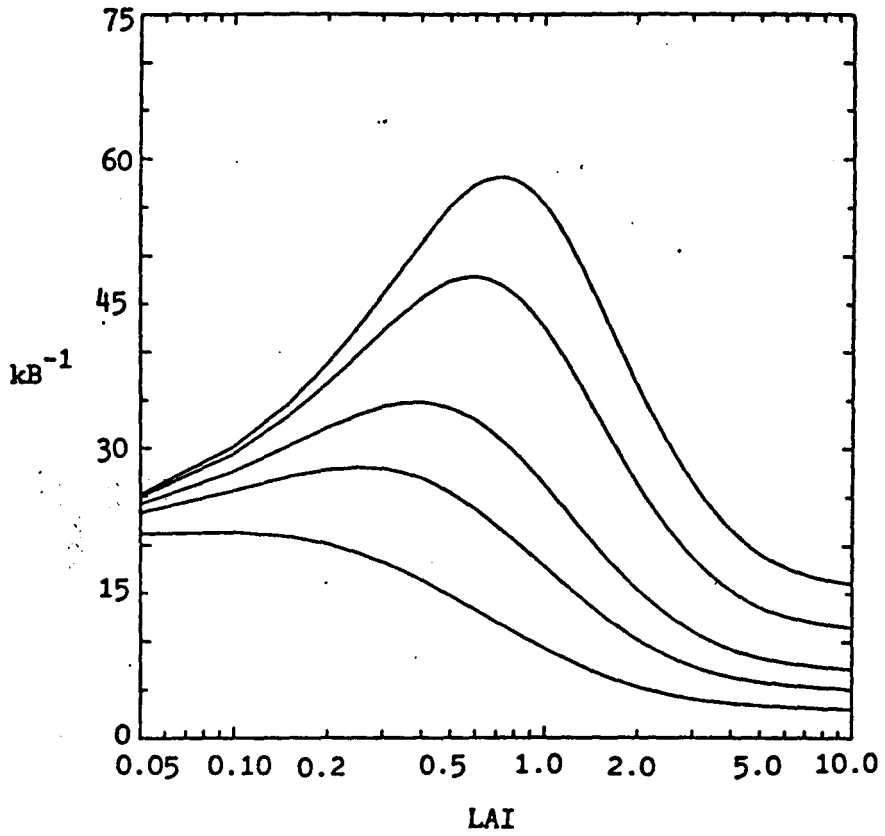

Figure 6.11: Same as figure 6.9, except f_m = 0.8.

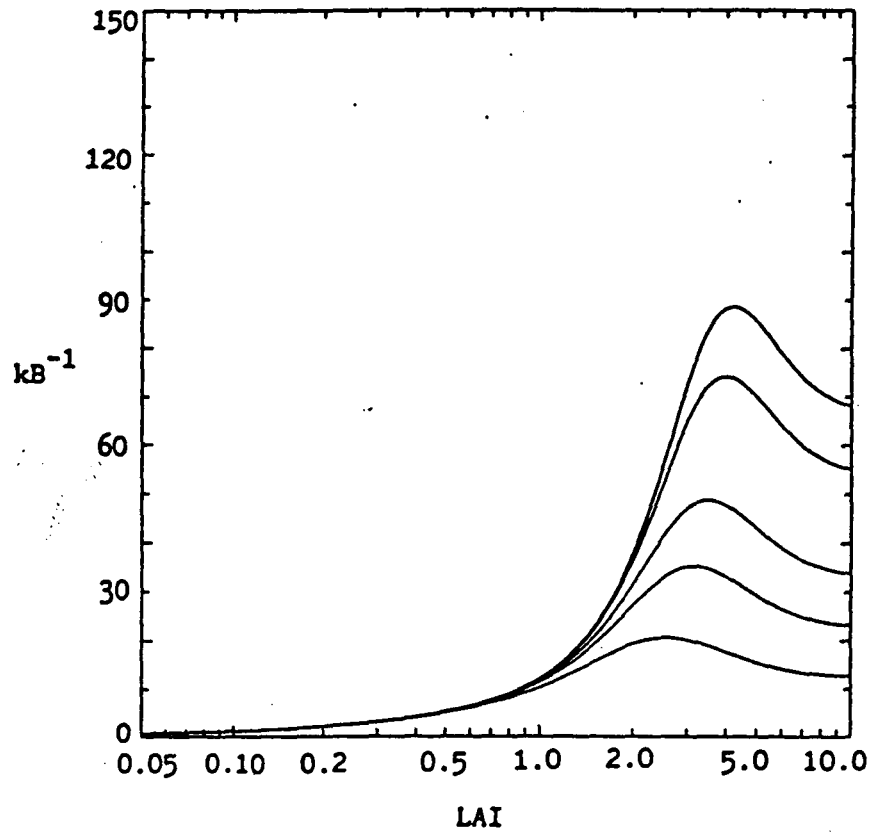

Figure 6.12: Same as figure 6.6, but now for an unstressed coniferous forest (f_m = 0.2).

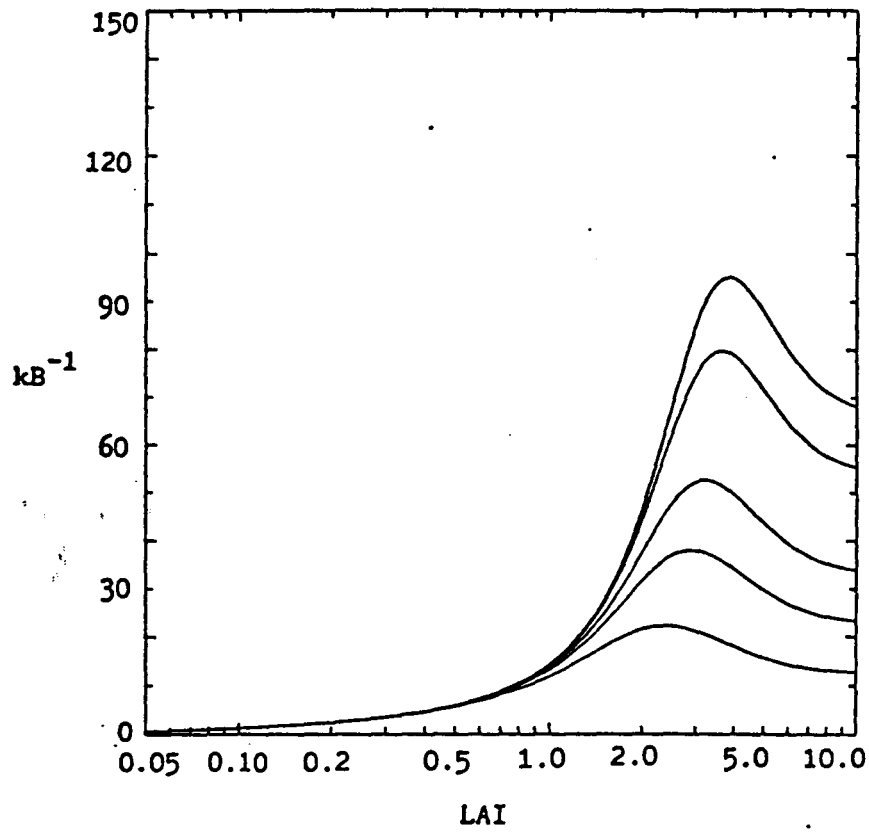

Figure 6.13: Same as figure 6.12, except ζ_m = 0.5.

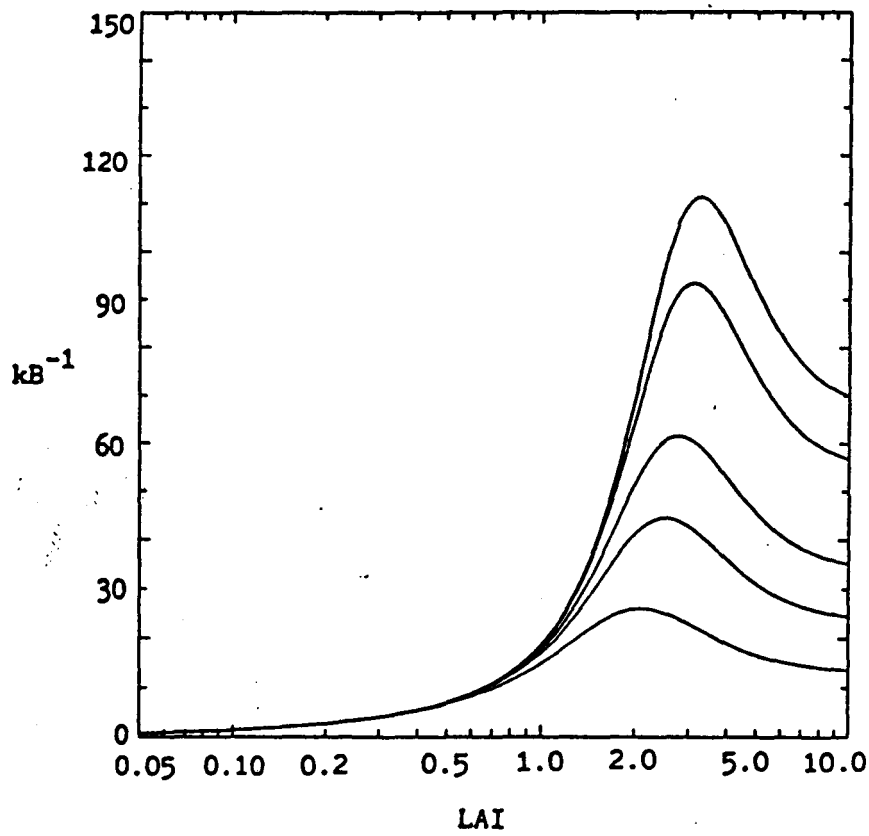

Figure 6.14: Same as figure 6.12, except J_m = 0.8.

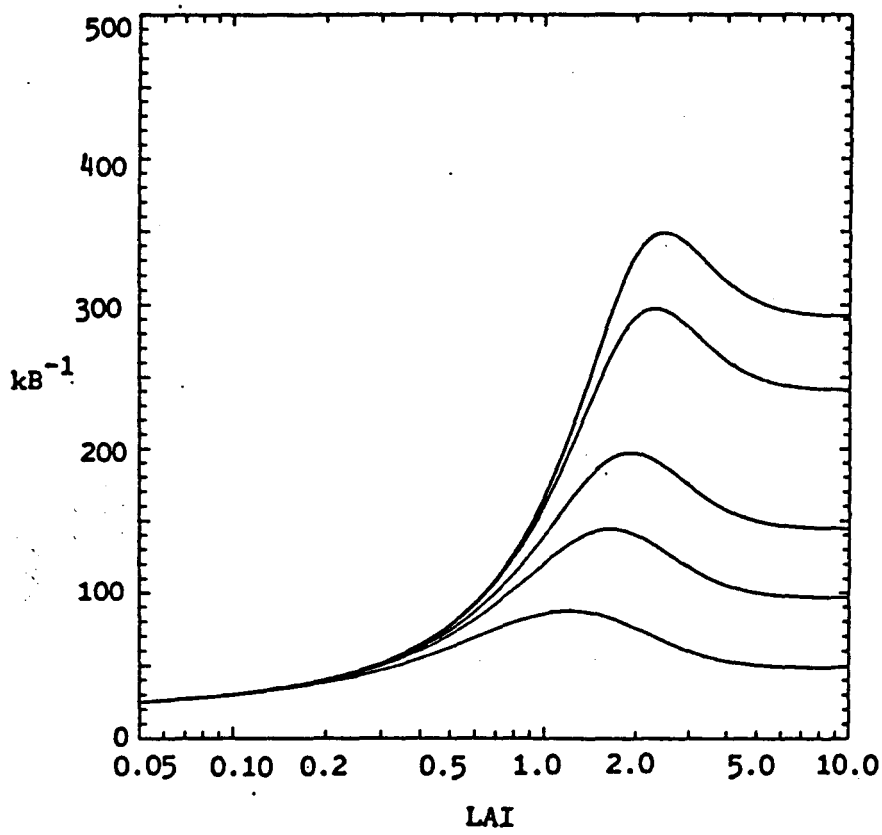

Figure 6.15: Same as figure 6.6, but now for a stressed coniferous forest (f_m = 0.2).

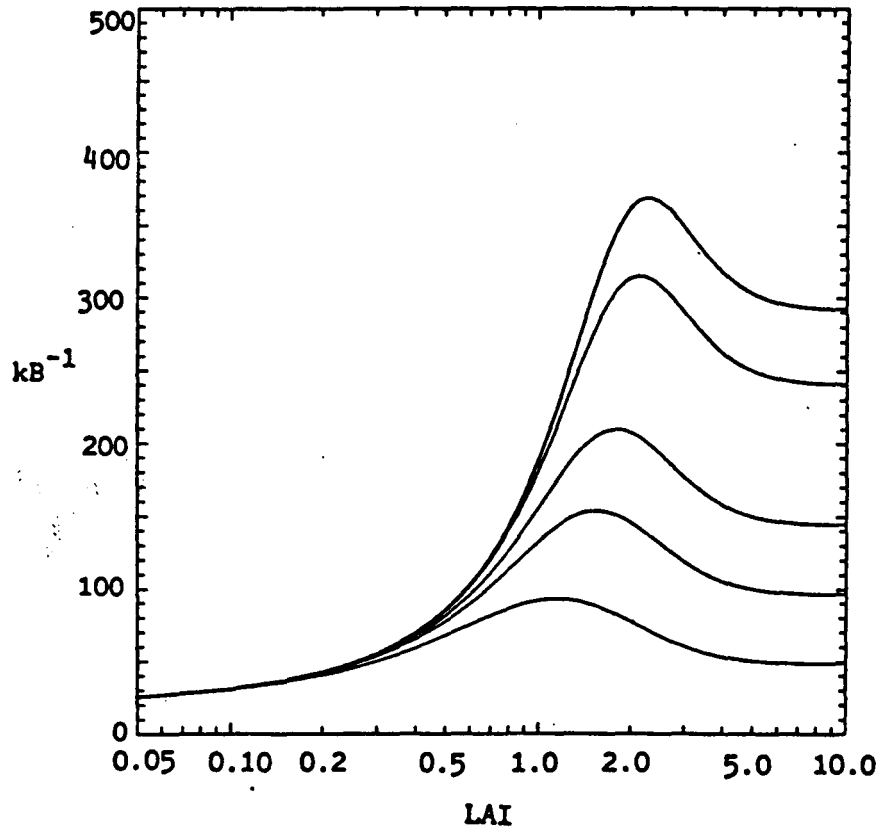

Figure 6.16: Same as figure 6.15, except $\mathfrak{f}_m$ = 0.5.

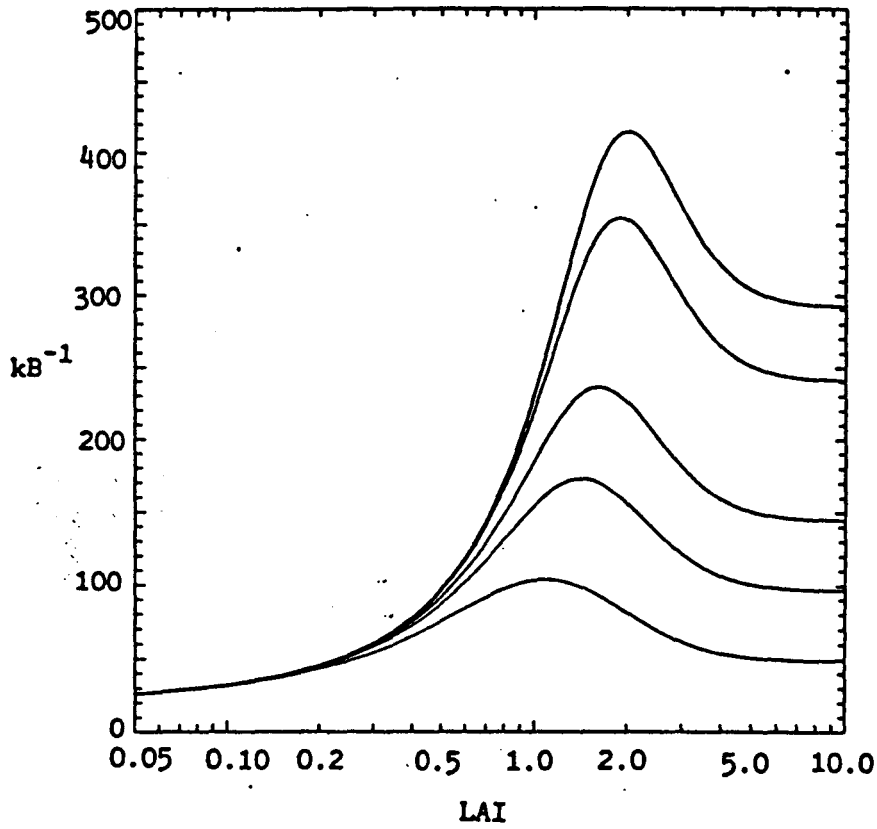

Figure 6.17: Same as figure 6.15, except ζ_m = 0.8.

6.4.4. Mutual aerodynamic interference of foliage elements

The effect of mutual aerodynamic interference of canopy elements is examined in the way described in section 2.4., i.e. the effective value of $C_d LAI$ is bound to a maximum of 0.50.

Figures 6.18 - 6.21 show the computed kB^{-1} values for the unstressed and stressed deciduous and coniferous forest, with $C_t' = 0.075$ in all cases. From these figures it can be seen, that including shelter effects reduces the kB^{-1} values for full canopies up to 70% for deciduous canopies, while the differences for coniferous canopies are much smaller (the largest reduction being 45% for a constant foliage distribution, assuming unstressed conditions). Furthermore, the figures show that kB^{-1} is far less dependent on the assumed shape of the foliage distribution than in the case of neglecting shelter effects.

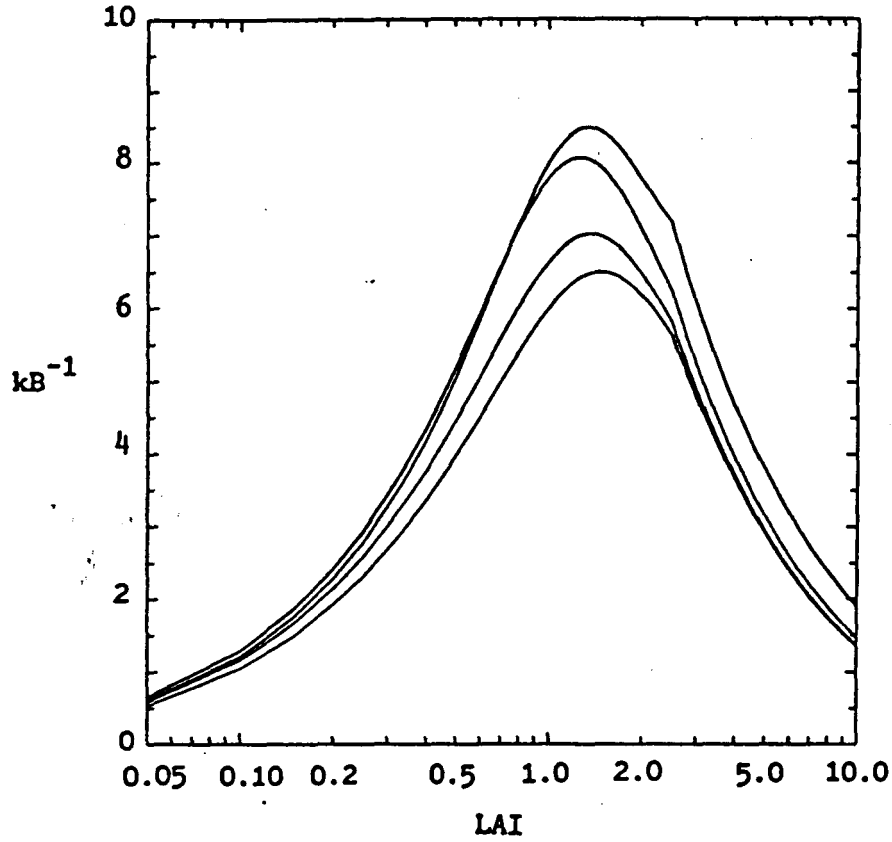

Figure 6.18: kB^{-1} for an unstressed deciduous forest as a function of LAI and foliage distribution, when shelter effects are included. The uppermost curve corresponds to a constant foliage distribution, and the lower three to triangular distributions, with (from top to bottom) f_m = 0.8, 0.5, and 0.2. In all cases C_t' = 0.075 (u_h = 1.0 m/s).

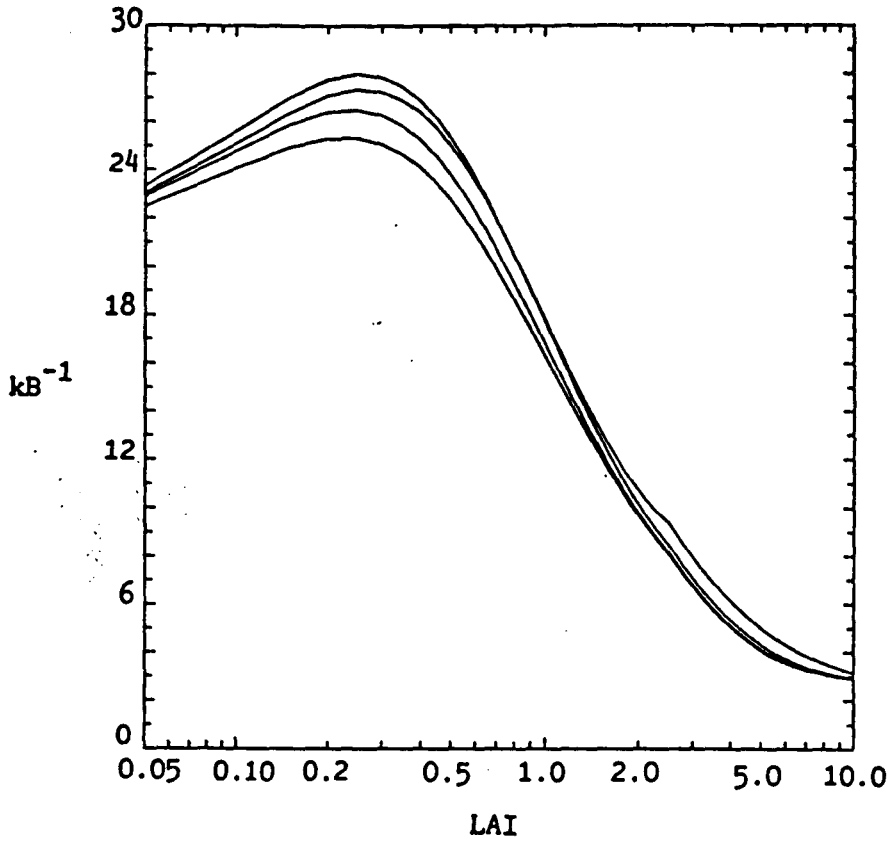

Figure 6.19: Same as figure 6.18, but now for a stressed deciduous forest.

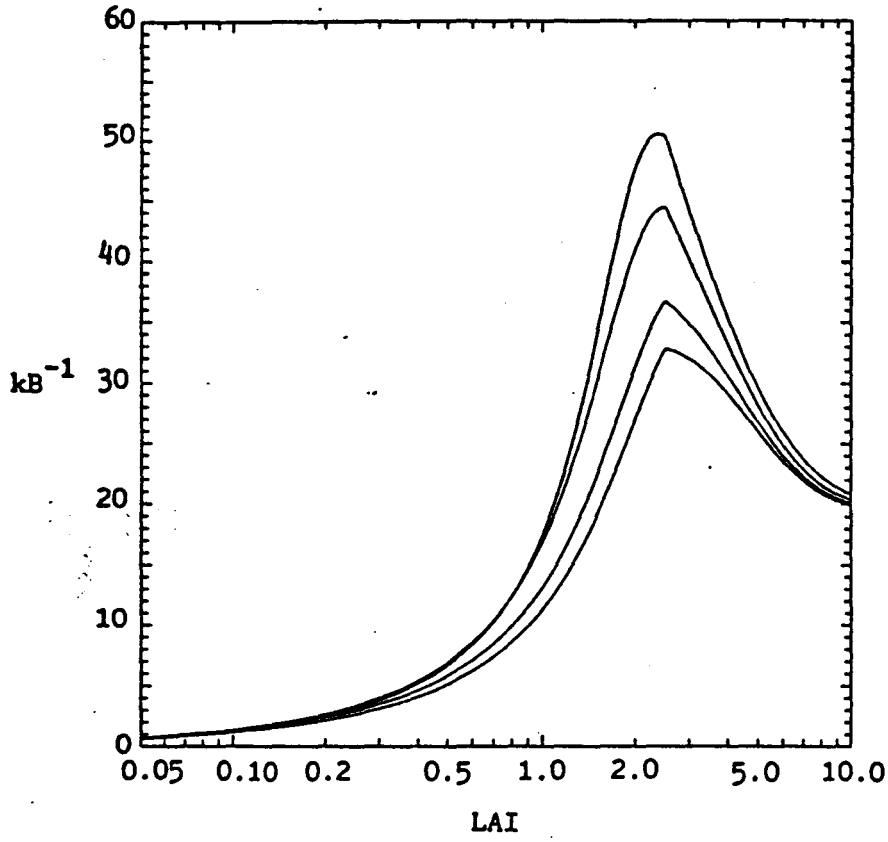

Figure 6.20: Same as figure 6.18, but now for the case of an unstressed coniferous forest.

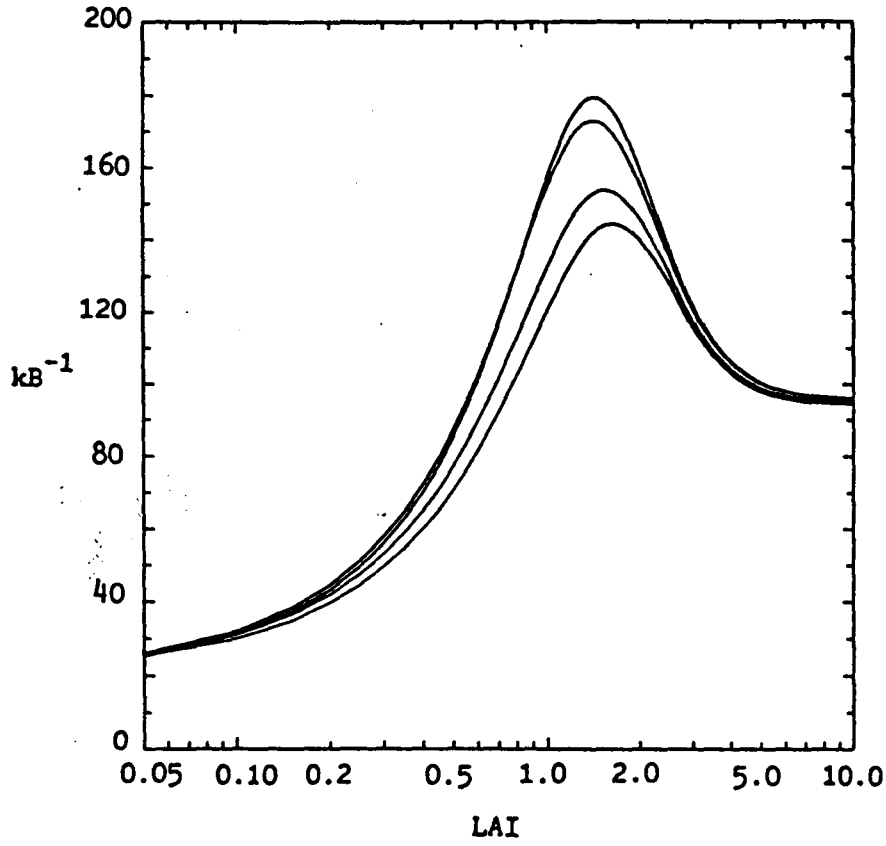

Figure 6.21: Same as figure 6.18, but for a stressed coniferous forest.

7. COMPUTATION OF THE CANOPY RESISTANCE

7.1. Introduction

In many studies (e.g. Szeicz and Long, 1969; Stewart and Thom, 1973; McNaughton and Black, 1973; Gash and Stewart, 1975) the transpiration from a forest canopy is estimated using the Penman-Monteith combination equation (7.1):

$$LE = \frac{s\,(Q_n - G) + \rho\, c_p\, E_r / r_{ah}}{s + \gamma\,(1 + r_{ah}/r_c)} \qquad (7.1)$$

where LE is the latent heat flux from the canopy (in W/m^2); Q_n is the net radiation (W/m^2); G is the soil heat flux (W/m^2); s is the change of saturation vapor pressure with temperature (kPa/K); γ is the psychrometric constant (kPa/K); c_p is the specific heat of air at constant pressure (J/kgK); E_r is the vapor pressure deficit at a reference height above the forest stand (kPa); r_{ah} is the aerodynamic resistance for heat exchange between the forest and the reference level (s/m); and r_c is the canopy resistance (s/m).

For dry canopies, the ability of this equation to give reasonable estimates of canopy transpiration is largely determined by the values applied for r_c (Gash and Stewart, 1975). An assumption commonly made is (e.g. Tan and Black, 1976), that the canopy resistance equals the bulk stomatal resistance $r_{s\ bulk}$, i.e. the resistance of all stomates acting in parallel, but objections can be raised against this assumption (e.g. Thom, 1975; Shuttleworth, 1976).

In this chapter, the results of this approach will be compared to values for the canopy resistance computed by solving a differential equation narrowly related to the exact transfer equation for water vapor (3.11).

7.2. Theory

As was pointed out in section 6.1., kB^{-1} is a measure for the discrepancy between the aerodynamic resistance for momentum exchange, and the aerodynamic resistance for heat or mass exchange. Therefore, in the case of water vapor transfer, its value is determined by the boundary layer resistance of the plant stand, as well as the canopy resistance. In the following, the boundary layer resistance r_b of a single leaf or needle in equation (3.5) is assumed to be small compared to the stomatal resistance r_s. Consequently, the water vapor transfer equation (3.11) changes into (7.2)

$$\frac{d^2E}{d\zeta^2} + \frac{1}{2}\frac{\chi'}{\chi}\frac{dE}{d\zeta} = \frac{f(\zeta)\, C_t'\, LAI\, \chi^{-1/4}\, E}{\alpha_k \sigma \mu r_s C_t' \chi^{1/4} u_h} \qquad (7.2)$$

Furthermore, the lower boundary condition on (7.2) is chosen to be

$$\left.\frac{dE}{d\zeta}\right|_{\zeta=0} = E'_0 = 0 \qquad (7.3)$$

i.e. a zero soil moisture flux. All other model parameters remain unaltered.

Now, solving the differential equation (7.2) results in kB^{-1} values, which only include the canopy resistance, and r_c can be computed from (7.4).

$$r_c = \frac{kB^{-1}}{k\, u_h\, (C_f/2)^{1/2}} \qquad (7.4)$$

Equation (7.5) gives an expression for the bulk stomatal (or bulk physiological) resistance, which is independent of foliage distribution.

$$r_{s\ bulk} = \left[\int_0^h \frac{a(z)}{r_s(z)}\, dz\right]^{-1} = \left[h \int_0^1 \frac{a(\zeta)}{r_s(\zeta)}\, d\zeta\right]^{-1} \qquad (7.5)$$

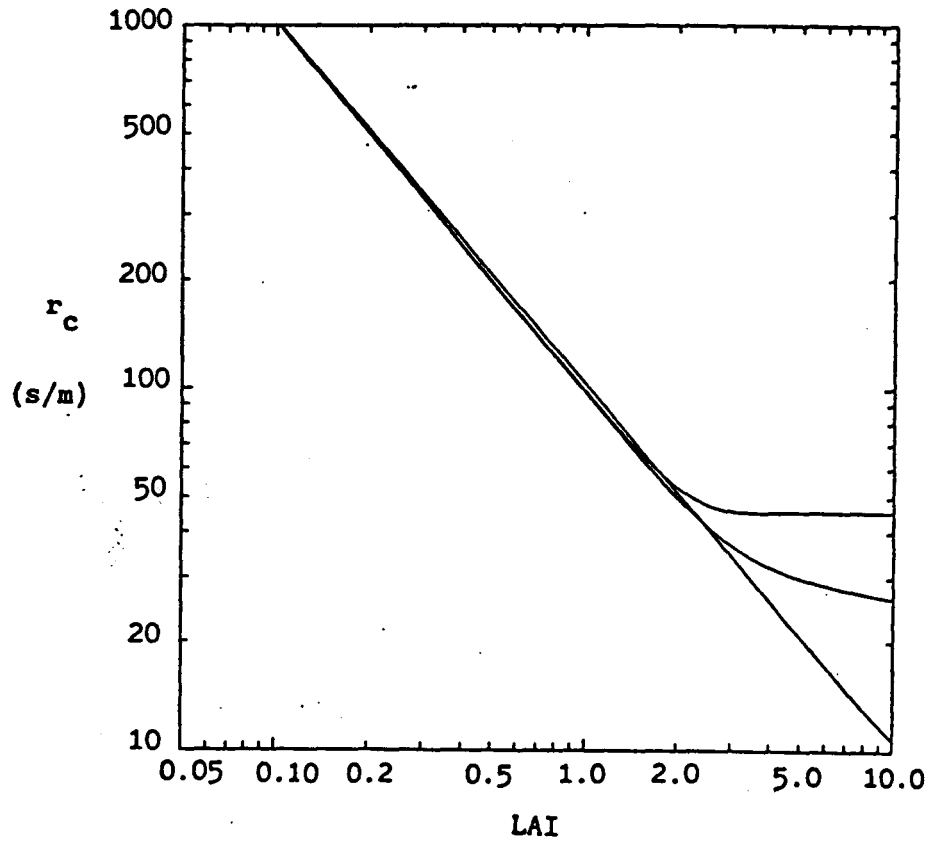

Figure 7.1: The canopy resistance r_c (s/m) as a function of LAI for an unstressed deciduous forest. The upper curve (for high values of LAI) represents the canopy resistance computed from (7.5), while the other two are computed using (7.4). The middle curve is associated with a triangular foliage distribution, and the upper one with a constant foliage distribution. For the latter two curves $C_t' = 0.075$, and no shelter effects are included.

7.3. Results

The figures 7.1 - 7.8 show the canopy resistance as a function of LAI as calculated from (7.4) and (7.5). Again, the cases of a deciduous and a coniferous forest are considered, under unstressed and stressed conditions.

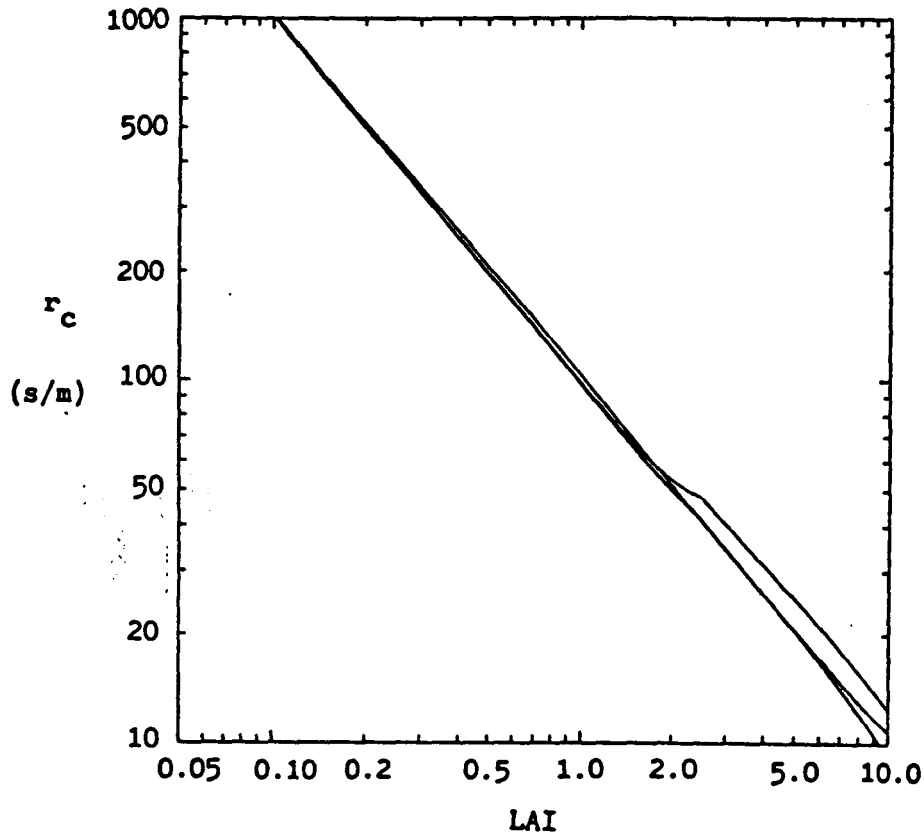

Figure 7.2: The canopy resistance as a function of LAI for an unstressed deciduous forest with shelter effects included. The upper curve (for large LAI) is associated with a constant foliage distribution, and the lower one with a triangular distribution. The middle curve represents canopy resistances computed with (7.5).

Three curves are presented in each figure, one representing the bulk stomatal resistance (which is independent of foliage distribution), one associated with a constant foliage distribution, and the canopy resistance computed using (7.4), and one associated with the triangular foliage distribution, r_c also being computed from (7.4). The height of maximum foliage density for the triangular distribution was not important, and therefore, only one curve is presented. Everywhere, $C_t' = 0.075$.

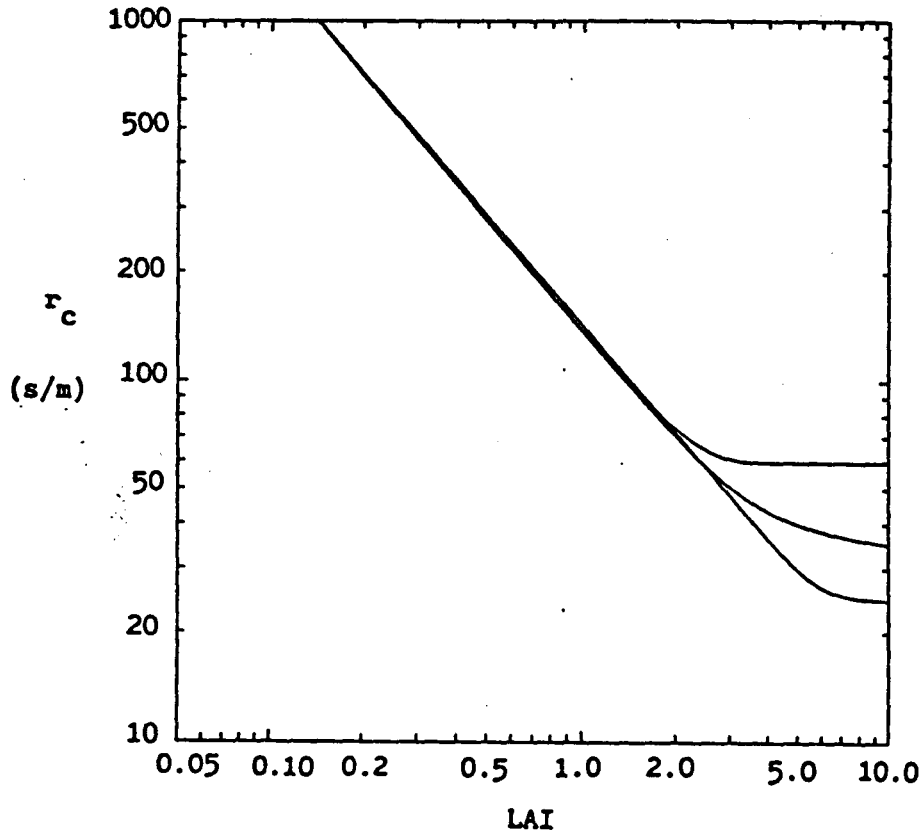

Figure 7.3: The canopy resistance as a function of LAI for a stressed deciduous forest without shelter effects. The sequence of the curves is the same as in figure 7.1.

From the figures for the case of a deciduous forest, it can be seen that the curves are very close for LAI values smaller than about 2 (differences always less than 10%). The same applies to the case of a coniferous forest for LAI < 3. For denser canopies however, the differences between the curves resulting from (7.4) and (7.5) increase considerably. The influence of including shelter effects in the model (again by restricting the effective C_dLAI to a maximum value of 0.5) is striking: without shelter differences of up to 300% occur for full canopies (figure 7.1), but with shelter effects these differences are within 20%.

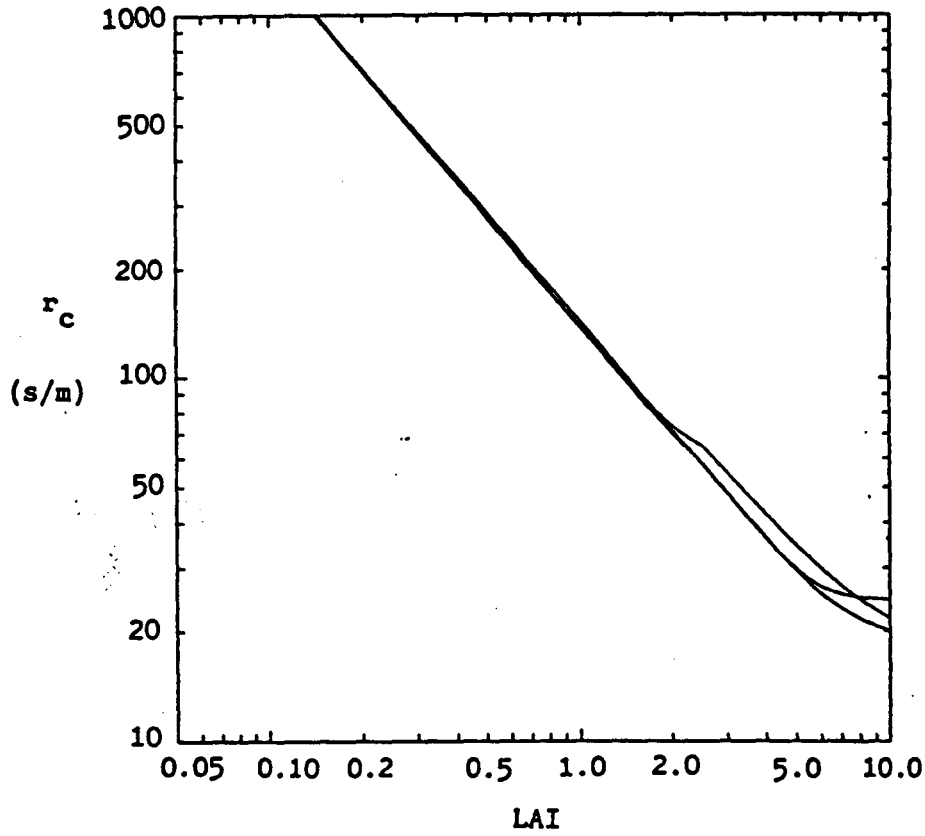

Figure 7.4: The canopy resistance as a function of LAI for a stressed deciduous forest with shelter effects. The upper curve (at LAI = 10) represents canopy resistances computed with (7.5), the middle one is associated with the constant foliage distribution, and the lower one with the triangular distribution.

Furthermore, the r_c values computed assuming a constant foliage distribution are always larger than those for a triangular distribution (the difference being about 80% in figure 7.1), but including shelter effects also tends to reduce these differences (about 25% in figure 7.2).

Finally, comparing all cases reveals, that the magnitude of the differences is also determined by the physiological and environmental parameters influencing the stomatal resistance (i.e. $r_{s\,min}$, A, B, g_1,

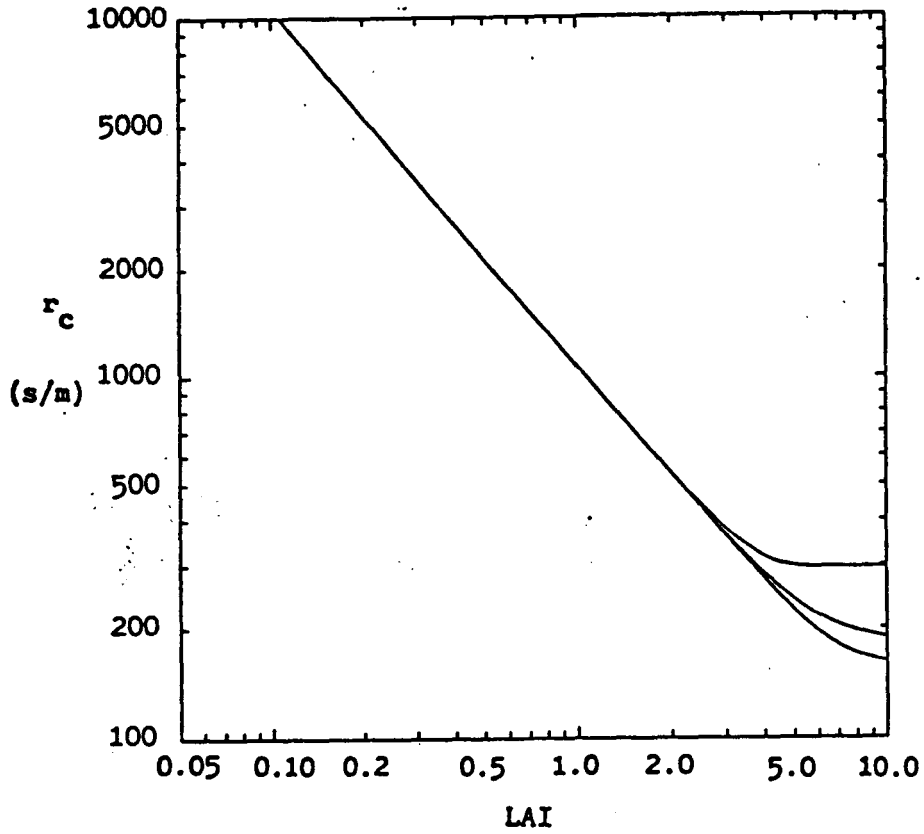

Figure 7.5: The canopy resistance as a function of LAI for an unstressed coniferous forest without shelter effects. The sequence of the curves corresponds to the sequence in figure 7.1.

E_1), the largest differences occurring for an unstressed deciduous forest, and the smallest for a stressed coniferous forest.

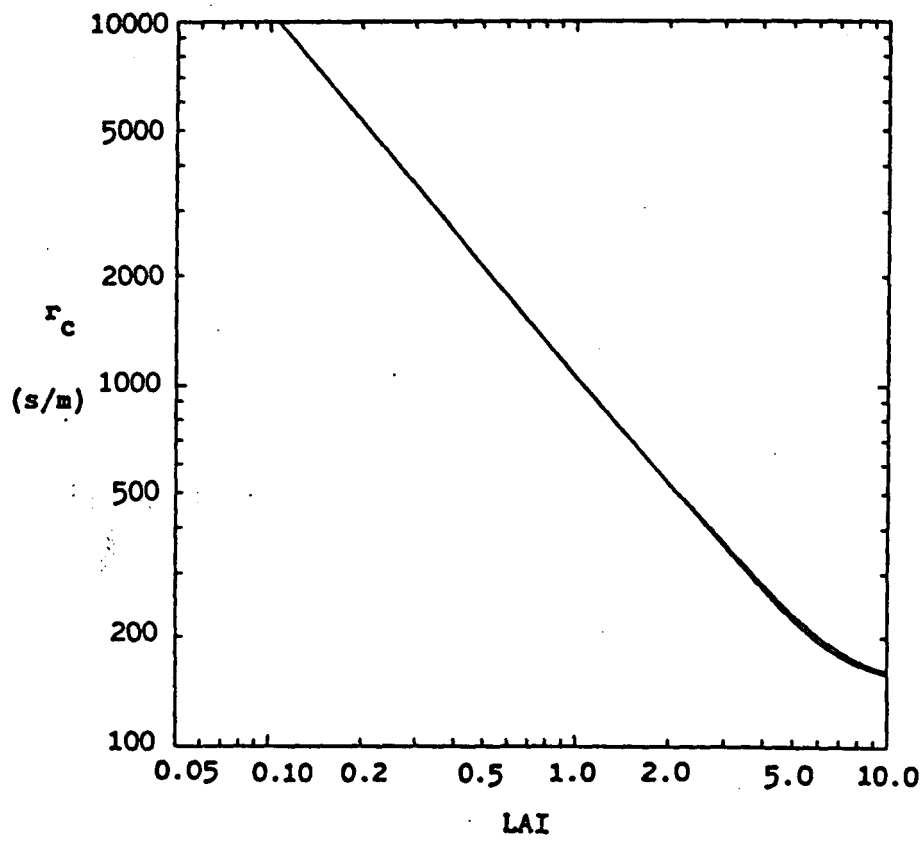

Figure 7.6: The canopy resistance as a function of LAI for an unstressed coniferous forest with shelter effects. The upper curve is associated with a constant foliage distribution, and the lower curve with a triangular foliage distribution. The middle curve is computed from (7.5).

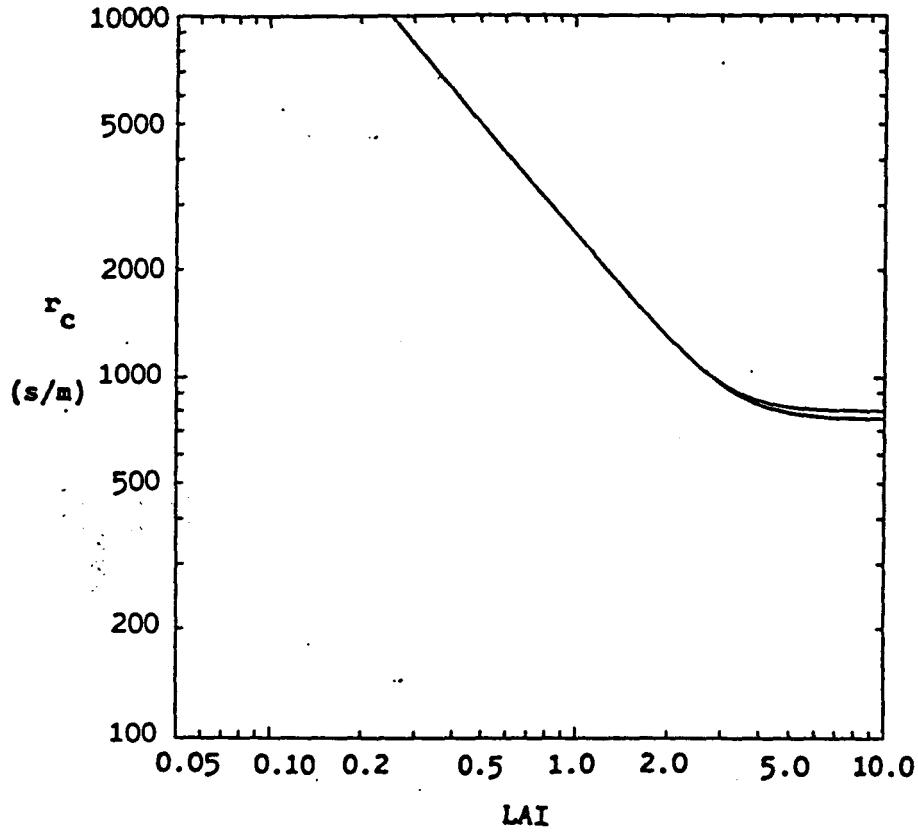

Figure 7.7: The canopy resistance as a function of LAI for a stressed coniferous forest without shelter effects. The upper curve is associated with a constant foliage distribution.

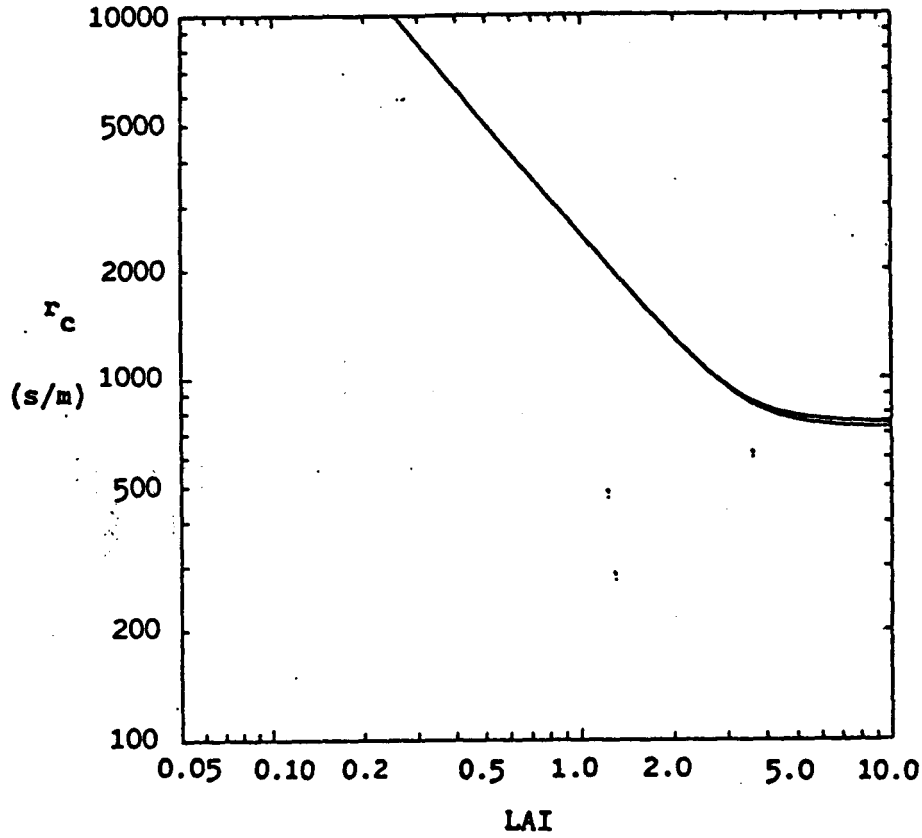

Figure 7.8: The canopy resistance as a function of LAI for a stressed coniferous forest with shelter effects. The upper curve (at LAI = 10) is computed from (7.5). The middle curve is associated with a constant foliage distribution, while the lower one is associated with a triangular distribution.

8. THE EXCHANGE OF GASEOUS AIR POLLUTANTS

8.1. Introduction

Presently, the deposition of gaseous air pollutants to vegetated surfaces is considered to be one of the major environmental problems. In order to quantify the (future) effects on the vegetation, it is necessary to estimate the uptake of the pollutants by leaves or needles.

In chapter 3 the transfer equation for water vapor (3.11) was derived from equations (3.1) - (3.3), assuming that $r_r = r_s$. For the transfer of gaseous air pollutants this is not necessarily true, because additional resistances, i.e. the mesophyll and cuticular resistance, might play a role.

The mesophyll resistance is influenced by the surface area of the mesophyll, and the solubility of the gas (Hill, 1971; O'Dell et al., 1977; Hosker and Lindberg, 1982), and is generally quite small: 10 - 50 s/m (Hosker and Lindberg, 1982). The cuticular resistance is affected by the chemical properties of the gas, and the characteristics of the leaf or needle surface. For many pollutants, the cuticular resistance is large, i.e. exceeding 1000 s/m, but in some cases the uptake through the surface can be significant, especially when the retention time on leaf surfaces is high (Hosker and Lindberg, 1982). Consequently, the transfer equation for gaseous air pollutants might differ slightly from the one for water vapor.

As an example, the transfer of ozone (O_3) from atmosphere to forest stand is described in the following sections. Values for the deposition velocity v_d are computed, and presented as a function of LAI and canopy structure. Also, the influence of mutual aerodynamic interference will be investigated.

8.2. The transfer of ozone from atmosphere to vegetation

8.2.1. The transfer equation for ozone

From (3.1) - (3.3) it can be derived that the transfer equation for gaseous air pollutants has the following form:

$$\frac{d^2C}{d\zeta^2} + \frac{1}{2}\frac{\chi'}{\chi}\frac{dC}{d\zeta} = \frac{f(\zeta)\, C_t'\, LAI\, \chi^{-1/4}\, C}{\alpha_k \sigma \mu (1 + r_r\, C_t'\, \chi^{1/4}\, u_h)} \qquad (8.1)$$

where $C = (c_f - c)/(c_f - c_h)$; $c_h = c(h)$ is the concentration of the pollutant in the air at canopy height; c_f is a constant throughout the depth of the canopy; $C_t' = C_1\, Re_h^{-1/2}\, Sc^{-2/3}$, but now with $Sc = \upsilon/\zeta$, where ζ is the molecular diffusivity of the pollutant in air; and

$$\frac{1}{r_r} = \frac{1}{r_{cut}} + \frac{1}{r_s + r_m} \qquad (8.2)$$

with r_{cut} the cuticular resistance, r_m the mesophyll resistance, and r_s the stomatal resistance.

In the case of ozone transfer it is assumed that the mesophyll resistance is zero, and that the cuticular resistance is very large compared to the stomatal resistance (Leuning et al., 1979). Therefore, like in the case of water vapor, $r_r = r_s$. These assumptions yield the following transfer equation for ozone

$$\frac{d^2C}{d\zeta^2} + \frac{1}{2}\frac{\chi'}{\chi}\frac{dC}{d\zeta} = \frac{f(\zeta)\, C_t'\, LAI\, \chi^{-1/4}\, C}{\alpha_k \sigma \mu (1 + r_s\, C_t'\, \chi^{1/4}\, u_h)} \qquad (8.3)$$

The molecular diffusivity of O_3 in air, ζ, is $\varepsilon/1.65 = 1.33\ 10^{-5}\ m^2/s$ (Leuning et al., 1979).

8.2.2. Boundary conditions

Since $C = (c_f - c)/(c_f - c_h)$, the upper boundary condition to (8.3) is simply

$$C(\zeta = 1) = C_1 = 1 \qquad (8.4)$$

Again, determining an appropriate lower boundary condition is the main problem. Due to lack of experimental data, it is very difficult to estimate values for the fluxes of gaseous air pollutants to the surface beneath the canopy. For the case of ozone transfer, it is assumed that the canopy is very effective in taking up ozone from the atmosphere, and that the surface uptake is not important. This is equivalent with assuming a zero concentration gradient at $\zeta = 0$.

$$\left.\frac{dC}{d\zeta}\right|_{\zeta=0} = C'_0 = 0 \qquad (8.5)$$

Although results will be presented for small values of LAI, one should be careful with these results, because the lower boundary condition is likely to be inappropriate in these cases.

8.2.3. Computation of the deposition velocity

The dry deposition velocity, v_d, is defined as the deposition flux, F, divided by the concentration of the gas in the air at a certain reference height, c_r, i.e.

$$v_d = -F/c_r \qquad (8.6)$$

(the minus sign is necessary to obtain positive values for v_d when the flux is directed downwards (negative flux)).

The deposition velocity can also be defined in terms of transport resistances, and is equal to the reciprocal of the total transfer resistance. Considering the case of ozone transfer outlined in the previous sections, the deposition velocity is given by (8.7).

$$v_d = (r_a + r_b + r_c)^{-1} \qquad (8.7)$$

where r_a is the aerodynamic resistance to momentum transfer at the reference height. Chosing this reference height to be equal to the canopy height, h, r_a can be computed from the stand drag coefficient, C_f, and the wind speed at the top of the canopy, u_h.

$$r_a = \left[\frac{u}{u_*^2}\right]_h = \frac{2}{C_f\, u_h} \qquad (8.8)$$

The term $r_b + r_c$ can be computed from the values obtained for kB^{-1}, following (8.9).

$$r_b + r_c = \frac{kB^{-1}}{k\, u_h\, (C_f/2)^{1/2}} \qquad (8.9)$$

8.2.4. Results

In the figures 8.1 - 8.4 the computed values for the deposition velocity v_d are presented as a function of LAI and canopy structure. In all figures, the canopy is assumed to be unstressed, i.e. E_1 = 0.2 kPa and $\varphi = 60^o$, and C_t' = 0.075 (u_h = 1.0 m/s). The figures 8.1 and 8.2 are for a deciduous forest, and 8.3 and 8.4 for a coniferous forest.

Figure 8.1 shows, that for full deciduous canopies differences of up to 60% in deposition velocity are possible, when a triangular foliage distribution is assumed instead of a constant distribution. The height of maximum foliage density for triangular distributions seems less important, leading to differences of maximum 10%. Including shelter effects (figure

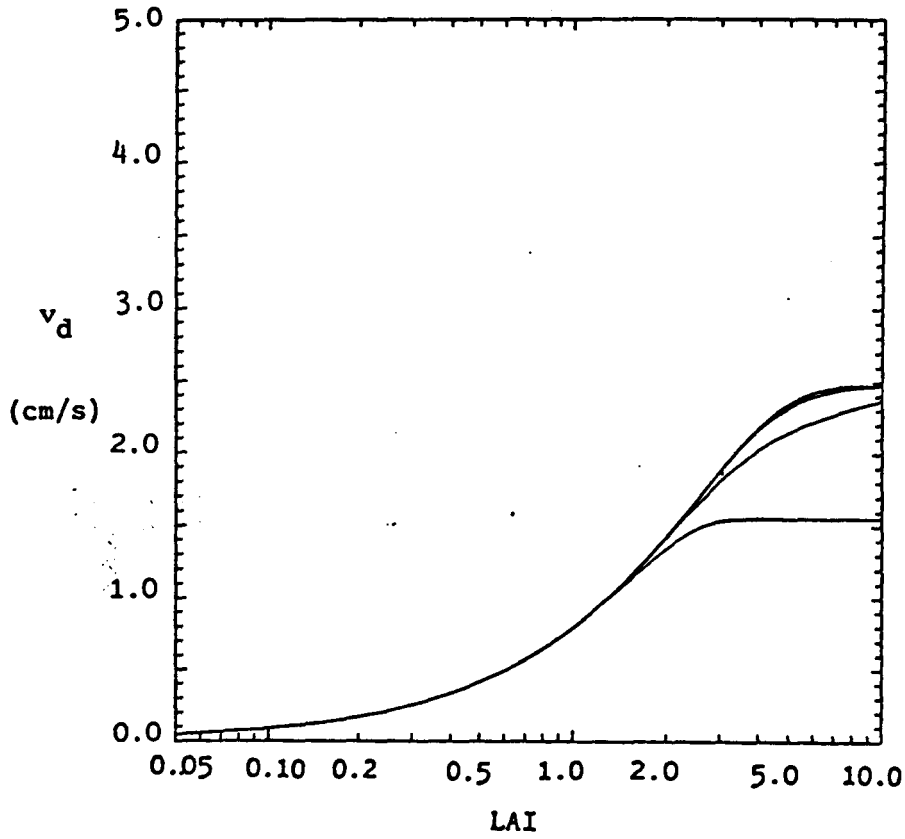

Figure 8.1: The deposition velocity v_d (cm/s) as a function of LAI and foliage structure for an unstressed deciduous forest without shelter effects. The upper three curves represent a triangular foliage distribution with, from to bottom, $\int_m$ = 0.2, 0.5, and 0.8. The lower curve is associated with a constant foliage distribution.

8.2) reduces the difference in v_d from the constant and triangular foliage distribution to about 20%. Furthermore, the values of the computed deposition velocities increase considerably (up to 150% in case of a constant foliage distribution), when shelter is included in the model.

The same accounts when a coniferous forest is considered: differences of up to 60% occur without shelter, but including the effects of mutual aerodynamic interference reduces these differences to a few percent.

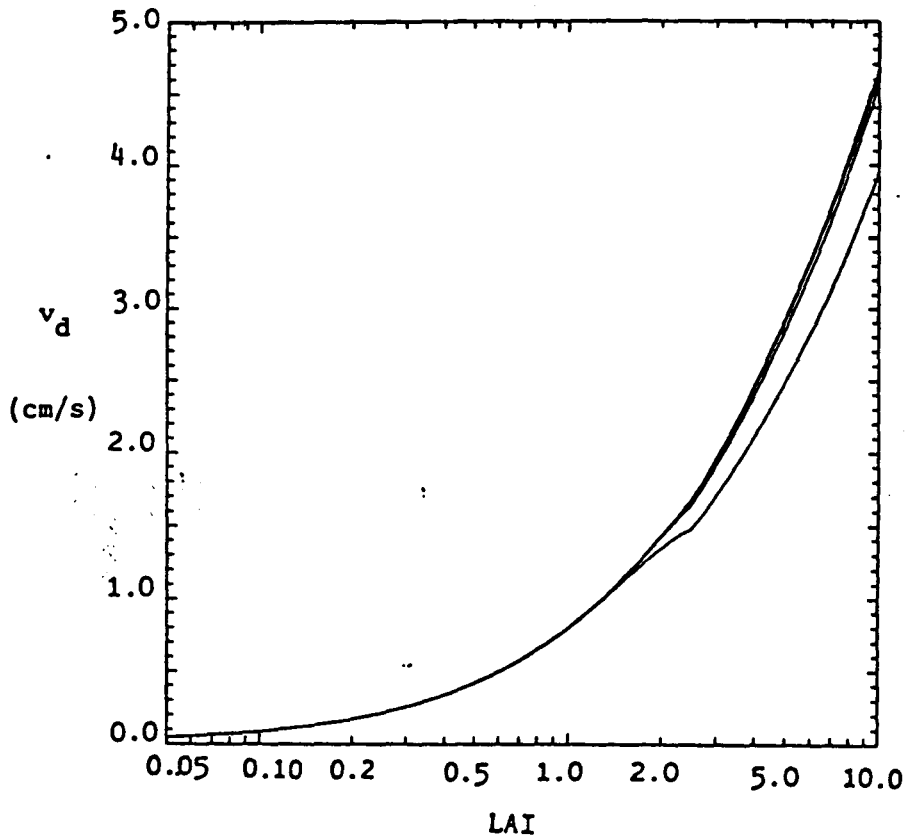

Figure 8.2: Same as figure 8.1, but now with the effects of shelter.

Finally, comparing the figures 8.2 and 8.4 reveals, that the computed deposition velocities for full coniferous canopies are about 8 times lower than those for deciduous canopies.

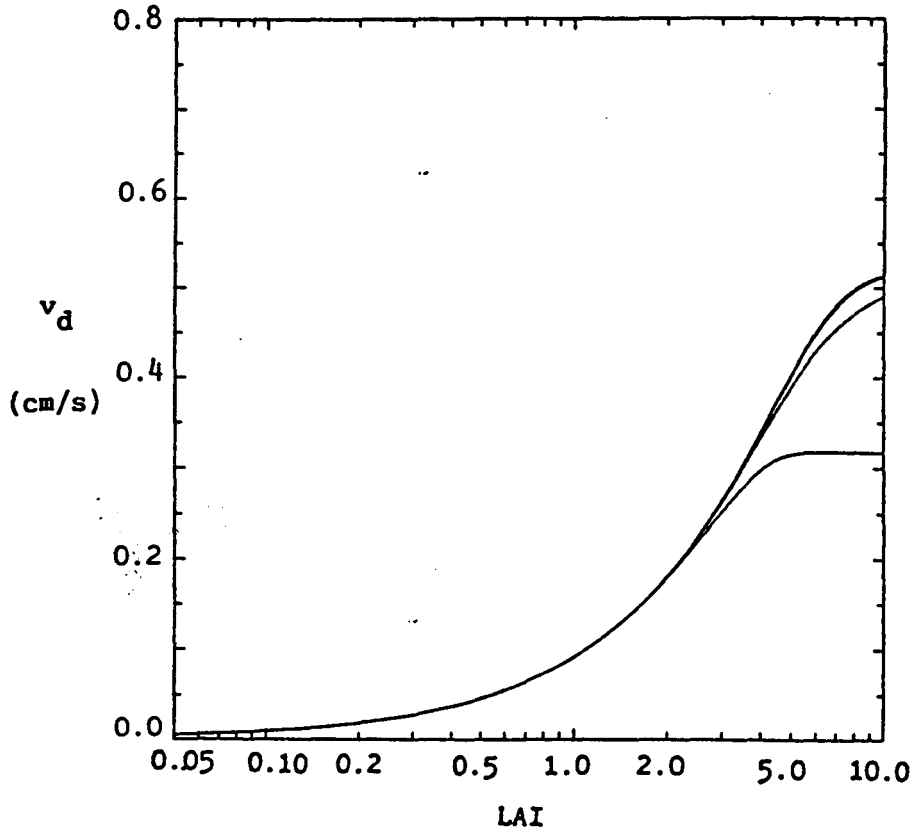

Figure 8.3: Same as figure 8.1, but for an unstressed coniferous forest (without shelter effects).

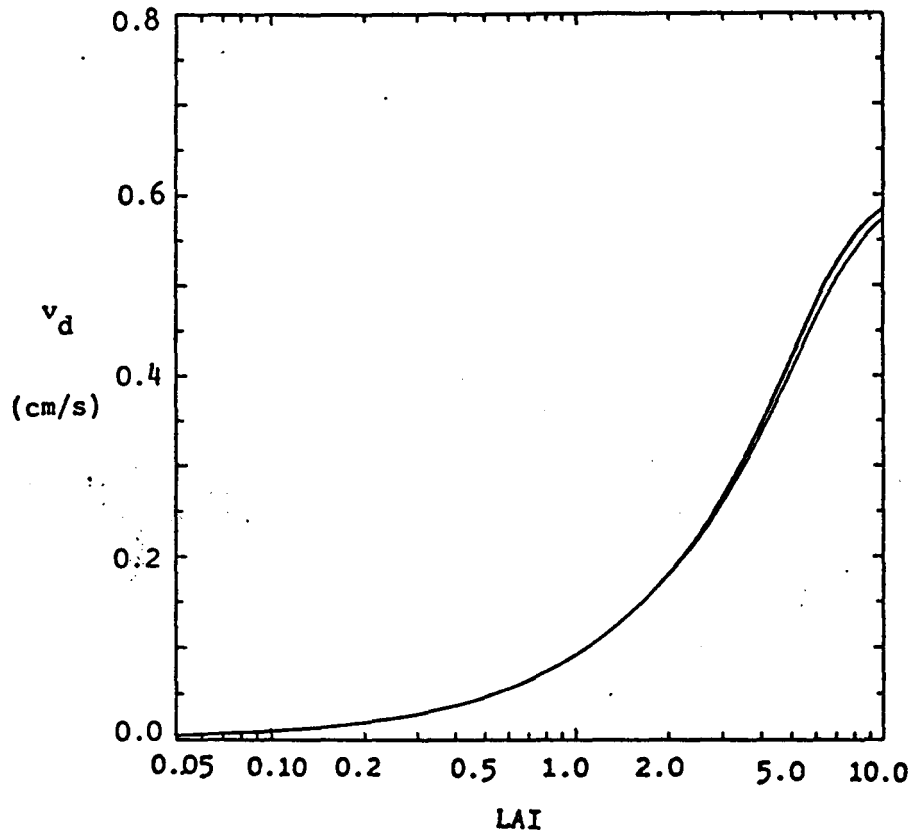

Figure 8.4: Same as figure 8.3, but with shelter effects.

9. DISCUSSION AND CONCLUSIONS

In the previous chapters, a model is derived to describe the exchange of mass between a vegetated surface and the atmosphere, using simple first-order closure assumptions, and including additional resistances in the transfer equation for momentum. Again, the application of the local gradient-diffusion concept is unable to account for all observed features in real canopies (e.g. Finnigan, 1985), but is preferred here over the complexity of more sophisticated methods.

Describing mass exchange between canopy and atmosphere, requires additional transfer resistances to be taken into account, which are associated with the transport through the boundary-layer surrounding the leaf or needle, and with the uptake by or removal from leaf tissue of the constituent under consideration. The boundary-layer resistance is expressed in terms of a leaf bulk transfer coefficient, for which the Pohlhausen model is assumed, because it seems relevant over a wide range of foliage types and Reynolds numbers. However, other models of leaf bulk transfer coefficients are available (e.g. Brutsaert, 1979; Gates, 1980). As proposed by Kaufmann (1982) for plants growing in their natural range, the stomatal resistance is assumed to be determined by two environmental factors only: (1) the within canopy profile of photosynthetic photon flux density, and (2) the water vapor pressure deficit between substomatal cavity and ambient air at the top of the canopy. However, for plants outside their natural environment other factors, like temperature, water stress, and CO_2 concentration might play an equally important role. The dependence of the stomatal resistance on water vapor pressure deficit is formulated following Jarvis (1976), and the radiation dependency is obtained from a photosynthesis model by Gates et al. (1985). Some calculations with the more commonly used formulation of Jarvis (1976) for the influence of PAR on stomatal resistance, showed that the specific form of this dependency was not important for the purposes of this study. Furthermore, it is assumed that: (1) the distribution of leaf inclination is spherical, (2) the foliage distribution is uniform, (3) the size of leaves or needles is

constant throughout the depth of the canopy, (4) leaf age has no influence on stomatal resistance, and (5) no adaptation to low light levels occurs in the lower part of the canopy. However, in many realistic canopies some or all of the above assumptions do not hold, but it is unknown to what extend this affects the presented results.

The mass transfer equation is solved numerically for the transport of water vapor from forest stand to atmosphere, and the removal of ozone from the atmosphere by forest canopies, assuming that (1) the displacement heights for momentum and mass are the same, and (2) the depths of the roughness sublayer for momentum and mass are equal. However, it can be argued that the ratio of the turbulent diffusivities for momentum and mass at the top of the canopy is unity (e.g. Raupach and Thom, 1981; Businger et al., 1971), and that the roughness sublayers for momentum and mass are equal (e.g. Garratt, 1980; Raupach and Legg, 1984).

For the case of water vapor transfer kB^{-1} values were presented as a function of leaf area index and canopy structure. The results for constant and triangular foliage distributions showed that canopy structure has considerable influence on kB^{-1} (differences of up to 100%). Also, for triangular distributions, decreasing the level of maximum foliage density causes a decrease in kB^{-1} of up to 40% for full canopies. However, when the effects of mutual aerodynamic interference of foliage elements were included in the model, kB^{-1} showed far less dependency on canopy structure. Furthermore, the kB^{-1} values for full canopies with shelter effects are considerably lower (up to 45% for coniferous forest, and up to 70% for deciduous forest) than without shelter. Unfortunately, no observed values of kB^{-1}, including the effects of the boundary-layer resistance as well as the stomatal resistance, are known. E.g. Chamberlain (1966), Garratt and Hicks (1973), and Stewart and Thom (1973) report values of kB^{-1} over a variety of surfaces between about 1 and 8, but in their studies only the boundary-layer resistance is taken into account. Computing canopy resistances from kB^{-1} revealed that the canopy resistance is a function of LAI, foliage distribution, and the physiological and environmental parameters determining the stomatal resistance, and that shelter effects play an important role. The commonly used assumption that

the canopy resistance is equal to the bulk stomatal resistance can probably lead to errors of up to 20% for full canopies.

For the case of ozone transport, the transfer equation is solved using a lower boundary condition of zero concentration gradient. Due to lack of experimental data it is not known whether this is appropriate or not, and especially for small values of LAI the deposition of ozone to the soil might be of importance. Deposition velocities were computed for deciduous and coniferous forest, and again, shelter effects proved to be of considerable importance. The computed values for v_d for full coniferous canopies range from about 0.15 to 0.6 cm/s (depending on LAI), which is in good agreement with values presented in the literature (Sehmel, 1980; Lenschow et al. 1982). Values obtained for full deciduous canopies are between about 1.0 and 4.7 cm/s, but unfortunately no values are known from the literature for this case.

REFERENCES

Abramowitz, M. and I.A. Stegun (eds.): 1964, **Handbook of Mathematical Functions**, National Bureau of Standards Applied Math. Ser. No. 55, Washington D.C., 1046 pp.

Anderson, M.C.: 1970, in: **Prediction and Measurement of Photosynthetic Productivity**, I. Setlik (ed.), Pudoc, Wageningen, 71-78

Avissar, R. and Y. Mahrer: 1982, 'Verification Study of a Numerical Greenhouse Microclimate Model', Trans. Am. Soc. Agric. Eng. 25, 1711-1720

Baldocchi, D.D., B.B. Hicks and P. Camara: 1987, 'A Canopy Stomatal Resistance Model for Gaseous Deposition To Vegetated Surfaces', Atmospheric Environment Vol. 21 No. 1, 91-101

Brutsaert, W.: 1979, 'Heat and Mass Transfer To and From Surfaces With Dense Vegetation or Similar Permeable Roughness', Boundary-Layer Meteorology 16, 365-388

Businger, J.A., J.C. Wyngaard, Y. Izumi and E.G. Bradley: 1971, 'Flux Profile Relationships in the Atmospheric Surface Layer', J. Atmos. Sci. 28, 181-189

Chamberlain, A.C.: 1966, 'Transport of Gases To and From Grass and Grass-like Surfaces', Proc. Roy. Soc. London A290, 236-265

Choudbury, B.J. and J.L. Monteith: 1986, 'Implications of Stomatal Response To Saturation Deficit for the Heat Balance of Vegetation', Agric. and Forest Meteorol. 36, 215-225

Corrsin, S.: 1974, 'Limitations of Gradient Transport Models in Random Walks in Turbulence', Adv. Geophysics 18A, 25-60

Cowan, I.R.: 1968, 'Mass, Heat and Momentum Exchange Between Stands of Plants and Their Atmospheric Environment', Quart. J. Roy. Meteorol. Soc. 94, 523-544

den Hartog, G. and R.H. Shaw: 1975, 'A Field Study of Atmospheric Exchange Processes Within a Vegetative Canopy', in D.A. DeVries and N.H. Afgan (eds.), Heat and Mass Transfer in the Biosphere, Scripta Books, Washington D.C., pp. 299-309

Dickinson, R.E.: 1983, 'Land Surface Processes and Climate-Surface Albedos and Energy Balance', Adv. In Geophys. 25, 305-353

Dolman, A.J.: 1986, 'Estimates of Roughness Length and Zero Plane Displacement for a Foliated and Non-Foliated Oak Canopy', Agric. and Forest Meteorol. 36, 241-248

Finnigan, J.J.: 1985, 'Turbulent Transport In Flexible Plant Canopies', in The Forest-Atmosphere Interaction, B.A. Hutchinson and B.B. Hicks (eds.), 443-480

Garratt, J.R. and B.B. Hicks: 1973, 'Momentum, Heat and Mass Transfer To and From Natural and Artificial Surfaces', Quart. J. Roy. Met. Soc. 99, 680-687

Garratt, J.R.: 1980, 'Surface Influence Upon Vertical Profiles in the Atmospheric Near-Surface Layer', Quart, J. Roy. Meteorol. Soc. 106, 803-819

Gash, J.H.C. and J.B. Stewart: 1975, 'The Average Surface Resistance of a Pine Forest Derived from Bowen-Ratio Measurements', Boundary-Layer Meteorol. 8, 453-464

Gates, D.M.: 1980, Biophysical Ecology, Springer-Verlag, New York Inc., New York, 611 pp.

Gates, D.M., J.A. Weber, T.W. Jurik and J.D. Tenhunen: 1985, 'Analysis of Gas Exchange In Seedlings of Acer saccharum: Integration of Field and Laboratory Studies', Oecologia (Berlin) 65, 338-347

Goudriaan, J.: 1977, Crop Micrometeorology: A Simulation Study, Wageningen, Wageningen Center for Agricultural Publishing and Documentation

Hill, A.C.: 1971, 'Vegetation: A Sink for Atmospheric Pollutants', J. Air Pollut. Control Assoc. 21, 341-346

Hosker, R.P. and S.E. Lindberg: 1982, 'Review: Atmospheric Deposition and Plant Assimilation of Gases and Particles', Atmospheric Environment 16 889-910

Inoue, E.: 1963, 'On the Turbulent Structure of Airflow Within Crop Canopies', J. Meteorol. Soc. Japan 41, 317-326

Jarvis, P.G.: 1976, 'The Interpretation of the Variations In Leaf Water Potential and Stomatal Conductance Found In Canopies In the Field', Phil. Trans. R. Soc. Lond. B. 273, 593-610

Kaufmann, M.R.: 1982, 'Leaf Conductance As a Function of Photosynthetic Photon Flux Density and Absolute Humidity Difference From Leaf To Air' Plant Physiol. 69, 1018-1022

Kimes, D.S.: 1984, 'Modeling the Directional Reflectance From Complete Homogeneous Vegetation Canopies With Various Leaf Orientation Distributions', J. Opt. Soc. Am. A 1, 725

Kondo, J. and A. Kawanaka: 1986, 'Numerical Study On the Bulk Heat Transfer Coefficient For a Variety of Vegetation Types and Densities', Boundary-Layer Meteorology 37, 285-296

Kuroiwa, S.: 1970, in: **Prediction and Measurement of Photosynthetic Productivity**, I. Setlik (ed.), Pudoc, Wageningen, 79-89

Landsberg, J.J. and A.S. Thom: 1971, 'Aerodynamic Properties of A Plant of Complex Structure', Quart. J. Roy. Meteorol. Soc. 97, 565-570

Lenschow, D.H., R. Pearson Jr. and B.B. Stankov: 1982, 'Measurements of Ozone Vertical Flux to Ocean and Forest', J. Geophysical Research 87, 8833-8837

Leuning, R., H.H. Neumann and G.W. Thurtell: 1979, 'Ozone Uptake by Corn: A General Approach', Agricultural Meteorol. 20, 115-135

Li, Z.J., D.R. Miller and J.D. Lin: 1985, 'A First-Order Closure Scheme to Describe Counter-Gradient Momentum Transport in Plant Canopies', Boundary-Layer Meteorol. 33, 77-83

Massman, W.J.: 1987a, 'A Comparative Study of Some Mathematical Models of the Mean Wind Structure and Aerodynamic Drag of Plant Canopies', Boundary-Layer Meteorology 40, 179-197

Massman, W.J.: 1987b, 'Heat Transfer To and From Vegetated Surfaces: An Analytical Method for the Bulk Exchange Coefficients', Boundary-Layer Meteorology 40, 269-281

McNaughton, K.G. and T.A. Black: 1973, 'A Study of Evapotranspiration from a Douglas-fir Forest Using the Energy Balance Approach', Water Resour. Res. 9, 1579-1590

Meyers, T. and U.K.T. Paw: 1986, 'Testing of a Higher-Order Closure Model for Modeling Air Flow Within and Above Plant Canopies', Boundary-Layer Meteorol. 37, 297-311

Monsi, M. and T. Saeki: 1953, 'Ueber den Lichtfaktor In den Pflanzengesellschaft und Seine Bedeutung Fuer die Stoffproduktion', Jap. J. Bot. 14, 22-52

O'Dell, R.A., M. Taheri and R.L. Kabel: 1977, 'A Model for Uptake of Pollutants by Vegetation', J. Air Pollut. Control Assoc. 27, 1104-1109

Owen, P.R. and W.R. Thomson: 1963, 'Heat Transfer Across Rough Surfaces', J. Fluid Mech. 15, 321-334

Pearman, G.I., H.L. Weaver and C.B. Tanner: 1972, 'Boundary Layer Heat Transfer Coefficients Under Field Conditions', Agric. Meteorol. 16, 83-92

Press, W.H., B.P. Flannery, S.A. Teukolsky and W.T. Vetterling: 1986, **Numerical Recipes: The Art of Scientific Computing**, New York, Cambridge University Press, 818 pp.

Raupach, M.R., A.S. Thom and L. Edwards: 1980, 'A Wind Tunnel Study of Turbulent Flow Close to Regularly Arrayed Rough Surfaces', Boundary-Layer Meteorology 18, 373-397

Raupach, M.R. and A.S. Thom: 1981, 'Turbulence In and Above Plant Canopies' Ann. Rev. Fluid Mechanics 13, 97-129

Raupach, M.R. and B.J. Legg: 1984, 'The Uses and Limitations of Flux-Gradient Relationships in Micrometeorology', Agric. Water Management 8, 119-131

Ross, J.K. and T.A. Nilson: 1965, in: **Aktinometriya i optika atmosfery (Actinometry and Atmospheric Optics)**, Valgus, Talinn, 263-281

Ross, J.: 1975, 'Radiative Transfer In Plant Communities', in: Vegetation and the Atmosphere, Vol. I, J.L. Monteith (ed.), London, Academic Press, 13-52

Seginer, I.: 1974, 'Aerodynamic Roughness of Vegetated Surfaces', Boundary-Layer Meteorology 5, 383-393

Sehmel, G.A.: 1980, 'Particle and Gas Dry Deposition: A Review', Atmosph. Environ. 14, 983-1011

Sellers, P.J.: 1985, 'Canopy Reflectance, Photosynthesis and Transpiration' Int. J. Remote Sensing Vol. 6 No. 8, 1335-1372

Sellers, P.J., Y. Mintz, Y. Sud and A. Dalcher: 1986, 'A Simple Biosphere Model (SiB) for Use within General Circulation Models', J. Atmos. Sci. 43, 505-531

Shaw, R.H.: 1977, 'Secondary Wind Speed Maxima Inside Plant Canopies', J. Appl. Meteorol. 16, 514-521

Shaw, R.H. and A.R. Pereira: 1982, 'Aerodynamic Roughness of a Plant Canopy a Numerical Experiment', Agric. Meteorol. 26, 51-65

Shuttleworth, W.J.: 1976, 'A One-Dimensional Theoretical Description of the Vegetation-Atmosphere Interaction', Boundary-Layer Meteorol. 10, 273-302

Smith, E.L.: 1937, 'The Influence of Light and Carbon Dioxide On Photosynthesis', J. General Physiol. 20, 807-830

Smith, E.L.: 1938, 'Limiting Factors In Photosynthesis: Light and Carbon Dioxide', J. General Physiol. 22, 21-35

Stewart, J.B. and A.S. Thom: 1973, 'Energy Budgets in a Pine Forest', Quart J. Roy. Met. Soc. 99, 154-170

Suits, G.H.: 1972, 'The Calculation of the Directional Reflectance of a Vegetative Canopy', Remote Sensing Environ. 2, 117

Szeicz, G. and I.F. Long: 1969, 'Surface Resistance of Crop Canopies', Water Resour. Res. 5, 622-633

Taconet, O., R. Bernard and D. Vidal-Madjas: 1986, 'Evapotranspiration over an Agricultural Region Using a Surface Flux/Temperature Model Based on NOAA-AVHRR Data', J. of Clim. Appl. Meteorol. 25, 284-307

Tan, C.S. and T.A. Black: 1976, 'Factors Affecting the Canopy Resistance of a Douglas-fir Forest', Boundary-Layer Meteorol. 10, 489-501

Thom, A.S.: 1971, 'Momentum Absorption by Vegetation', Quart. J. Roy. Meteorol. Soc. 97, 414-428

Thom, A.S.: 1975, 'Momentum, Mass and Heat Exchange of Plant Communities', in Vegetation and the Atmosphere Vol. I, J.L. Monteith (ed.), London, Academic Press, 57-109

Warren-Wilson, J.: 1967, J. Appl. Ecol. 4, 159-165

Wilson, N.R. and R.H. Shaw: 1977, 'A Higher Order Closure Model for Canopy Flow', J. Appl. Meteorol. 16, 1197-1205

Yamada, T.: 1982, 'A Numerical Model Study of Turbulent Air Flow In and Above a Forest Canopy', J. Meteorol. Soc. Japan 60, 439-454